Enhancement of Heat Transfer with Nanofluids

PhD Thesis

By

SANDESH S. CHOUGULE

DISCIPLINE OF MECHANICAL ENGINEERING

INDIAN INSTITUTE OF TECHNOLOGY INDORE

JUNE 2015

Enhancement of Heat Transfer with Nanofluids

A THESIS

Submitted in partial fulfillment of the requirements for the award of the degree

of

DOCTOR OF PHILOSOPHY

by

SANDESH S. CHOUGULE

DISCIPLINE OF MECHANICAL ENGINEERING

INDIAN INSTITUTE OF TECHNOLOGY INDORE

JUNE 2015

INDIAN INSTITUTE OF TECHNOLOGY INDORE

CANDIDATE'S DECLARATION

I hereby certify that the work which is being presented in the thesis entitled **"Enhancement of Heat Transfer with Nanofluids"** in the partial fulfillment of the requirements for the award of the degree of **DOCTOR OF PHILOSOPHY** and submitted in the **Discipline of Mechanical Engineering, Indian Institute of Technology Indore**, is an authentic record of my own work carried out during the time period from July 2012 to May 2015 under the supervision of **Dr. S. K. Sahu, Assistant Professor, Indian Institute of Technology Indore.**

The matter presented in this thesis has not been submitted by me for the award of any other degree of this or any other institute.

Signature of the student with date

(SANDESH S. CHOUGULE)

This is to certify that the above statement made by the candidate is correct to the best of my/our knowledge.

Signature of Thesis Supervisor with date

(Dr. S. K. SAHU)

Sandesh S. Chougule has successfully given his Ph.D. Oral Examination, held on **…………**

Signature of Thesis Supervisor Date:	Convener, DPGC Date:
Signature of PSPC Member Date:	
Signature of PSPC Member Date:	Signature of External Examiner Date:

AKNOWLDGEMENTS

I would like to express my sincere gratitude to my honorific supervisor **Dr. S. K. Sahu** for his valuable guidance and endless encouragement during my research tenure at IITI. His positive attitude towards excellent ideas helped me to grow as a quality researcher. His continuous advice on both research as well as on my career has been priceless.

I am very grateful to doctorate research progress committee members **Dr. E. Anil Kumar** and **Dr. Apurba Das** for their valuable suggestions and comments during this work.

I am thankful to **Dr. Devendra L. Deshmukh**, **Dr. Amod C. Umarikar**, **Dr. Kiran Bala** and **Dr. Parasharam M. Shirage**. Their academic support and personal cheering are greatly appreciated.

I am also extremely indebted to **Prof. Pradeep Mathur** (Director, Indian Institute of Technology Indore) for sanctioning financial support to present research work in abroad conferences.

Very special thanks go to **Prof. S. H. Pawar** (Vice Chancellor, D. Y. Patil University, Kolhapur) and **Dr. S. Suresh** (Assistant Professor, National Institute of Technology, Trichy) who played a significant role in thesis work and opened doors of nanotechnology science for me.

Dr. Thomas J. MaKrell (Research Scientist, Massachusetts institute of technology, USA) and **Prof. William M. Worek** (Associate Dean for Research and Graduate Studies, Stony Brook University, USA) provided very practical suggestions during the research work. During the research, they responded rapidly to my twists and turns. Their contributions made a significant difference to the overall shape of the dissertation.

I would not have studied this PhD without the wise counsel of **Prof. Ashok T. Pise** (Deputy Director, Directorate of Technical Education, Mumbai) who have been steady hands to steer me through my postgraduate career at Government College of Engineering, Karad.

It is a pleasure to acknowledge with gratitude the financial support of **Science and Engineering Research Board** and **Council of Scientific & Industrial Research, New Delhi, India** to present research work in reputed ASME conferences **ICNMM-2014**, **Chicago, USA** and **MNHMT-13, Hong kong, China**, respectively. I acknowledge the **Ministry of Human Resource Development, Government of India** and **Indian Institute of Technology Indore** for providing scholarships to pursue doctoral studies.

I also wish to thanks, **Anand Petare** and **Arun Kumar Bhagwaniya** who helped in the fabrication of test facility at IIT Indore. I am grateful for the time spent with backpacking buddies and our memorable trips into the mountains of **Panchmadhi**. I am ever indebted to friends for their cooperation, encouragement and moral support. I wish to thank my friends, Javed Shaikh, Manish Agrawal, Vinod Sharma, Sambhaji Kadam, Yogesh Madaria, Hari Mohan Kushwah, Aniket Kulkarni, Rajan Lanjekar, Pramod Mane, Balmukund Dhakar, Mayur Sawant, Sagar Nikam, Kratika Pathak, Mayank Modak, Agnel D'souza and Vinayak Yadav.

This thesis would not have been possible without the support of my family. I am grateful to them for their never-ending love, patience and encouragement. Words cannot express how grateful I am to my **Aai**, **Papa**, **Deepika** and **my wife** for all of the sacrifices that they have made on my behalf.

- **Sandesh Surendra Chougule**
Indore, May 2015

Dedicated to beloved Aai, Papa and Teachers

Abstract

The present dissertation reports the experimental study pertaining to enhanced heat transfer performance of nanofluids compared to water in several thermal devices. The objective of the present study is to analyze the thermal performance of nanofluids for various practical applications including heat exchanging equipments, automobile radiators, flat plate solar collector and cooling of electronics components.

In this study, efforts have been made to study the heat transfer performance of various thermal devices. Tests have been performed to study the forced convection and heat transfer characteristics of Al_2O_3/water and carbon nanotube/water nanofluids through uniformly heated horizontal circular pipe with helical twisted tape inserts (HI). The experiments are performed with varied range of particle volume concentration (0.15%, 0.45%, 0.60% and 1%) and helical tape inserts of twist ratio (TR) = 1.5, 2.5 and 3. Next, an experimentally study has been carried out to evaluate the convective heat transfer characteristics of CNT/water and Al_2O_3/water and nanofluids in an automobile radiator. The effects of various parameters, namely synthesis method, variation in pH values and nanoparticle concentration on the Nusselt number are examined through the experimental investigation. The comparison of thermal performance for CNT/water and Al_2O_3/water nanofluids is reported in the present investigation. The heat pipes are integrated into flat plate solar water heater to evaluate the thermal performance of solar flat plate collector. Here, two different fluids such as: CNT/water nanofluids and pure water are used as working fluid in the heat pipe. The effect of the tilt angle, filling ratio, nanoparticle concentration and coolant flow rate on the thermal performance of the solar collector has been discussed in the study. Further, an attempt has been made to evaluate the thermal performance of nanofluid (CNT/water) charged heat pipe with phase change material (PCM) as energy storage material (ESM) for electronic

cooling. Tests are conducted for two different ESM (water and paraffin), different fan speeds and heating powers in the PCM cooling module. The temperature variations in PCM are obtained during charge/discharge processes.

Keywords: Nanofluid, CNT/water, Al_2O_3/water, heat transfer, helical screw tape inserts Nusselt number, Reynolds number, friction factor, thermal performance, automobile radiators, heat pipe, solar flat plate collectors, phase change material, electronics cooling

Table of Content

List of Figures

List of Table

Nomenclature

A	Surface area, (m^2)
A_{coll}	Collector effective area, m^2
C_p	Specific heat, (J/kg K)
D	Test section diameter, (m)
D_{hy}	Hydraulic diameter, (m)
F_R	Heat removal factor
h	Convective heat transfer coefficient, ($W/m^2\ {}^0C$)
I	Current, (A)
I_t	Total solar radiation, (W/m^2)
k	Thermal conductivity, (W/m K)
L	Test section length, (m)
$\dot{m}$	Mass flow rate, (kg/s)
M	Mass of phase change material, (kg)
Nu	Nusselt number, (hD/k)
P	Pitch of the helical screw tape insert, (m)
Pe	Peclet number, ($\rho C_p uD/k$)
Q, Q_{in}	Heat input, (W)
Re	Reynolds number, ($\rho uD/\mu$)
t	Time, (s)
T	Temperature, (${}^0C$)
Q_g	Thermal energy gain, (W)
u	Fluid velocity, (m/s)
U_L	Overall loss coefficient of solar collector, (W/m^2 K)
V	Voltage, (V)
Greek Symbols	
φ	Volume concentration, (%)
μ	Dynamic viscosity, (kg/m^2s)
ρ	Density, (kg/m^3)

$\tau\alpha$	Absorptance-transmittance product
η	Thermal Performance factor, dimensionless
η_{coll}	Collector instantaneous efficiency, dimensionless

Subscripts

a	Ambient
b	Bulk
bf	Basefluid
eff	Effective
exp.	Experimental
i	Inserts
in	Inlet
l	Nanolayer
nf	Nanofluid
out	Outlet
p	Nanoparticle
pt	Plain tube
w	Wall

Abbreviations

ESM	Energy storage material
EST	Energy storage tank
FR	Filling ratio
FCNT	Functionalized CNT
HI	Helical Screw Tape inserts
ID	Inner diameter
MWCNT	Multi walled carbon nanotube
OD	Outer diameter
PCM	Phase change material
SSA	Specific surface area
SCNT	Surface treated CNT
TR	Twist ratio

Chapter 1

Introduction and Literature Review

1.1 General Background

Transfer of heat energy plays a vital role in various engineering and scientific applications. Several processes such as: heating, cooling and heat transfer by phase change are frequently encountered during engineering applications. It is observed that the heat transfer due to convection plays a significant role in different industrial applications. The heat transfer by convection depends on various hydrodynamic parameters and thermophysical properties of the fluid. For a given hydrodynamic parameters, the heat transfer characteristics of a fluid can be enhanced by increasing the thermal conductivity.

Conventional single phase fluids such as: water, engine oil and ethylene glycol are used as coolant in various industrial applications including automobile radiators, manufacturing units and electronics applications. However, the heat transfers capability of these conventional single phase fluids are limited. At this juncture, there is a need to develop new engineering fluids with improved heat transfer characteristics compared to the conventional fluids. It is observed that metals have higher thermal conductivity compared to conventional single phase fluids. Therefore, it is a logical approach to develop new heat transfer fluids containing solid particles to enhance the thermal conductivity. Therefore, new engineering fluids have been developed by dispersing nanoparticles in the conventional heat transfer fluids, termed as *nanofluids* [1]. Apart from the miniaturized devices, larger units (heat exchanger, evaporator), conventional thermal or nuclear power plants and non-conventional energy devices need an efficient cooling system with greater cooling capacities and decreased sizes. Among various methods, enhancing the heat transfer capacity of coolant (nanofluids) is considered to be a useful technology to enhance the cooling capacity. In this chapter, the introduction of nanofluids, the associated heat transfer mechanism, various applications and a brief review of the literature on the use of nanofluids in various engineering and scientific application are discussed. Also, the objectives of this investigation are enumerated.

1.2 Applications of Nanofluids

Nanofluid can be utilized in various thermal devices to improve the heat transfer rates and energy efficiency. Some of the industrial applications are listed below.

Solar water heating

Solar energy is often used in various applications such as: electricity generation, chemical processing and solar heating. Solar collectors absorb the incoming solar radiation, convert it into heat and transfer the heat to a fluid (air, water and oil) flowing through the collector. Solar water heaters are mostly used to obtain hot water. Although, the flat plate solar collectors are the most cost-effective, they usually have lower thermal efficiency. In order to improve the thermal efficiency, nanofluids are used directly as a coolant or one can utilize nanofluid charged heat pipes to transfer the heat energy to the coolant.

Cooling of electronics

Removal of higher heat flux is a major challenge in the design of future electronic devices. Commonly, water is used as a single-phase coolant in combination with microchannel heat sinks for cooling electronics, as it possesses the most adequate thermal and hydrodynamic transport properties in the required range of operating temperatures. However, the thermal conductivity of water is two to three orders of magnitude lower compared to of most metals and metal oxides. Therefore, an innovative way to elevate the thermal conductivity of fluids may be the addition of nanometer-sized metal or metal oxide particles into a basefluid, most suitable water. Novel concepts of heat pipes using a nanofluid as a working fluid can be used for electronics cooling.

Engine cooling management

The automobile engine utilizes a heat exchanger device, termed as a radiator, in order to remove the heat from the cooling jacket of the engine. The radiator is considered as an important component of the cooling system of the engine. In general, ethylene glycol and water mixture is used automotive coolant. However, ethylene glycols possess inferior heat removal capacity compared to water. The addition of nanoparticles to the engine coolant has the potential to improve the cooling rates in the case of automotive and heavy-duty engines. In such a case, a smaller cooling system can be used to remove the engine heat. Smaller coolant systems results in smaller and lighter radiators, resulting in the reduction of the drag and fuel consumption.

Medical applications

Nanofluids are widely used in biomedical applications such as: magnetic cell separation, drug delivery and hyperthermia. Based on the specific requirements, suitable functionalization and synthesis methods are adopted to obtain the required properties. It may be noted that the colloidal stability of biocompatible water-based magnetic fluids is an important issue that affect the successful application.

Heat exchanger

Cooling is one of the important challenges faced by many industries. The conventional way to increase cooling rates is to increase the heat transfer area, change the flow geometry to generate turbulence and increase the flow rate. With the increase of heat transfer area, the size of the thermal system increases. The addition of nanoparticle may help to decrease size of the heat exchanger by increasing heat transfer capacity of the base fluid or coolant.

Other applications

The nanocoolants also have potential application in various devices, namely, chillers, refrigerators, electric transformer, fuel cells, and nuclear reactors. Also, the nanofluids are widely used as coolant for different machining processes.

1.3 What is Nanofluid?

From last few decades, efforts have been made to enhance the thermal conductivity of liquids by adding solid particles in liquids. Earlier, Maxwell [2] has made an attempt to disperse millimeter/micrometer-sized particles in liquids. This approach encountered two major problems, namely, quick settlement of particles and lower conductivities of these suspensions at low particle concentrations. Also, these suspensions were found to clog the tiny channels of micro devices.

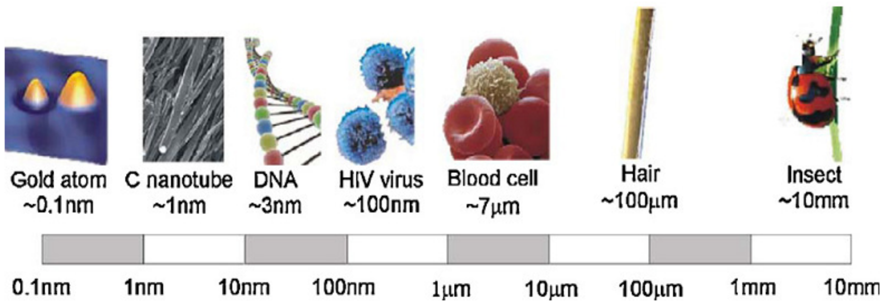

Figure 1.1: Length scale and some examples related [3]

Later on, modern nanotechnology enabled the production of metallic or nonmetallic nanoparticles with average crystallite sizes below 100 nm. The mechanical, optical, electrical, magnetic, and thermal properties of nanoparticles are superior to the conventional bulk materials. Choi [1] conceived the novel concept to utilize these excellent properties of nanoparticles in colloidal suspension. Nanofluids are a new class of nanotechnology based heat transfer fluids engineered by dispersing nanometer-sized particles with typical length scales on the order of 1 to 100 nm (preferably, smaller than 10 nm in diameter) in traditional heat transfer fluids. Choi [1] developed nanoparticles and reported an enhancement in thermal conductivity by dispersing the nanoparticle in conventional heat transfer fluids and termed as nanofluids. These fluids found to exhibit superior thermal properties compared to their base fluids. Serrano et al. [3] provided excellent examples of various length scales (nano, micro and millimeter) as applied in various scientific and day to day is applications (Fig. 1.1).

Nanofluids are found to possess following advantages compared to conventional fluids and are elaborated below [4]

- Higher specific surface area and therefore more heat transfer surface between particles and the fluids.
- Higher dispersion stability with predominant Brownian motion of particles.
- Reduced pumping power as compared to conventional liquid to achieve equivalent heat transfer intensification.
- Reduced particle clogging compared to conventional slurries, thus promoting system miniaturization.
- Adjustable properties, including thermal conductivity and surface wettability, by varying particle concentrations to suit different applications

1.4 Mechanism of Heat Flow in Nanofluid

The effective thermal conductivity of mixture originates from continuum formulation usually involves only the particle size/shape and the volume fraction. These formulations assume diffusive heat transfer in both fluids and solid phases. This method provides good prediction pertaining to the heat transfer characteristics of micrometer and large size solid/fluid system. However, the theory could not explain the unusual heat transfer characteristics of nanofluids. In view of this, various theories have been proposed in order to explain the anomalous increase in the heat transfer of nanofluids [5] and are elaborated below.

Brownian motion

Two different modes of Brownian motion are encountered in nanofluids. This includes the collision between Brownian nanoparticles and convection induced by Brownian nanoparticles. The collision between nanoparticles occurs due to Brownian motion of nanoparticles. This is considered to be the first dynamic mechanism for the enhancement of thermal conductivity of nanofluids. However, the enhancement in the thermal conductivity due to the collision between Brownian nanoparticles is negligible. This may be due to the fact the Brownian nanoparticle is much slower compared to the thermal diffusion. On the contrary, nanoparticles move through the liquid and convection is induced due to the Brownian motion of nanoparticles leading to an increase in the thermal conductivity.

Liquid layering at liquid/particle interface

Liquid molecules form a layer near the solid surface of nanoparticle termed as nanolayer. The nanolayer structure was proposed by Keblinski et al. [5] and considered to be the first static mechanism to explain the enhancement in the thermal conductivity of nanofluids. Fig. 1.2 shows the schematic diagram of a nanolayer around the nanoparticle surface. Nanolayers act as a thermal bridge between the solid nanoparticle and the bulk liquid and improve the thermal transport in a suspension. The thermal conductivity of the nanolayer is higher than that of the bulk liquid.

Heat transport by ballistic phonon transport

The ballistic phonon transport of the nanoparticles plays a significant role in the increase in thermal conductivity. In crystalline solids, heat is transported by phonons due to lattice vibrations. The ballistic phonon initiated in one particle can persist in the liquid and propagates to the adjacent particle. This increases the effective thermal conductivity of nanofluids [5].

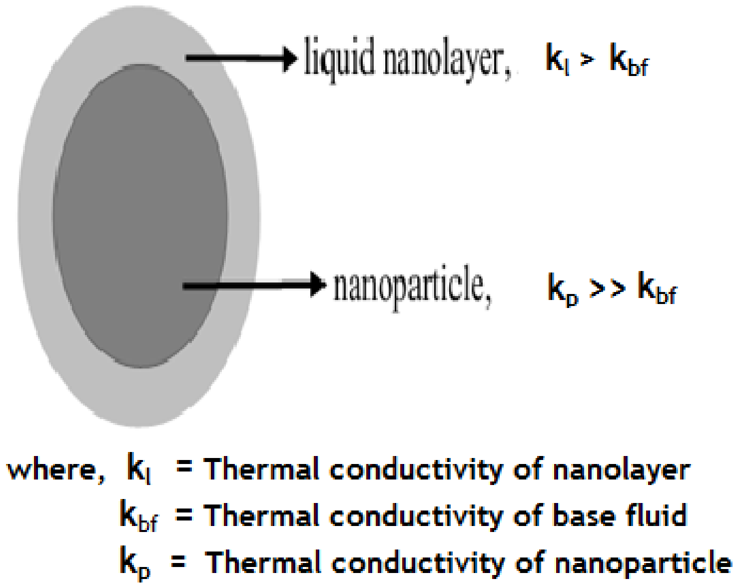

Figure 1.2: Schematic illustration representing the liquid layering around nanoparticles [5]

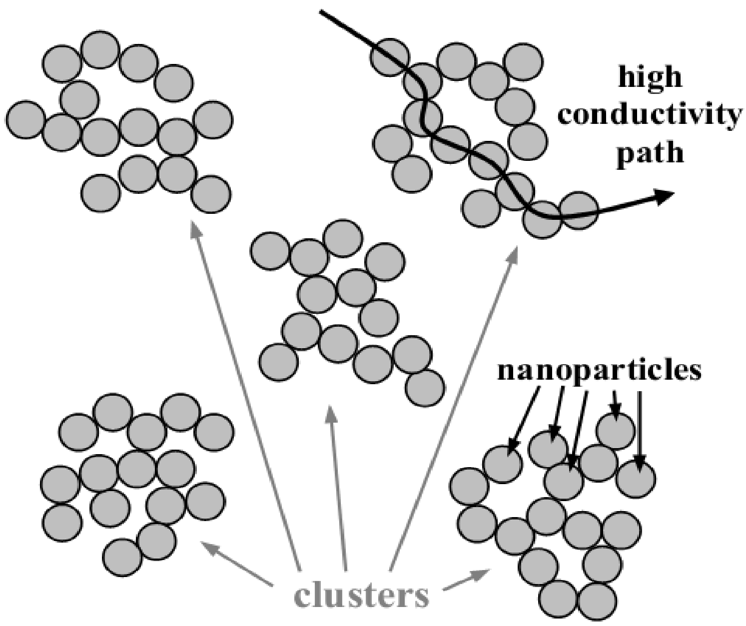

Figure 1.3: Schematic of clustering phenomenon of nanoparticles and the heat transfer paths.

Effect of nanoparticles clustering

Enhancement in heat transfer of nanofluids also occurs due to the clustering of nanoparticles. Clustering of nanoparticles increases the thermal conductivity of the basefluid because of higher concentration of nanoparticles. On the contrary, because of clustering of particles the mass increases and leads to the sedimentation of the nanoparticles. The clustering is usually found at higher concentrations of nanofluid, where the interparticle distances between particles are very small, leading to agglomeration. Evans et al. [6] proposed that clustering can result in fast transport of heat for a longer distance since heat can be conducted much faster by solid particles when compared to the liquid matrix. This phenomenon is illustrated schematically in Fig. 1.3

1.5 Review of Literature

Nanofluids offers several benefits such as: higher cooling rates, decreased pumping power for same heat loads, smaller and lighter cooling systems and the reduced inventory of heat transfer fluids. Because of these advanced features, nanofluids have been used widely in several applications including manufacturing, transportation, energy and electronics cooling. In addition, nanofluids charged heat pipes are used for solar heating and electronics cooling applications. A variety of studies involving both theoretical and experimental investigations have been carried out to study the heat transfer enhancement of nanofluids. A brief review of some of the important studies is presented here.

1.5.1 Experimental investigation

Several experimental studies have been made to study the heat transfer capability of nanofluids. In view of this, various researchers performed tests to evaluate the thermal conductivity of nanofluids. In addition, efforts have been to study the heat transfer characteristics of nanofluids through uniform heated pipes with and without inserts, automobile radiator, solar collectors and nanofluid assisted heat pipe for electronics cooling and boiling heat transfer.

Thermal conductivity enhancements with nanofluids

The heat transfer by convection can be enhanced by increasing the flow geometry, creating turbulence and thermal conductivity of the fluid. For a given design condition, the heat transfer rate of the thermal device can be enhanced by increasing the thermal conductivity of coolant. While, it is observed that the thermal conductivities of conventional coolants such as: water, ethyl glycol and engine oil usually have several orders lower compared to that of copper. In view of this, efforts have been made to increase the thermal conductivity of coolant by suspending micro-sized particles in the base fluid. This is due to the fact that the thermal conductivity of solid nanoparticles is significantly higher compared to the basefluid as shown in Table 1.1 [7-11].

Nanofluids exhibit the significant increase in the heat transfer rate. Among other reasons, it is observed that the effective thermal conductivity of nanofluids is higher compared to the base fluid and plays a role in the enhancement in the heat transfer rate. The increase in the thermal conductivity of nanofluids was found to depend on various factors such as: particle volume concentration, particle composition, particle size, particle shape, base fluid, temperature, pH level and additives used [10, 12-17]. The magnitude of enhancement in thermal conductivity for various cases is summarized in Table1.2.

The enhanced thermal conductivity of nanofluids offer several benefits such as higher cooling rates, decreased pumping power needs, smaller and lighter cooling systems, reduced inventory of heat transfer fluids, reduced friction coefficients, and improved wear resistance. Thermal conductivity of nanofluids is found to be an attracting characteristic for many applications. Those benefits make nanofluids promising for applications like coolants in various heat exchanging equipments.

Table 1.1: Thermal conductivities of various solids and liquids

Solids/liquids	Material	Thermal conductivity (W/m K)
Metallic solids	Silver (Ag)	429
	Copper (Cu)	401
	Aluminum (Al)	237
	Gold(Au)	317
Nonmetallic solids	Diamond	3300
	Carbon nanotubes (CNT)	3000
	Silicon (Si)	148
	Alumina (Al_2O_3)	46
	Titania (TiO_2)	8.4
	Copper oxide (CuO)	69
	Silica (SiO_2)	1.2
	Iron oxide (Fe_3O_4)	80.4
Liquids	Water	0.613
	Ethyl glycol	0.253
	Engine oil	0.145
	Kerosene	0.15

Convective heat transfer in plain tube

The heat transfer characteristic of water flowing through a duct plays a significant role in many scientific and industrial applications. In order to enhance the heat transfer rate, one needs to modify the flow geometry or increase the flow rate through the duct. However, in both the cases higher pumping power is needed to achieve the higher heat transfer rate. In view of this, various researchers utilized nanofluids (water based)

Table 1.2: Summary of various experimental studies that report the thermal conductivity of nanofluids [18]

	Particle	Base fluid	Average particle size	Volume fraction	Thermal conductivity enhancement
Metallic nanofluids	Cu	Ethylene glycol	10 nm	0.3%	40%
	Cu	Water	100 nm	7.5%	78%
	Fe	Ethylene glycol	10 nm	0.55%	18%
	Au	Water	10-20 nm	0.026%	21%
	Ag	Water	60-80 nm	0.001%	17%
Non-metallic nanofluids	Al_2O_3	Water	13 nm	4.3%	30%
	Al_2O_3	Water	33 nm	4.3%	15%
	Al_2O_3	Water	68 nm	5%	21%
	CuO	Water	36 nm	3.4%	12%
	CuO	Water	50 nm	0.4%	17%
	SiC	Water	26 nm	4.2%	16%
	TiO_2	Water	15 nm	5%	30%
	MWCNT	Synthetic oil	25nm-diameter 50µm-length	1%	150%
	MWCNT	Decene/ethylene glycol/ water	15nm-diameter 30µm-length	1%	20%/13%/7%
	MWCNT	Water	100nm-diameter 70µm-length	0.6%	38%

to enhance the heat transfer rate. It has been observed that with the use of nanofluids, the heat transfer rate increases while reducing the pumping power costs compared to conventional single phase fluids (water). The researchers have used various nanofluids with the varied range of flow rate and nanoparticle concentration. Some of the important studies are elaborated below.

Several researchers [19- 43] conducted experimental studies to evaluate the heat transfer characteristics of nanofluids in various pipes. Wen and Ding [19] performed their experiments by using Al_2O_3/water nanofluids in the entrance region under laminar flow conditions. The convective heat transfer was found to increase with the Reynolds number, and particle concentration. In the entrance region, the improvement in heat transfer was significant while it decreases in the axial direction. Heyhat et al. [23] reported the heat transfer and friction factor characteristics of Al_2O_3/water nanofluids inside a tube for constant wall temperature conditions. The authors conducted tests for the varied range of volume concentration 0.1–2 vol.% and reported that the heat transfer coefficient increases approximately by 32% in the fully developed region for 2 % particle volume concentration. CNTs have attracted many researchers due to their higher thermal conductivity and higher aspect ratio for preparing nanofluids. It is observed that nanofluids with CNT nanoparticles can be kept stable for months if the nanoparticles are functionalized or dispersed with a surfactant. Ding et al. [24] showed the heat transfer behavior of aqueous suspensions flowing through a horizontal tube. The flow condition, CNT concentration and the pH level have the significant impact on heat transfer behavior. The effect of pH on the heat transfer was found to be very minimal. The heat transfer augmentation was found to depend on the axial distance from the inlet of the test section. The heat transfer enhancement increases, attain the highest value and decreases in the axial distance. Wang et al. [29] reported the heat transfer and pressure drop of nanofluids containing carbon nanotubes (CNT) in a horizontal circular

Table 1.3: Summary of forced convection experimental studies on nanofluids

Author	Nanofluid	Particle Size(nm)	Flow regime	Heat transfer enhancement
Wen and Ding [19]	Al_2O_3/water	26-56	Laminar (600-2200)	47% for h at 1.6 vol.% and Re=1600
Anoop et al. [20]	Al_2O_3/water	45	Laminar (500-2500)	31% for h at 4 wt.% and Re=1550
Hwang et al. [21]	Al_2O_3/water	30	Laminar (500-800)	8% for h at 0.3 vol.% and Re=700
Esmaeilzadeh et al. [22]	Al_2O_3/water	15	Laminar (400-2000)	24.5% for h at 1 vol.% and Re=1300
Heyhat et al. [23]	Al_2O_3/water	40	Laminar (300-2100)	32% for h at 2 vol.% and Re=2100
Ding et al. [24]	MWCNT/Water	d=10, l=100 μm	Laminar (800-1200)	375% for h at 0.5wt.% and Re=800
Garg et al. [25]	MWCNT/Water	d=10-20, l=0.5-40μm	Laminar (600-1200)	32% for h at 1 wt.% and Re=600
Amrollahi et al. [26]	FWCNT/Water	150-200	Laminar and Turbulent (1500-5000)	12% for h at 0.12 wt.% and Re=1592 40% for h at 0.25 wt.% and Re=1592
Liu and Liao [27]	MWCNT/Water	d=10-20, l=1-2 μm	Turbulent (10^4 to $50x10^4$)	70% for h at 2 wt.%
Abreu et al. [28]	MWCNT/Water	d=50-80, l=10-20μm	Laminar (1650-2060)	47% for h at 0.5 vol.% and Re=2060
Wang et al. [29]	MWCNT/Water	d=30, l=30 μm	Laminar (20-250)	190% for h at 0.24 vol.% and Re =120
Arani and Amani [30]	TiO_2/water	30	Turbulent (8000-51000)	72% for h at 0.02 vol.% and Re=8000
Kayhani et al. [31]	TiO_2/water	15	Turbulent (6000-16000)	8% for h at 2 vol.% and Re=11800

Table 1.3: Summary of forced convection experimental studies on nanofluids (Cont.)

Author	Nanofluid	Particle Size(nm)	Flow regime	Heat transfer enhancement
Sajadi and Kazemi [32]	TiO_2/water	30	Turbulent(5000-30000)	22% for h at 0.25 vol.% and Re=5000
He at al. [33]	TiO_2/water	95	Laminar and Turbulent(800-6500)	40% for h at 1.1 vol.% and Re=5900
Fotukian and Esfahany [34]	CuO/water	30-50	Turbulent(6000-31000)	42% for h at 0.15 vol.% and Re= 24450
Selvakumar and Suresh [35]	CuO/water	27-37	Turbulent (2985–9360)	29.63 % for h at 0.2 vol.% and Re= 9360
Heris et al. [36]	CuO/water	10	Laminar (660- 2050)	27% for Nu at 1.5 vol.%
Xuan and Li [37]	Cu/water	<100	Turbulent (10000-25000)	39% for h at 2 vol.%
Azmi et al. [38]	SiO_2/water	22	Turbulent (5000–27000)	38.5% for h at 3 vol.%
Ferrouillat et al. [39]	SiO_2/water	22	Laminar and Turbulent (200 < Re < 10,000)	50% for h at 18.93 vol.% and Re > 1000
Julia et al. [40]	SiO_2/water	12	Turbulent ($3x10^3$-10^5)	300% for h at 5 vol.% and Re =$3x10^4$
Bontemps et al. [41]	SiO_2/water	22	Laminar and Turbulent (100<Re<10000)	100% for h at 19 vol.%
Yu et al. [42]	SiC/water	170	Turbulent (3300- 13000)	50-60 % for h at 3.7 vol.%
SyamSundar et al. [43]	Fe_3O_4/water	36	3000 < Re < 22,000	30.96% for h at 0.6 vol.% and Re =22000

tube. A significant enhancement in the average convective heat transfer was observed with nanofluids compared to the distilled water. At Reynolds number of 120, the enhancement in heat transfer for nanofluids was found to be 70% and 190% for 0.05% and 0.24% particle volume concentration, respectively. The authors observed that the enhancement in the thermal conductivity was less than 10%. It was argued that the significant enhancement in heat transfer cannot be solely attributed to the enhanced thermal conductivity. Arani and Amani [30] investigated the effect of nanoparticle volume fraction on the convection heat transfer characteristics and pressure drop of TiO_2/water nanofluids. The nanoparticle volume fraction is varied between 0.002 and 0.02 and the Reynolds number is varied within 8000 and 51,000 during the experimental investigation through a horizontal double tube counter flow heat exchanger. The heat transfer performance was found to be higher compared to the distilled water results. The heat transfer and pressure characteristics of TiO_2/water nanofluids for both laminar and turbulent conditions were studied experimentally by He et al. [33]. The results exhibited that the convective heat transfer coefficient increases with the increase in the Reynolds number for both laminar and turbulent flows. The enhancement in heat transfer in the laminar flow is found to be much smaller compared to the turbulent flow regime. For 1.1 vol. % of TiO_2 nanofluids, the maximum enhancement in the heat transfer was found to be 12% and 40% for Reynolds number of 1500 and 5900, respectively. The turbulent convective heat transfer and pressure drop characteristics of CuO/water nanofluid flowing through a circular tube were investigated experimentally by Fotukian and Esfahany [34]. The authors reported that the addition of small amounts of CuO nanoparticles with the basefluid significantly increases the heat transfer performance. The authors obtained 25% increase in heat transfer coefficient with 20% penalty in pressure drop. The forced convective heat transfer and friction factor characteristics of nanofluids with SiO_2 nanoparticle in the turbulent flow regime was studied by Azmi et al. [38]. For 3.0% nanoparticle volume concentration, the Nusselt number and friction factor was found to be 32.7% and 17.1% higher compared to pure water results. Bontemps et al. [41] reported the convective heat transfer and pressure drop characteristics of SiO_2/water nanofluids under constant heat flux boundary condition. The authors reported that the heat transfer enhancement is significant in the turbulent flow region compared to the laminar flow region. The heat transfer enhancements of nanofluids was found to be 30% and 100% higher compared to pure water results with nanoparticle volume concentration of 2.3% and 19.0%, respectively. The convective heat transfer and friction factor characteristics of Fe_3O_4 nanofluid through a circular tube is evaluated experimentally by Syam Sundar et al. [43]. The experiments were carried out for Reynolds number varying within 3000-22000 and the nanoparticle concentration is varied between 0-0.6%. The heat transfer coefficient and friction factor of nanofluids were found to be 30.96% and 10.01% higher compared to pure water results for similar operating conditions. The forced convection heat transfer and friction factor characteristics of various nanofluids through ducts with constant heat flux boundary conditions are summarized in Table 1.3.

Convective heat transfer in tube with inserts

The heat transfer enhancement techniques are broadly divided into two categories such as: active method which needs an external power source and the passive method which does not need any external power source. The passive technique method mainly involves the use of twisted tapes, wire coil inserts and helical screw tapes in the ducts leading to the increase in the heat transfer rate [44-45]. The passive method uses inserts to generate the swirl in the bulk fluids and disturb the thermo-hydrodynamic boundary layer, it leads to increase in effective surface area, residence time and consequently heat transfer coefficient in existing system. In may be noted that with the combination of inserts with nanofluids, the heat transfer rate can be enhanced due to enhanced thermal conductivity of nanofluids and improvement in fluid mixing.

Several studies have been carried out to investigate the heat transfer and friction factor characteristics of helical screw tapes and twisted tapes in pipe flow using nanofluids [11, 46-53]. The heat transfer coefficient and friction factor for transition flow in a tube with twisted tape inserts and Al_2O_3/water nanofluid has been investigated experimentally by Sharma et al. [46]. The heat transfer coefficient of nanofluid flowing through a tube with 0.1% volume concentration was found to be 23.7% higher compared to water results at 9000 Reynolds number. For 0.1 % volume concentration of nanofluid, the maximum friction factor with twisted tape was found to be 1.21 times of the water results for a plain tube. The heat transfer and friction factor characteristics of Al_2O_3/water nanofluid in a circular tube with twisted tapes of various twist ratios have been reported by Syam Sundar et al. [47]. The authors carried out experiments for varied range of volume concentration (0.02%, 0.1% and 0.5%) and Reynolds number (10,000-22000). For 0.5% volume concentration of Al_2O_3/water nanofluid, the enhancement in heat transfer coefficient and friction factor was found to be 33.51% and 1.096 times, higher compared to water results. In addition, the authors [48] studied the turbulent convective heat transfer and friction factor behavior of Al_2O_3/nanofluid in a circular tube with longitudinal strip inserts. Tests were carried out for varied range of volume concentration (0-0.5%), Reynolds number (22000>Re>3000) and aspect ratio (0-18). The heat transfer coefficient was found to increase with nanofluid volume concentration and decrease with the aspect ratio. The heat transfer, friction factor and thermal performance characteristics of CuO/water nanofluid in a circular tube fitted with modified twisted tape with alternate axis were studied experimentally by Wongcharee and Eiamsaard [49]. For 0.7% volume concentration of CuO/water and Reynolds number of 1990, the twisted tape with alternate axis exhibits the maximum increase in thermal

Table 1.4: Summary of forced convection experimental studies on nanofluids with inserts

Author	Nanofluid	Type of insert	Flow regime	Remarks
Wongcharee and Eiamsaard [49]	CuO/water	twisted tape with alternate axis	830 -1990	The increase in Nusselt number found to be 12.8 and 7.2 times using CuO/water nanofluid in a tube with twisted tape and alternative twisted tape compared to pure water results.
Chandrasekar et al. [50, 51]	Al_2O_3/water	wire coil inserts	600 – 2275 and 2500 to 5000	The maximum enhancement in heat transfer are 23.69% and 20% at Re=2275 and Re=5000 with pitch ratio of 3, compared to distilled water.
SyamSundar et al. [11]	Fe_3O_4/water	twisted tape	3000 < Re < 22000	Heat transfer and friction factor enhancement of 0.6% volume concentration of Fe_3O_4 nanofluid in a plain tube with twisted tape insert of twist ratio H/D = 5 is 51.88% and 1.231 times compared to water flowing in a plain tube at Re=22,000
Kahani et al. [55]	Al_2O_3/water and TiO_2/water	helical coil inserts	500–4500	The maximum thermal performance factor is found to be 3.82 for Al_2O_3/water nanofluid (φ = 1%) with insert at Re= 1865. Al_2O_3/water nanofluids show more heat transfer enhancement compared with TiO_2/water.
Saeedinia et al. [56]	CuO/Base oil	Wire coil	10-120	In average, 45% increase in heat transfer coefficient and 63% penalty in pressure drop is observed at Re=90

performance factor. The heat transfer and friction factor characteristics of wire coil inserts with various pitch ratios in Al_2O_3/water nanofluid through a circular tube was experimentally investigated by Chandrasekar et al. [50-51]. The use of nanofluids increases the heat transfer rate with negligible increase in friction factor in the plain tube and the tube fitted with wire coil inserts. The comparative study on thermal performance of helical screw tape inserts with various twist ratios (1.78, 2.44 and 3) with different nanofluids such as: Al_2O_3/water and CuO/water was reported by Suresh et al. [52-53]. The thermal performance factor of helical screw tape inserts using CuO/water nanofluid was found to be higher compared to the values obtained by using Al_2O_3/water. The heat transfer and friction factor characteristics of Fe_3O_4 /water nanofluid through a uniformly heated horizontal circular tube with and without twisted tape inserts for turbulent flow condition were studied experimentally by Syam Sundar et al. [11]. For 0.6% volume concentration of Fe_3O_4/water nanofluid, the increase in the heat transfer and friction factor of twisted tape insert was found to be 51.88% and 1.231 times higher compared to water results. The heat transfer and friction factor characteristics of water/propylene glycol based CuO nanofluids through a horizontal circular tube fitted with and without helical inserts for transition flow regime was reported by Naik et al. [54]. Tests were carried out for the varied range of twist ratios (0-9) and Reynolds number (2500-10,000). For 0.5% volume concentration of CuO nanofluids, the Nusselt number was found to be 28% higher compared to the plain tube.

Automobile radiator

In the heat exchange the fluid flows through a pipe or system of pipes, where heat is transferred from one fluid to another. Heat exchangers are very common in everyday life and can be found in various applications including conditioners and automobile radiators. Hot fluid flows through a system of pipes and cold fluid flows over the pipes resulting in the exchange of heat from the hot fluid to the cool fluid. The automobile engine utilizes a heat exchanger device, termed as a radiator, in order to remove the heat from the cooling jacket of the engine. The radiator is considered as an important component of the cooling system of the engine and shown in Fig. 1.4.

In general, the mixture of ethylene glycol and water is used as a coolant in the radiator of automobile engines. These fluids posses poor heat transfer performance compared to water because of lower thermal conductivity. Choi [57] reported the limitations of the existing cooling system in the heavy vehicle engines and are as below:

- Liquid-side: convectional fluids and oils have inherently poor heat transfer properties.
- Air-side: suitable fin designs have been already been adopted in order to improve the heat removal rate.

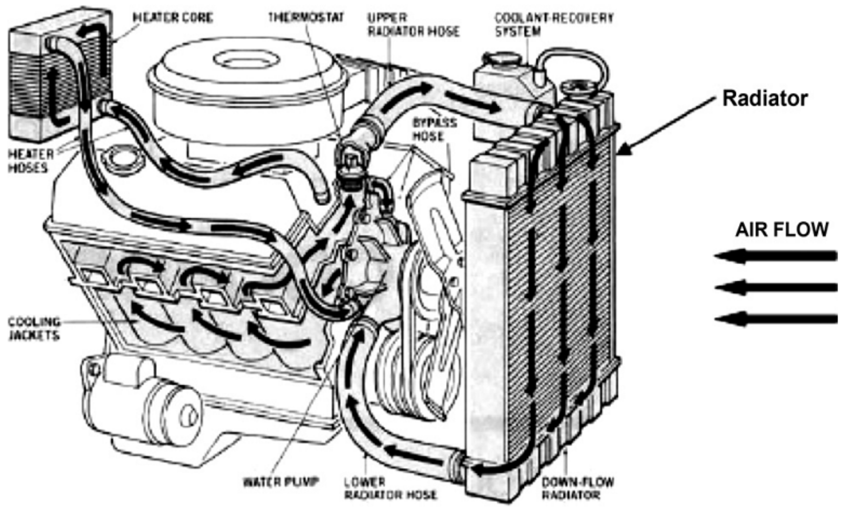

Figure 1.4: Photographic view of radiator of an engine [4]

It is observed that conventional fluids are unable to meet the increasing demand in cooling in high energy applications including automobile engines. In view of this, the new technique is needed to improve the existing cooling performance of heavy vehicle engines. It may be noted that, the use of nanofluid in an automobile radiator can enhance the heat removal rate leading to the reduction in size the cooling system. In addition, the smaller size could reduce the drag leading to lesser fuel 0.4% volume concentration, nanofluid exhibited the increase in the overall consumption. Several researchers utilized nanofluids in the automobile radiator and elaborated below.

The application of Al_2O_3/water nanofluids has been used as a jacket coolant in diesel electric generator by Kulkarni et al. [58]. The authors observed a reduction in cogeneration efficiency. This may be due to the decrease in the specific heat that influences the waste heat recovery from the engine. On the contrary, the efficiency of waste heat recovery heat exchanger with nanofluid is higher because of its superior convective heat transfer coefficient. The laminar flow and heat transfer behavior of two different nanofluids, namely, Al_2O_3 and CuO in the ethylene glycol/water mixture through the flat tubes of an automobile radiator was numerically studied by Vajjha et al. [59]. The heat transfer enhancement was significant with the use of nanofluids. Peyghambarzadeh et al. [60] reported the tube side heat transfer coefficient of a car radiator by using Al_2O_3/water nanofluids. The heat transfer coefficient of nanofluid was evaluated for various volume concentrations (0.1-1 %), mass flow rate (2-5 lit/min) and inlet temperature (37-49^{0}C). The enhancement in heat transfer was found to be of 45% higher compared to the pure water under highly turbulent flow condition. The use of ethylene glycol based copper nanofluids in an automobile cooling system was studied by Leong et al. [61]. With the addition of 2% copper particles in a base fluid, the enhancement in heat transfer was found to be 3.8%. Peyghambarzadeh et al. [62] studied the addition of Al_2O_3 nanoparticle in various fluids such as: pure water, ethylene glycol and their binary mixtures. The authors observed that nanofluids improve the cooling performance of the car radiator. The enhancement in heat transfer was found to be 40% higher compared to the base fluid. The overall heat transfer coefficient of CuO/water nanofluids in a car radiator was investigated experimentally by

Naraki et al. [63]. The overall heat transfer coefficient was decreased with the increase in nanofluid inlet temperature from 50^0C to 80^0C. For the 0.4% volume concentration, nanofluid exhibited the increase in the overall heat transfer coefficient up to 8% compared to water.

Nanofluid assisted heat pipes for solar collectors

The operation of a heat pipe [64] is easily understood by using a cylindrical geometry, as shown in Fig.1.5 (a). The components of a heat pipe are a sealed container (pipe wall and end caps), a wick structure, and a small amount of working fluid. The length of a heat pipe is divided into three parts: the evaporator section, adiabatic (transport) section, and condenser section. Heat applied externally to the evaporator section is conducted through the pipe wall and wick structure, where it vaporizes the working fluid. The resulting vapor pressure drives the vapor through the adiabatic section to the condenser, where the vapor condenses, releasing its latent heat of vaporization to the provided heat sink. The capillary pressure created by the menisci in the wick pumps the condensed fluid back to the evaporator section. Therefore, the heat pipe can continuously transport the latent heat of vaporization from the evaporator to the condenser section. This process will continue as long as there is a sufficient capillary pressure to drive the condensate back to the evaporator.

In certain application, the heat pipes work under gravity with the condensing region above the evaporating region and the return flow of the condensate to the heating zone occurs because of the gravity force. This type of heat pipes are termed as gravity assisted heat pipes, wickless heat pipes or thermosyphon (Fig. 1.5 (b). Therefore, the wickless heat pipe has been used in wide variety of industrial application, namely boilers, air-conditioning system, heat exchangers and solar water heating system [64]. The wickless heat pipes are usually integrated with a flat absorber plate of the solar heating system to enhance the thermal performance. The operation of the thermosyphon is sensitive to the fill volume of working

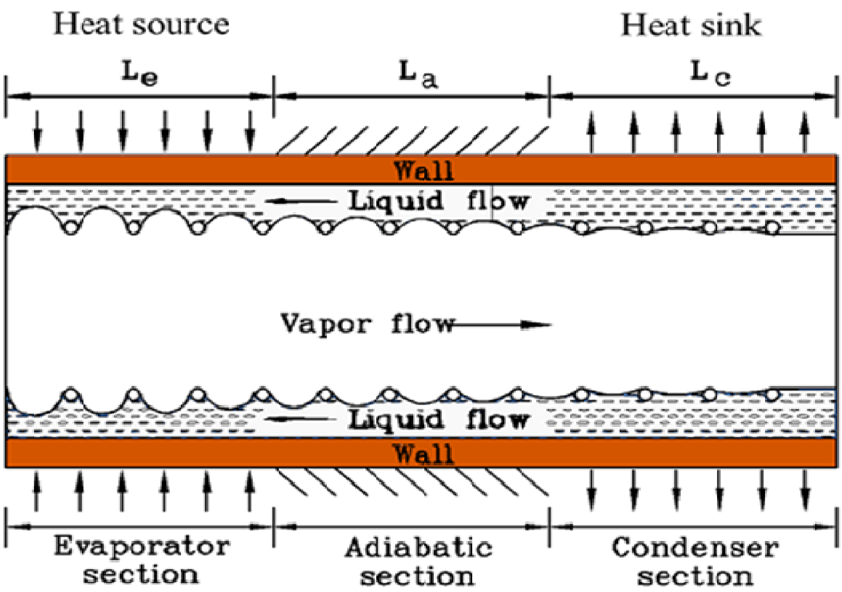

Figure 1.5 (a): Axial variation of the liquid–vapor interface [64]

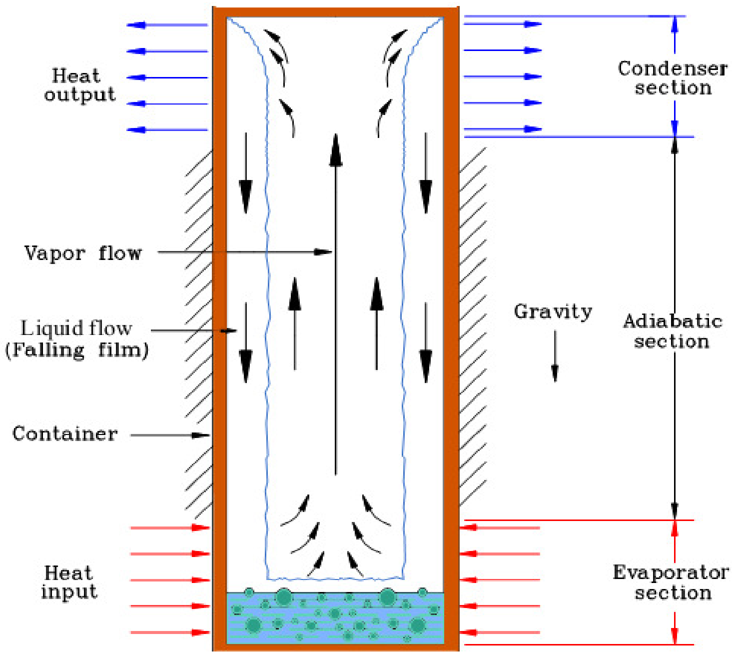

Figure 1.5 (b): Gravity-assisted wickless heat pipe (two-phase closed thermosyphon) [64]

fluid. For thermosyphons without wicks, it has been shown experimentally that the maximum rate of heat transfer increases with the amount of the working fluid up to a certain value. A wick structure is sometimes included in the design of thermosyphons to postpone flooding and improve the contact between the wall and the liquid.

Because of the enhanced heat transfer characteristics of nanofluid, several researchers applied nanofluid in tubular thermosyphon to improve the heat transfer performance. Liu et al. [65] carried out experiments to study the effect of nanoparticle parameters in a closed two-phase thermosyphon using CuO/water nanofluids as working fluid. For the optimal nanoparticle concentration (1%), the maximum enhancement in heat transfer coefficient and critical heat flux was found to be 160% and120%, respectively. The thermal performance of closed thermosyphon has been studied by Liu et al. [66] using CNT/water suspensions as working fluid. The results exhibited the maximum enhancement in heat transfer rate for optimal nanoparticle mass concentration of 2%. Gabriela et al. [67] performed experiments with addition of 5.3% (by volume) iron oxide nanoparticle with water. The thermal performance of Fe_3O_4/DI-water was found to be better compared to DI water. Shanbedi et al. [68] reported the effect of addition of multiwalled carbon nanotubes (MWCNTs) in deionized water (DI water) to study the heat-transfer performance of a two-phase closed thermosyphon. The authors conducted experiments by using CNT/water nanofluid with concentration of 1 % by weight and the maximum thermal efficiency was found to be 93% for the given input power of 90 W. Noie et al. [69] investigated the heat transfer performance of two-phase closed thermosyphon using Al_2O_3/water nanofluid. The enhancement in efficiency was found to be 14.7% by using Al_2O_3/water nanofluid when compared with water as the working fluid. Paramatthanuwat *et al.* [70] studied the heat transfer of Ag/water nanofluid in a thermosyphon. The effects of filling ratio (30%, 50%, 80%), the operating temperature (40°C, 50°C, 60°C), the ratio of length and diameter (5, 10, 20), and the diameter (7.5, 11.1, and 25.4 mm) on the heat transfer performance were investigated in detail. Results show that the heat transfer capacity can be enhanced up to 70% by adding Ag nanoparticles. In addition, experimental study has been carried out to study the thermal performance of open thermosyphon with CuO/water nanofluids in an indoor environment [71]. For mass concentration of 1.2%, CuO/water nanofluid exhibits a maximum enhancement in heat transfer rate compared to the operation with DI water.

Electronics cooling

The modern trend in electronic devices is to increase the level of integration by minimizing the device size (high-density packaging) and increasing the performance of the device (higher frequency). This results in an increase in both power dissipation and power density on the device increasing the local heat flux which needs to be dissipated. Heat pipes are the one of the available technologies to deal with the high-density electronic cooling due to their high thermal conductivity, reliability and lower weight. Heat pipes are two-phase heat transfer devices with high effective thermal conductivity [72]. During the last decade, application of heat pipes to the electronic component has been rapidly growing.

Various researchers reported the application of heat pipes and thermosyphons for electronics cooling. Kim et al. [73] observed that the acoustic noise of the fan can be reduced by using heat pipes during cooling of CPU. Chang et al. [74] experimentally investigated the thermal performance of the heat pipe cooling system for electronics equipment. It is observed that both the evaporation resistance and the condensation resistance grow with the increase in the heating power and decrease in the filling ratio. Flooding phenomenon is found during the flow of vapor and liquid in the opposite direction in a closed two-phase system. This phenomenon is observed at the fill ratio of 20% with heating power higher than 120 W. The heat sink with embedded L-shaped heat pipes and plate fins for electronic cooling application was studied experimentally by

Wang [75]. Results exhibited that the heat sink with six heat pipes carry 160 W and attained a minimum thermal resistance of 0.22^{0}C/W. Computational fluid dynamics simulations were used to obtain the proper design conditions for the CPU cooling heat sinks. The simulation results were validated with the test data [76]. With the increasing demand for the higher power and smaller size, the cooling of the electronic component plays a crucial role for its performance. In view of this, it is essential to improve the heat removal capacity of the heat pipes. In such a case, one can select a suitable working fluid in the heat pipe that can transfer maximum heat energy. The researchers applied nanofluid in heat pipe assembled electronics cooling module to improve the heat transfer performance. Nandy et al. [77] reported the use of nanofluid in heat pipe liquid-block for the thermoelectric cooling of electronic equipment. It is observed that the heat pipe liquid-block and thermoelectric cooler improves the thermal performance by using nanofluid. Yousefi et al. [78] investigated the performance of CPU coolers by using Al_2O_3–water nanofluid charged heat pipe. Results indicate that the thermal resistance decreases by 15% and 22%.For the heat load of 10 W and 25 W, respectively. Jahani et al. [79] reported the thermal performance of micro pulsating heat pipe (MPHP). The experimental results show that the optimum charging ratio for water and nanofluid is 40% and 60%, respectively. The nanofluid charged MPHPs have a lower thermal resistance compared to the water charged micro pulsating heat pipe.

Boiling heat transfer

The heat transfer phenomena during boiling plays an important role in various industrial processes and applications such as: refrigeration, power generation, heat exchangers, cooling of high-power electronics components and cooling of nuclear reactors. Therefore, there is need to enhance the heat transfer rate during boiling. In view of this various researchers have used nanofluids as the working fluid to enhance the heat transfer rates during boiling in various thermal devices.

Kim et al. [80] reported the pool boiling heat transfer characteristics of various nanofluids such as: Al_2O_3/water, ZrO_2/water and SiO_2/water. It was observed that nanoparticles deposit on the heater surface after the boiling process and an irregular porous structure was formed at the surface. The authors further studied the deposition of nanoparticles on the surface. This deposition was found to increase the wettability. It was argued that the enhancement in the wettability is due to two reasons such as: increase in adhesion tension and the increase in the surface roughness [80]. Tu et al. [81] reported the heat transfer characteristics of Al_2O_3/water nanofluids on a “nanoscopically smooth” vapor-deposited heating surface. The authors reported an enhancement in the heat transfer rate and four-time increase in the nucleation site. The boiling heat transfer characteristics of Al_2O_3/water nanofluids on a stainless steel disc of micron-sized surface roughness were studied by Wen and Ding [82]. In another study, the authors [82] reported 50% enhancement in the heat transfer by using TiO_2/water nanofluids. The authors did not observe much particle deposition. Truong [83] reported the higher enhancement in the heat transfer by using various nanofluids such as: SiO_2/water and Al_2O_3/water during pool boiling studies. Ahn et al. [84] reported the heat transfer characteristics of nanostructured surfaces with refrigerants. The surfaces were prepared by using the chemical vapor deposition of multiwalled carbon nanotubes. The heat transfer enhancement was found to be19-33 % during the nucleate boiling. Bang and Chang [85] reported the enhancement in critical heat flux (CHF) of Al_2O_3/water nanofluids on stainless steel surface. The authors observed the particle deposition on the surface that increases the surface wettability. In their experimental study, Das et al. [86] reported the deposition of nanoparticle on the surface after boiling of Al_2O_3/water nanofluids. The authors reported the increase in the wall superheat and decrease in the boiling heat transfer during their experimental investigation. Kwark et al. [87] reported the decrease in the boiling heat transfer coefficient with the increase in the nanoparticle concentration. This may be due to the thickening of the boundary layer resulting in increase in the thermal resistance.

Figure 1.6 summarizes pictorially the main factors affecting nanofluid boiling enhancement. It has been shown by researchers that there are several factors that individually or in combination can play an important role in the nanofluid boiling enhancement. Most of these studies report the enhancement in the heat transfer varies between 15–68% [88] during the experimental investigation. The studies used several materials and geometries for nanoparticles and heaters. Most of the studies reported deposition of nanoparticles on the heater surface after boiling. In addition, the deterioration in boiling heat transfer is observed by various authors. This may be due to the fouling of the heater surface due to boiling.

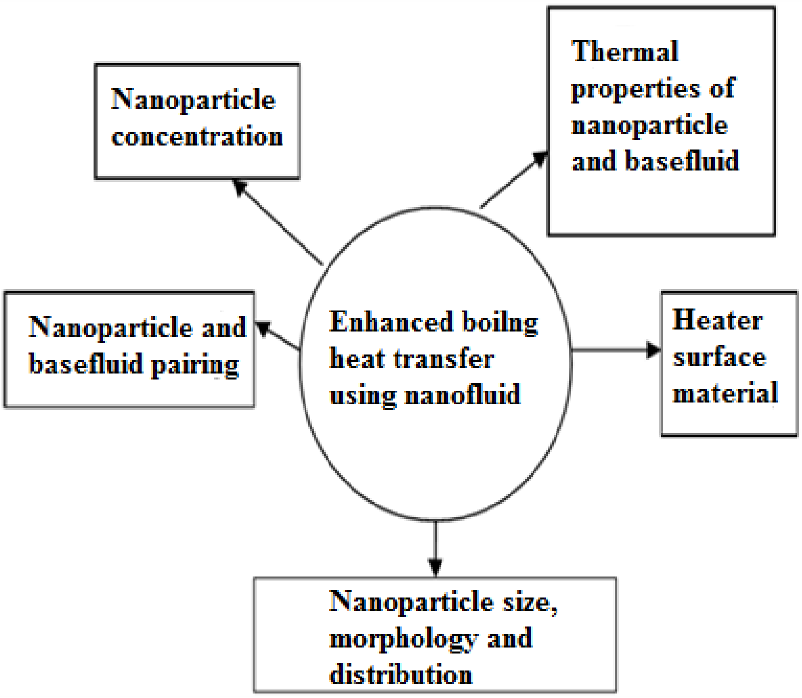

Figure 1.6: Factors affecting on boiling heat transfer enhancement using nanofluid

1.5.2 Theoretical modeling

Theoretical studies have been carried out for nanofluids. These studies mainly propose theoretical models to evaluate the thermophysical properties such as: thermal conductivity and viscosity of nanofluids. Some of important studies are discussed below.

Thermal conductivity

The thermal conductivity of nanofluids is considered to be responsible for the enhancement of heat transfer performance of nanofluids. In view of this, numerous theoretical studies have been carried out by various researchers to predict the effective thermal conductivity of solid particles suspended in base fluids. Some of the important studies are elaborated below.

Maxwell [2] was the first to develop a theoretical model to determine the effective thermal conductivity of liquid–solid suspensions. This model is applicable to statistically homogeneous and low volume fraction liquid–solid suspensions with randomly dispersed, uniformly sized and non-interacting spherical particles. The Maxwell equation is expressed as:

$$k_{eff} = \frac{k_p + 2k_{bf} + 2(k_p - k_{bf})\varphi}{k_p + 2k_{bf} + 2(k_p - k_{bf})\varphi} k_{bf} \qquad (1.1)$$

Where, k_p and k_b denote the thermal conductivity of the particle and the base fluid, respectively. While, φ represents the particle volume fraction in the suspension. Later on, Hamilton and Crosser [89] extended the Maxwell's model by introducing a shape factor to account for the effect of the shape of particles. Bruggeman [90] proposed a model to analyze the interactions among randomly distributed particles. This model can be used to evaluate the thermal conductivities of suspensions containing spherical particles and applicable for the varied range of nanoparticle concentration. It is observed that for low solid concentrations, the Bruggeman model [90] exhibits good agreement with the Maxwell model. While, at higher concentration, the Maxwell model [2] fails to provide a good agreement with the test data. However, the Bruggeman model was found to agree well with the test data [90]. Yu and Choi [91]

Table 1.5: Various models to evaluate the effective thermal conductivity of mixtures

Investigator	Equation	Year
Maxwell [2]	$k_{eff}=\frac{k_p+2k_{bf}+2(k_p-k_{bf})\varphi}{k_p+2k_{bf}+2(k_p-k_{bf})\varphi}k_{bf}$	(1873)
Hamilton and Crosser [89]	$k_{eff}=\frac{k_p+2k_{bf}+2(k_p-k_{bf})\varphi}{k_p+2k_{bf}+2(k_p-k_{bf})\varphi}k_{bf}$ where 'n' is the empirical shape factor given by $3/\psi$ and ψ is the particle sphericity, For spherical particle the value of n is 3. For particles of other shapes, the factor n can be allowed to vary from 0.5 to 6.0.	(1962)
Bruggeman [90]	$k_{eff}=\frac{1}{4}[(3\varphi-1)k_p+(2-3\varphi)k_{bf}+{k_{bf}}/{4\sqrt{\Delta}}$ $\Delta=\left[(3\varphi-1)^2\left(\frac{k_p}{k_{bf}}\right)^2+(2-3\varphi)^2+2(2+9\varphi+9\varphi^2\left(\frac{k_p}{k_{bf}}\right)\right]$	
Yu and Choi [91]	$k_{eff}=\frac{k_{pe}+2k_{bf}+2(k_{pe}-k_{bf})(1-\beta)^3\varphi}{k_{pe}+2k_{bf}+2(k_{pe}-k_{bf})(1+\beta)^3\varphi}k_{bf}$ where, $k_{pe}=\frac{\left[2(1-\gamma)+(1+\beta)^3(1+2\gamma)\gamma\right]}{-(1-\gamma)+(1+\beta)^3(1+2\gamma)}k_p$, $\gamma=k_l/k_p$ is the ratio of nanolayer thermal conductivity to particle thermal conductivity and $\beta=h/r$ is the ratio of the nanolayer thickness to the original particle radius.	(2003)
Koo and Kleinstreuer [92-93]	$k_{eff}=\frac{k_p+2k_{bf}+2(k_p-k_{bf})\varphi}{k_p+2k_{bf}+2(k_p-k_{bf})\varphi}k_p+5\times10^4\beta\varphi\rho_s c_s\sqrt{\frac{k_B T}{\rho_s D}}f(T,\varphi)$	(2005)
Prasher et al. [94]	$k_{eff}=\left(1+ARe^mPr^{0.333}\varphi\right)\left[\frac{k_p+2k_{bf}+2(k_p-k_{bf})\varphi}{k_p+2k_{bf}+2(k_p-k_{bf})\varphi}\right]$ where, $h=k_{bf}/a(1+ARe^mPr^{0.333}\varphi)$ and A and m are constants, $Re=\frac{1}{v}\sqrt{\frac{18k_{bf}T}{\pi\rho_p d_p}}$	(2006)

reported a theoretical model that incorporates the thermal conductivities of intermediate nanolayers in the model. Koo and Kleinstreuer [92-93] proposed a model that considers the effects of particle size, particle volume fraction, properties of the base fluid, temperature of nanofluids and Brownian motion of nanoparticles. In their study, Prasher et al. [94] reported that convection induced by Brownian motion of the nanoparticles is responsible for the enhancement of the effective thermal conductivity of nanofluids. The authors modified the Maxwell model by incorporating the effect of the convection of the liquid near the particles due to Brownian movement.

It is observed that the proposed theoretical models include various mechanisms in the model. This includes the effect of nanoparticle-matrix interfacial layer, nanoparticle Brownian motion and clustering of nanoparticles. In general, these models depend on the exact value of a suitable empirical parameter to evaluate the value of thermal conductivity. These parameters need to be obtained before they can be used to predict the thermal conductivity of a nanofluid. This requirement limits the use of these correlations. In addition, the enhancement in the effective thermal conductivity is found to depend on two or more mechanisms. Therefore, further research is needed to develop suitable models that can successfully correlate the test data.

Viscosity

Viscosity plays an important role during the analysis of the thermohydrualic behavior of nanofluids. In addition, in the case of flow through ducts, the pressure drop and the pumping power requirements depends on the viscosity of the fluids. It is observed that although the nanofluids increase the heat transfer performance, these fluids exhibit an enhancement in the viscosity compared to the base fluid. In view of this, various theoretical models have been proposed to evaluate the viscosity of nanofluids. The studies show that the viscosity of the nanofluid depends on the particle shape, particle size, volume fraction and temperature of the nanofluids. Some of the important studies on this are elaborated below.

Einstein [95] was the first to propose a model to evaluate the effective viscosity of a suspension involving spherical solids. Einstein [95] evaluated the viscosity of a viscous fluid containing a dilute suspension of small spherical particles. It was assumed that the disturbance of the flow pattern of the base fluid caused by a given particle does not overlap with the disturbance of the flow caused by the presence of a second suspended particle. The following equation is proposed by Einstein.

$$\mu_{eff} = (1+2.5\varphi_p)\mu_{bf} \tag{1.2}$$

The model [95] does not consider the structure, particle-particle interaction within the solution and higher particle concentrations. In view of this, efforts have been made to extend the Einstein model in three major areas. The first theory extends the Einstein's viscosity equation to higher particle volume concentrations by incorporating some of the particle-particle interactions. The theoretical equation for the effective viscosity of the mixture is expressed as [96]:

$$\mu_{eff} = (1+c_1\varphi_p+c_2\varphi_p{}^2+c_3\varphi_p{}^3+...)\mu_{bf} \tag{1.3}$$

The second theory extends the Einstein's equation (1.3)which takes into account of the fact that the effective viscosity of a mixture becomes infinite at the maximum particle volume concentration. This theoretical equation usually has the term $\mu_{eff} = \left[1\text{-}(\varphi_p/\varphi_{p\,max})\right]^{\alpha}$ in the denominator and α denotes the thermal expansion coefficient. While, this term can be expressed in a form similar to Eq. 1.3.

Some of the frequently used theoretical models used to predict viscosity of mixture are summarized in Table 1.6. It is observed that the various models [95-97], frequently used for prediction of the effective viscosity of nanofluids, underestimate the viscosity of nanofluids. This may be due to the fact that these models consider only the particle volume

Table 1.6: Various models to evaluate the effective viscosity of mixtures

Investigator	Equation	Year
Einstein [95]	$\mu_{eff}=(1+2.5\varphi_p)\mu_{bf}$	(1906)
Brinkman [97]	$\mu_{eff}=\frac{1}{(1-\varphi_p)^{2.5}}\mu_{bf}$	(1952)
Batchelor [98]	$\mu_{eff}=(1+2.5\varphi_p+6.2\varphi_p^2)\mu_{bf}$	(1977)
Tseng and Lin [99]	$\mu_{eff}=13.47\exp(35.98\varphi_p)\mu_{bf}$	(2003)
Maïga et al. [100]	$\mu_{eff}=(1+7.3\varphi_p+123\varphi_p^2)\mu_{bf}$	(2004)
Maïga et al. [101]	$\mu_{eff}=(1-0.19\varphi_p+306\varphi_p^2)\mu_{bf}$	(2004)
Kulkarni et al. [102]	$\ln\mu_{eff}=-(2.8751+53.54\varphi_p+30107.12\varphi_p^2)+(1078.3+15857\varphi_p+20587\varphi_p^2)(1/T)$	(2006)

concentration. The nanoparticles usually form clusters in the suspension and experience surface adsorption. This leads to an increase in the hydrodynamic diameter and increase in the viscosity of the suspension. Test data for the effective viscosity of nanofluids are limited to certain nanofluids. In addition, the ranges of the parameters such as: the particle volume concentration and temperature are limited in the literature. The test data exhibits higher values of effective viscosity compared to values obtained from the theoretical models. In view of this attempt has been made to develop theoretical models for specific applications. This includes the studies involving Al_2O_3 in water [99], Al_2O_3 in ethylene glycol [100], TiO_2 in water [98] and CuO in water with incorporating the change in temperature [101]. However, it is noticed that these equations do not reduce to the Einstein equation at lower particle volume concentration and therefore, lack a sound physical basis.

1.6 The Scope of Present Investigation

In the past few decades a significant volume of work has been undertaken in the synthesis and applications of various nanofluids. An extensive review of selected studies pertaining to present investigation has been reported here. The literature discussed in this report includes the experimental studies to evaluate the thermal conductivity of various nanofluids, enhancement in convective heat transfer of nanofluids in plain tube and tube with inserts, thermal performance of nanofluid through automobile radiator, nanofluid charged heat pipes for solar water heating and electronics cooling. Also, various theoretical models to evaluate the thermal conductivity and viscosity of nanofluids have been discussed. However, there are certain issues that need further investigation are enlisted below.

1. The synthesis of CNT/water nanofluid using functionalization method and its applications in thermal devices has not been reported extensively.
2. The heat transfer and friction factor characteristic of helical screw tape inserts with CNT/water nanofluids through tubes has not been reported in the literature.
3. The comparative study of heat transfer characteristic of CNT/water nanofluid with various nanofluids in different thermal devices has not been reported extensively in literature.
4. It is observed that conventional fluids are unable to meet the increasing demand in cooling in automobile engines. The

nanofluids can be used to improve the existing cooling performance of automobile radiator.

5. The nanofluids can enhance the thermal performance of heat pipe and thermosyphon. Therefore, emphasis should be given to improve the thermal performance of solar thermosyphon/heat pipe collector.
6. The use of nanofluid charged heat pipe with PCM as energy storage material and their hybrid effect on heat dissipation performance in electronics cooling is rarely reported in the literature.
7. Studies with hybrid nanofluid have not been reported extensively in the literature.

The present investigation have been planned to obviate some of the limitations mentioned above. This work primarily aims to synthesize stable CNT/water nanofluid, measure its thermal and rheological properties and application of CNT/water nanofluid to various thermal applications. An effort has been made to propose a design scheme for test facilities to examine the thermal performance of CNT/water nanofluid in forced convection with inserts, automobile radiator, thermosyphon solar collector and heat pipe cooling module. In addition, tests have been performed to evaluate the thermal performance of both CNT/water and Al_2O_3/water nanofluid in pipe flow and automobile radiators. An attempt has been made to study the thermal performance of the heat pipe using CNT with water as the working fluid. Various concentrations of nanoparticles are used to find the optimal concentration for the maximum performance. The effect of the tilt angle of the solar collector has been discussed in the study. The present study reports the nanofluid charged heat pipe module with PCM for electronics cooling. The study compares the thermal performance of heat pipe module with CNT/water nanofluid and water as the working fluid.

The Organization of the thesis is as follows:

Chapter 1: It introduces about nanofluid and the mechanism of heat flow in nanofluids. A brief review of thermal conductivity of nanofluid and its applications in various thermal devices has been reported. Finally, the objectives of the present investigation are enumerated.

Chapter 2: It presents the various synthesis methods for CNT/water and Al_2O_3/water nanofluids. In addition, various methods are adopted to inspect the stability of the nanofluid suspension. The experimental value of thermal conductivity and viscosity of nanofluids at the varied range of particle volume fraction and temperature are reported.

Chapter 3: This chapter presents the design, development and fabrication of test facility to evaluate the convective heat transfer and friction factor characteristics of various nanofluids through ducts with and without inserts. The results obtained from the experiments have been discussed.

Chapter 4: Tests have been performed to investigate the thermal performance of automobile radiator by using CNT/water nanofluid. The comparison of thermal performance CNT/water and Al_2O_3/water nanofluid in automobile radiator is presented here.

Chapter 5: The solar heat pipe collectors are fabricated and their thermal performance is investigated by using CNT/water nanofluid. Efforts have been made to investigate the thermal performance of CNT/water nanofluid charged heat pipe cooling module with PCM for electronics cooling applications.

Chapter 6: Conclusions obtained from the present investigations are reported here. In addition, the scope for further investigation is discussed.

Chapter 2

Synthesis and Characterization of Nanofluids

2.1 Introduction

Miniaturization of electronic devices and enhanced rate of data storage leads to serious problems in the thermal management system. In addition, several devices, namely, lasers, high power X-rays, scientific measurements, heat exchangers, transportation units, thermal and power plants need an efficient cooling system with greater cooling capacities and decreased sizes. Nanofluids are considered as a better medium to transfer heat in various devices. However, the preparation of nanofluids need special attention since the preparation methods affect various important thermo physical properties and stability of the dispersion. The stability of nanofluids is a key issue that influences the nanofluid properties and its heat transfer performance in thermal devices. It is observed that preparation of nanofluids is a challenging issue because of several reasons such as: stable and durable suspension, negligible and no chemical change of particles or fluid and maintain a stable colloidal state independent of time [103]. The selection of proper synthesis method is an important task to prepare nanofluids stable over a long time, with negligible agglomeration and without chemical change of the fluid properties [104].

In view of this, efforts have been made to prepare nanofluids by employing various methods. In this study, two different nanoparticles carbon nanotube (CNT) and Al_2O_3 have been received from the M/S Nanoshel LLC (USA). The morphology of individual nanoparticles was studied by using scanning electron microscopy (Model: SUPRA 55, Make: Carl Zeiss Microscopy, Germany). Here, CNT/water and Al_2O_3/water nanofluids have been prepared by adopting the two-step technique. Various techniques such as ultrasonic vibration, functionalized, and the addition of surfactant have been employed to prepare the nanofluids. After dispersing the nanoparticles in the water, the DLS technique is employed to measure the mean particle size and the particle size distribution of the nanoparticles in the suspension by using a particle sizing system (Model: Nicomp 380, Make: Santa Barbara, USA). In addition, the electrophoresis behavior of individual nanoparticles in the suspension is studied by measuring the zeta potential of the suspension to evaluate the stability of nanofluids. The wettability characteristics of nanofluids with various nanoparticle concentrations are studied through the contact angle measurements. In order to evaluate the thermal performance, one needs to measure accurately the thermo-physical properties such as thermal conductivity and viscosity. In this study**,** the effective thermal conductivity of the nanofluids was measured by using thermal property analyzer (Model: KD2 Pro., Model: Decagon Devices, USA) with isothermal temperature bath. The viscosity of the nanofluid was measured by using cone and plate viscometer (Model: Brookfield DV-II+ Pro, Make: Brookfield Engineering Laboratories, USA). The variation of thermal conductivity and viscosity of various nanofluids such as: CNT/water and Al_2O_3/water are reported for different nanoparticle concentration and temperature of nanofluids. The details of the microscopic examination of nanoparticles, nanofluid preparation, inspection of stability and method of measurement of thermal conductivity and viscosity are elaborated below.

2.2 Nanoparticles and Microscopic Examination

Among various nanoparticles, carbon nanotubes (CNTs) have attracted many researchers due to their higher thermal conductivity and very high aspect ratio, for preparing nanofluids. It can be noticed that CNTs nanofluids can be kept stable for months if the nanoparticles are functionalized or dispersed with surfactant [104]. Multi-walled carbon nanotubes (MWCNTs) were received from the M/S Nanoshel LLC (USA). The MWCNT is written as CNT in the remaining text for the convenience. The physical properties of CNT are listed in Table 2.1. The morphological characterization for CNT was obtained by using scanning electron microscopy (Model: SUPRA 55, Make: Carl Zeiss Microscopy, Germany) and is shown in Fig. 2.1 (a).

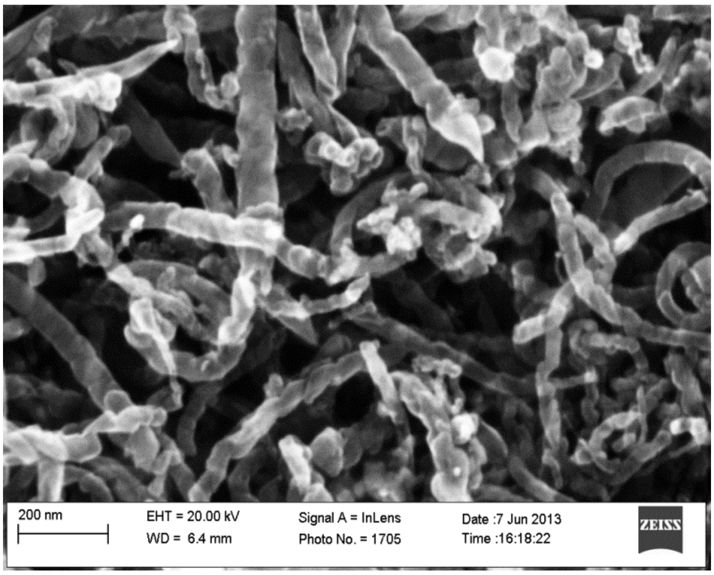

(a)

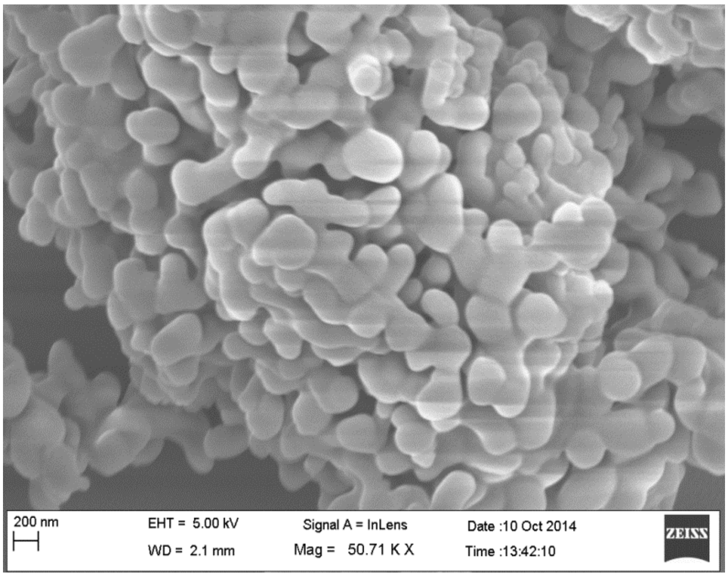

(b)

Figure 2.1: SEM image at magnification of **(a)** 10,000x of CNT particles and **(b)** 50,000x of CNT particles

Table 2.1: Geometrical specifications and characteristics of Al_2O_3 and CNT nanoparticles

Material	Al_2O_3	MWCNT
Appearance	White powder	Black powder
Purity	99.99%	>99.5%
Diameter	<100 nm	20-30 nm
Length	—	3-8 µm
pH value	6.6	—
Specific surface area	15-20 m^2/g	90- 350 m^2/g
Specific Density	3.428 g/cm^3	3.250 g/cm^3

It is observed that alumina is the most cost effective and widely used material in various applications. Also, it is found that, regardless of the base fluid, Al_2O_3 based nanofluids exhibits good stability for several weeks only by sonication method with adjusting the pH value. In this study, Al_2O_3 were received from the M/S Nanoshel LLC (USA). The physical properties of Al_2O_3 are listed in Table 2.1. The morphological characterization for Al_2O_3 was obtained by using scanning electron microscopy (Model: SUPRA 55, Make: Carl Zeiss Microscopy, Germany) and is shown in Fig. 2.2 (b).

2.3 Preparation of Nanofluids

Preparation of stable nanofluids is a challenging issue because of various reasons. Several techniques have been proposed to prepare nanofluids. These include sonication, pH control and addition of surface activators and/or dispersants such as: thiols, oleic acids, laurate salts [105]. Nanofluids are usually synthesized by employing either one-step or two-step production method. Two important elements such as: nanoparticle material and base fluid are needed for preparing the nanofluids.

Nanoparticles used in nanofluids are made of various materials, such as: oxide ceramics (Al_2O_3, CuO), nitride ceramics (AlN, SiN), carbide ceramics (SiC, TiC), metals (Cu, Ag, Au), semiconductors (TiO_2, SiC) and carbon nanotubes. The common host liquids are water, ethylene glycol, and oil [106].

Single-step technique

In this method, the manufacturing of nanoparticle and preparation of nanofluid are carried out simultaneously. The nanoparticles can be directly prepared by physical vapor deposition (PVD) technique or through the liquid chemical method. In this method, the metal is vaporized in vacuum chamber, condensed and collected in the heat transfer fluids. By using this method the agglomeration of nanoparticles is minimized and the stability of the nanofluids is improved. A disadvantage of this method is that it is impossible to scale it up for industrial application [107].

Two-step technique

In this technique, the dry nanoparticles are first produced, and these nanoparticles are dispersed in a suitable liquid (base fluid). However, the problem of agglomeration of nanoparticles is observed in this process. Two step techniques have been extensively used for the synthesis of nanofluids because of the simple preparation procedure and the availability of various nanopowders by several companies [107].

In the present study, we have adopted the two-step technique for preparing the nanofluids. Various techniques such as sonication, functionalization and addition of the surfactant (sodium dodecyl sulfate) have been employed to obtain nanofluids. This has been elaborated below.

Preparation of nanofluids by functionalized method

Here, nanofluids with different nanoparticle concentration (φ= 0.15%, 0.45%, 0.60% and 1%) were prepared by the functionalization acid treatment method [108]. According to this method, simple acid treatment provides good stability in water to carbon nanotubes suspension.

This was caused by a hydrophobic-to-hydrophilic conversion of the surface nature due to the generation of a hydroxyl group.

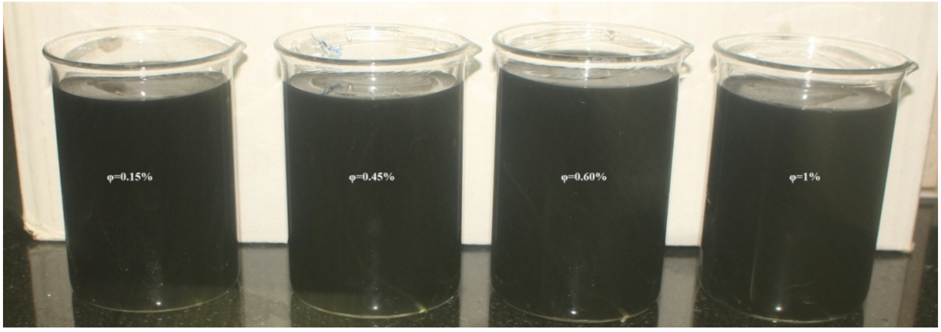

Figure 2.2: Photographic view of CNT/water nanofluids with various volume fractions

In this procedure, CNTs were immersed in a mixture of H_2SO_4/HNO_3 (3:1) at room temperature. Later on, CNTs were treated in an ultrasound bath (Model: USBT- 9.0L Ultrasonic Cleanser, 200 W, Make: Rico Scientific Industries, India) for 2 hours and upheld for 15 hours. Subsequently, this solution was neutralized with ammonium hydroxide and filtered with a 0.22 mm cellulose acetate membrane. The CNTs were washed several times by using deionized water until the pH is adjusted to 5.5, 6.5 and 9.0. When a surface suffers oxidation, the chemical elements are adsorbed forming functional groups. These groups are either positively or negatively charged. In this case, hydroxyl and carboxylic groups are inserted on the nanotubes surface; these groups are equally charged. The presence of similar charged particles on the surface of CNTs enables the CNTs to repel each other, keeping the solution in a dispersed form. The nanofluid prepared by functionalized method is termed as functionalized carbon nanotubes (CNT or FCNT) nanofluids.

Preparation of nanofluids with addition of surfactant

The use of the surfactant is one of the methods widely used to avoid the agglomeration of nanoparticles in the base fluid. Surfactants can improve the stability of nanoparticles in aqueous suspensions. The reason may be due the fact that the hydrophobic surfaces of nanotubes are modified to act as hydrophilic and vice versa. A repulsive force between the suspended particles is developed due to the surface charge of the suspended particles in the base fluid. Various surfactants such as: sodium dodecyl sulfate (SDS), sodium dodecyl benzene sulfonate (SDBS), salt and oleic acid, gum arabic and cetyl trimethyl ammonium bromide (CTAB) has been used by various researchers. It may be noted that the selection of suitable activators/dispersant depends on the properties of the solutions and particles [109].

Here, sodium dodecyl sulfate (SDS) is used as the surfactant for preparing the nanofluids. It is observed 0.25 wt.%. of sodium dodecyl sulfate is required to obtain better stability of CNT/water nanofluid [109]. In this study, CNT/water nanofluids are prepared by adding various CNT nanoparticle concentration (φ= 0.15%, 0.45%, 0.60% and 1%) and 0.25 wt.% of sodium dodecyl sulfate (SDS). Subsequently, the solution is placed in an ultrasonic bath (Make: USBT- 9.0L Ultrasonic Cleanser, 200 W, Model: Rico Scientific Industries, India) for a period of 45 min. in order to attain the complete dispersion of the nanoparticles. The nanofluid prepared in this method is termed as SCNT in the rest of the thesis.

Ultrasonic vibration

The ultrasonic vibration procedure is commonly used to eliminate the agglomeration of nanoparticles. In this procedure, the ultrasonic vibration produces high-frequency ultrasonic wave in the nanofluid kept inside the ultrasonic bath and excites the nanoparticles, breaks up the agglomerates of the nanoparticles and form a suspension of isolated nanoparticles. Here, Al_2O_3/water nanofluids with different nanoparticle concentration (φ= 0.15%, 0.45%, 0.60% and 1%) were prepared by dispersing a specified amount of Al_2O_3 nanoparticles in water by using an ultrasonic vibrator (Rico Scientific Industries, India). The ultrasonic vibrator generates ultrasonic pulses of 40 kHz at 200 W. In order to get a uniform dispersion and stable suspension which determine the final properties of nanofluids, the nanofluids are kept under ultrasonic vibration continuously for 5 h [103]. No surfactant was used as they may have some influence on the effective thermal conductivity of nanofluids [110].

Figure 2.3: Photographic view of Al_2O_3/water nanofluids with various volume fractions

The pH of the prepared nanofluids at different concentrations were measured and found to be around 6.2 which is far from the isoelectric point of 9.2 for alumina nanoparticles [103]. This ensures the nanoparticles are well dispersed and the nanofluid is stable because of very large repulsive forces among the nanoparticles. Thus, the Al_2O_3/water nanofluid prepared in the present work was found to be very stable for several weeks without sedimentation. This is observed through visual observation.

2.4 Stability of Nanofluids

The stability of nanofluids is considered an important issue as this affects the heat transfer performance. The stability inspection includes the particle size distribution of nanoparticles in the suspension and electrophoretic behavior of individual nanoparticles. Various techniques have been adopted to evaluate the stability of nanofluids and are elaborated below [105, 111].

2.4.1 Dynamic light scattering test (DLS)

The DLS methodology is commonly used to measure the mean particle size and particle size distribution of the nanoparticles in the suspension. In this method, a continuous-wave laser beam (wavelength of

632.8 nm range) passes through a colloidal suspension sample and the particles scatter some of the light in all directions (Rayleigh scattering) [112]. This is due to the smaller particle size compared to the laser wavelength. In addition, the small particles in the suspension move randomly resulting in the fluctuation in the scattered light in the detector plane. This fluctuation is related to the diffusion rate of the particles, and the diffusion coefficient of the particles is given by the Stokes-Einstein relation:

$$D_C = \frac{k_B T}{6\pi\mu r} \tag{2.1}$$

Where, D_C, K_B, T, r and μ denote the diffusion coefficient, Boltzmann constant, the absolute temperature, the radius of the particles and viscosity of the solvent, respectively. The diffusion coefficient of particles is determined by analyzing the fluctuation data. Therefore, the DLS system measures the effective hydrodynamic diameter by treating the particles as spherical.

In this study, the DLS methodology is used to measure the mean particle size and the particle size distribution of the nanoparticles in the suspension by using a particle sizing system (Model: Nicomp 380, Make: Santa Barbara, USA). Figs. 2.4 (a-f) show the statistical graph of intensity (%) versus the hydrodynamic diameter (nm) of the nanoclusters for two different nanofluids such as: CNT/water and Al_2O_3/water nanofluids with various nanoparticle concentrations. The DLS tests are carried out after 1 month of preparation. The average hydrodynamic diameters for functionalized CNTs in water with 0.15% and 1% particle volume fraction was found to be 63.5 nm and 82 nm, respectively. While, the average hydrodynamic diameters for surface treated CNTs in water with 0.15% and 1% particle volume fraction was found to be 106 nm and 155 nm, respectively. On the contrary, the average Al_2O_3 nanoparticle in water with 0.15% and 1% particle volume fraction show the hydrodynamic diameter of 121 nm and 184 nm, respectively.

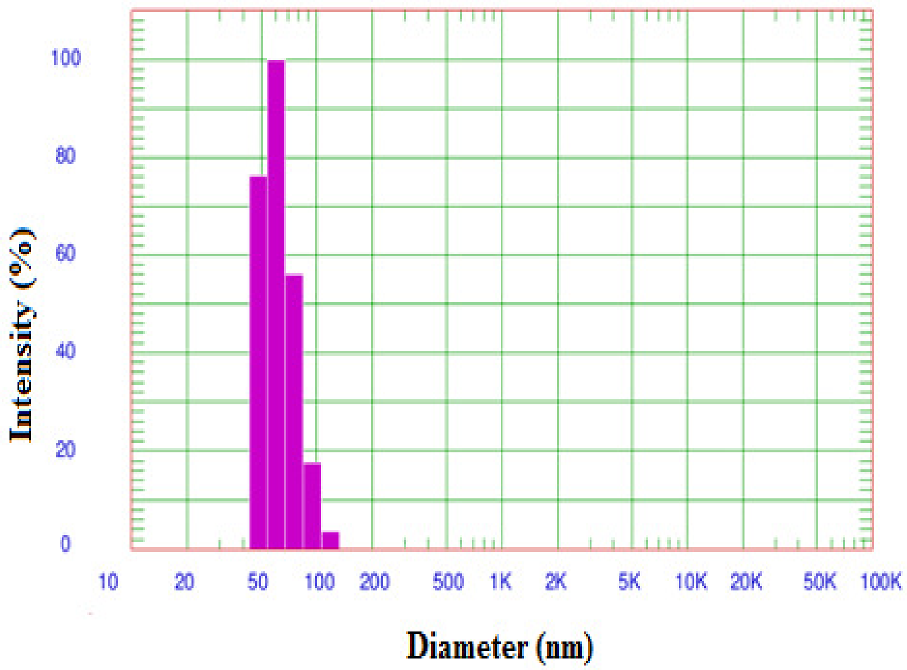
100
80
60
40
20
0
Intensity (%)
10
20
50
100
200
500
1K
2K
5K
10K
20K
50K
100K
Diameter (nm)

(a)

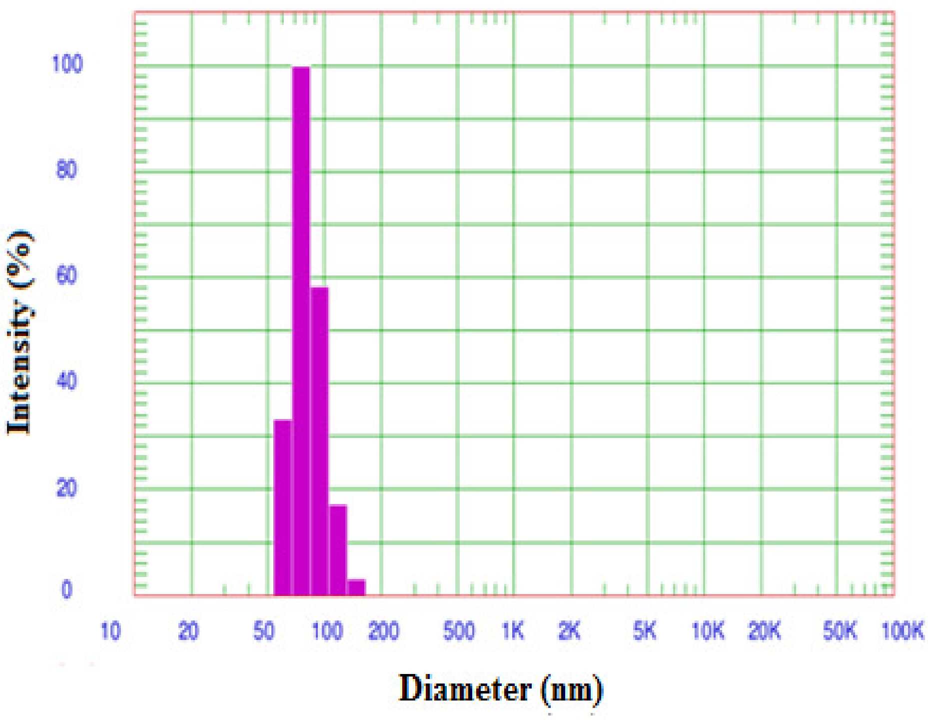
100
80
60
40
20
0
Intensity (%)
10
20
50
100
200
500
1K
2K
5K
10K
20K
50K
100K
Diameter (nm)

(b)

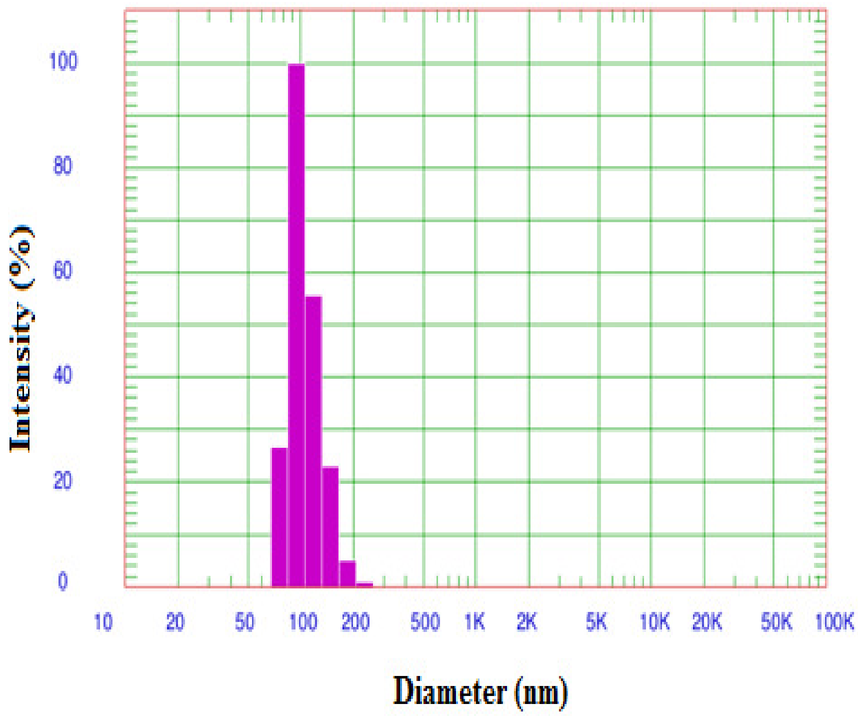
100
80
60
40
20
0
Intensity (%)
10
20
50
100
200
500
1K
2K
5K
10K
20K
50K
100K
Diameter (nm)

(c)

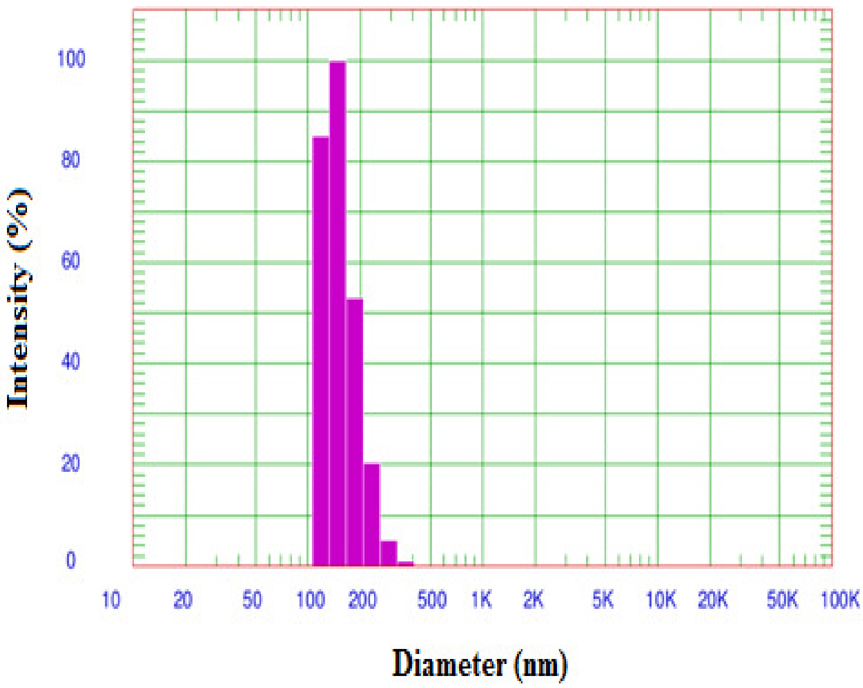
100
80
60
40
20
0
Intensity (%)
10
20
50
100
200
500
1K
2K
5K
10K
20K
50K
100K
Diameter (nm)

(d)

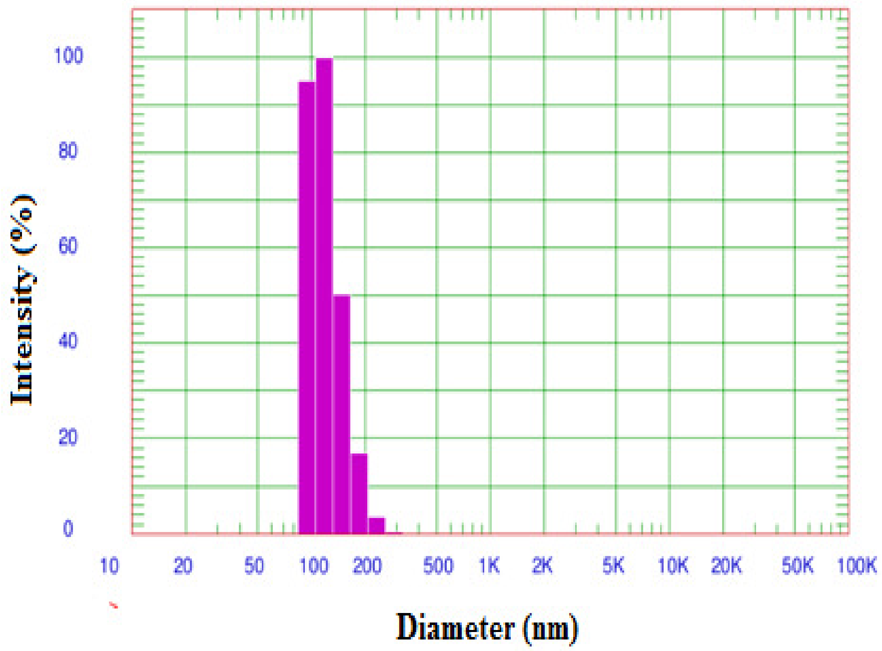

(e)

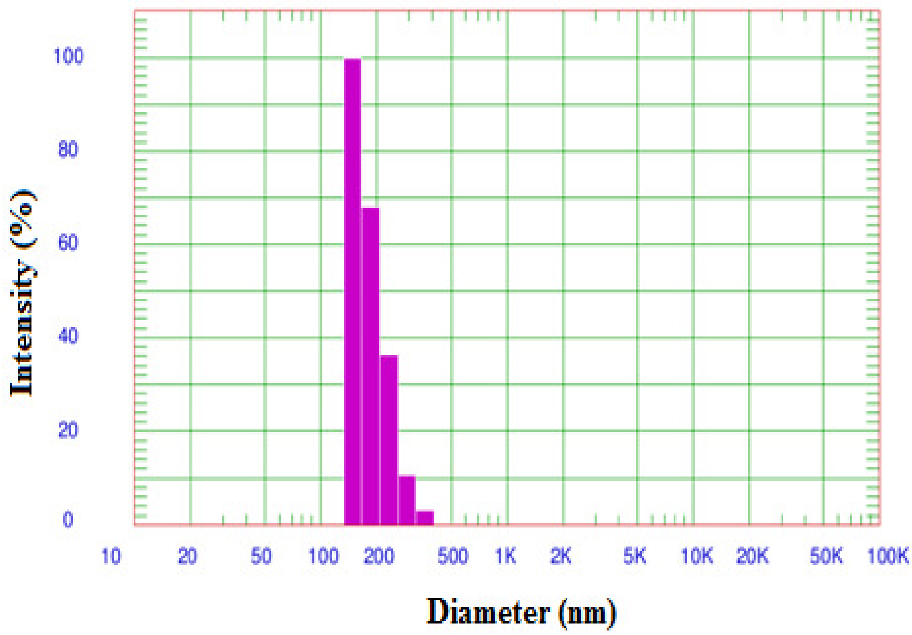

(f)

Figure 2.4: Hydrodynamic diameter of nanoparticles in the dispersed state for **(a)** FCNT nanofluid (φ=0.15%), **(b)** FCNT nanofluid (φ=1%), **(c)** SCNT nanofluid (φ=0.15%), **(d)** FCNT nanofluid(φ=1%), **(e)** Al_2O_3/ nanofluid (φ=0.15%) and **(f)** Al_2O_3/water nanofluid (φ=1%)

It is observed that at higher particle volume concentration, nanoparticles agglomerate due to strong interparticle interactions resulting in sedimentation of the nanofluid. On the contrary, lower nanoparticle concentration reduces the interparticle interactions and enhances the stability of nanofluid leading to the lower value of the effective hydrodynamic diameter of nanoparticles. The increase in particle agglomeration is observed with the increase in the nanoparticle concentration.

2.4.2 Zeta potential test

In general the electrostatic repulsion is considered as the mechanism to stabilize the colloidal suspensions. In many cases, the colloidal particles are charged and leads to the mutual repulsion of particles at extended distances. These repulsive forces are sufficiently strong to overcome the attractive force caused by Vander waals forces. Zeta potential is the measure of the repulsive forces between particles. According to the stabilization theory [113], the electrostatic repulsions between the particles increase if the zeta potential has a higher absolute value. This may be due to the fact that at the higher surface charge, the repulsion between the particles increases resulting in lesser agglomeration. The measured values of the zeta potential at room temperature for various nanofluids are summarized in the Table 2.2. It is argued that the suspension exhibits good stability if the zeta-potential value is higher than 30 mV [105, 114-115].

Table 2.2: Zeta potential of various nanofluids

Concentration (φ)	Zeta potential of various Nanofluid (mV)		
	FCNT/water nanofluid	SCNT/water nanofluid	Al_2O_3/water nanofluid
0.15 %	57	50	48
0.45 %	48	45	42
0.60 %	45	40	36
1 %	39	35	32

2.4.3 Wettability characterization

The nanoparticles should be hydrophilic in nature so that it forms stable dispersion in medium like water. One of the fundamental methods of characterizing the hydrophobic or hydrophilic properties of a solid surface is to determine the contact angle [116]. The contact angle is a measure of the wetting behavior of a particular liquid on the surface under investigation and directly relates to the interfacial energies of the systems. The contact angle on the solid surface gets changed merely by changing the chemistry of the outermost layer.

Depending on the wettability of a solid surface by a liquid, it is classified into two groups such as hydrophobic and hydrophilic. The contact angle (θ) for the hydrophilic surface is less than 90^0 and for the hydrophobic surface is greater than 90^0. Here, the hydrophilic nature of the nanofluid was tested by the static wettability test. It may be noted that static wetting occurs when a small liquid droplet is deposited on a smooth, homogeneous stationary copper surface. The degree of static wetting is usually defined by the equilibrium contact angle (θ_e). For the higher values of contact angle (θ_e>90°), the wetting is considered to be poor. While, for a lower contact angle (θ_e<90°), the liquid wets the solid surface. With the decrease in the contact angle, the degree of wetting increases and the complete wetting is achieved for zero value of contact angle (θ_e=0). In the present study, tests have been carried out to measure the contact angle of various fluids such as: water, CNT/water nanofluid and Al_2O_3/water nanofluid with a plain copper solid surface by using the contact angle meter (Model: HO-IAD-CAM-01A, Make: Holmarc Opto-Mechatronics Pvt. Ltd., India) and the results are shown in Fig. 2.5 (a-c). The contact angle was found to be 57.62^0, 48.45^0 and 44.82^0 for water, Al_2O_3/water nanofluid (φ=0.15%) and CNT/water nanofluid (φ=0.15%), respectively. This shows that the addition of nanoparticle increases the surface wettability.

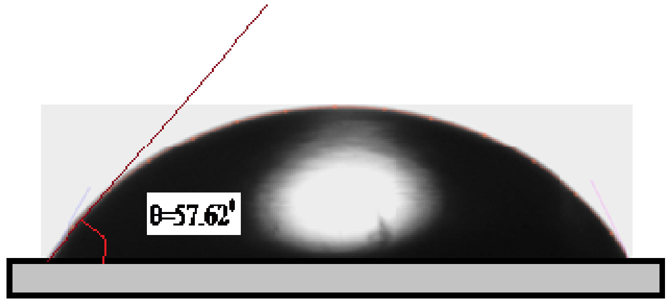

(a)

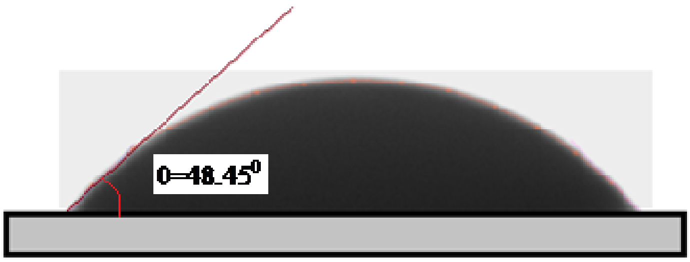

(b)

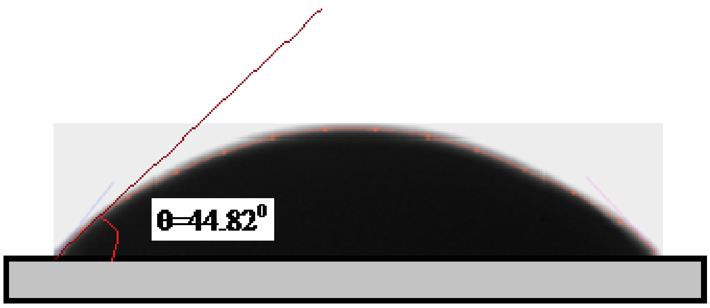

(c)

Figure 2.5: Equilibrium contact angle of a droplet resting on a plain copper surface **(a)** pure water, **(b)** Al_2O_3/water nanofluid and **(c)** CNT/water nanofluid

2.5 Measurement of Various Properties of Nanofluids

Accurate measurement of various properties including thermal conductivity and viscosity plays an important role in evaluating the thermal performance of nanofluids. The details of measurement for thermal conductivity and viscosity of nanofluids are elaborated below.

2.5.1 Thermal conductivity measurements

The thermal conductivity of nanofluids depend on various parameters such as: chemical composition of nanoparticle and base fluid, nanoparticle concentration, particle shape, particle size, temperature of the base fluid and the additives (surfactants) used in the solution. Several techniques have been proposed to measure the thermal conductivity of nanofluids. In general two types of methods are used to measure the thermal conductivity such as: steady-state method and transient method. In the case of steady state methods, the heat loss cannot be quantified and the natural convection gives rise to higher values of thermal conductivity. The transient methods includes, hot-wire method, temperature oscillation method and 3-omega method. While, the steady-state method include parallel plate type, cylindrical cell type. Among these methods, the transient hot-wire method (TWH) has been used extensively because of several advantages of this method over other techniques. TWH method is very fast compared to other techniques and eliminates the error due to the natural convection. In addition, the design of the hotwire apparatus is simple compared to the other techniques. In view of this, it is advantageous to use the transient methods to measure the thermal conductivity.

In the case of TWH method, a thin metallic wire is used to supply heat source and temperature probes are used to measure the rise in the temperature. A wire (infinitely long) is suspended inside and surrounded by a fluid whose thermal conductivity is to be measured. The hot wire is heated by sending the electrical current through it. The temperature change over a given period of time is recorded to evaluate the thermal conductivity of the fluid.

In this study, the effective thermal conductivity of the nanofluid was measured by using the thermal property analyzer (Model: KD2 Pro., Model: Decagon Devices, USA) with isothermal temperature bath. The measurement is based on the transient hot-wire method. The minimum amount of nanofluid required for the measurement of thermal conductivity is found to be 45 ml. The sensor needle, KS-1, is made of stainless steel with 60 mm long and 1.3 mm diameter. This configuration can be considered as the infinite line heat source. The thermal conductivity measurement assumes several parameters such as: (i) the sensor needle is considered to be infinitely long heat source (ii) the medium is considered to homogeneous, isotropic and at uniform initial temperature. The sensor needle can be used to measure the thermal conductivity of fluids in the range of 0.2–2 W/m K with an accuracy of ±5%. Here, the experiment lasts for 90 s. The thermal conductivity of the fluid is calculated according to the equation,

$$k = \frac{q(\ln t_2 - \ln t_1)}{4\pi(T_2 - T_1)} \tag{2.2}$$

where q is applied electric power to an infinitely long and small line source. Here, (T_2-T_1) represents the temperature rise of the wires between times t_1 and t_2, respectively.

The KD2 Pro thermal properties analyzer meets both ASTM D5334 and IEEE 442-1981 standards. Before conducting the experiments, the calibration of the sensor needle is carried out by measuring the thermal conductivity of various known fluids such as: distilled water, glycerin and ethylene glycol. The measured thermal conductivity values for distilled water, glycerin and ethylene glycol are found to be 0.613, 0.292 and 0.263 W/mK, respectively. This is in good agreement with the literature values of 0.613, 0.285 and 0.252 W/mK for water, glycerin and ethylene glycol,

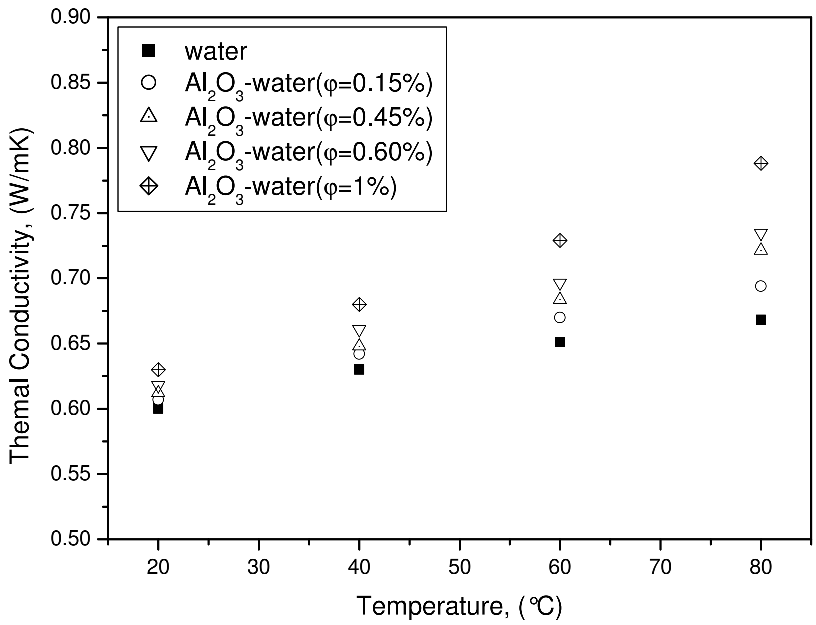

(a)

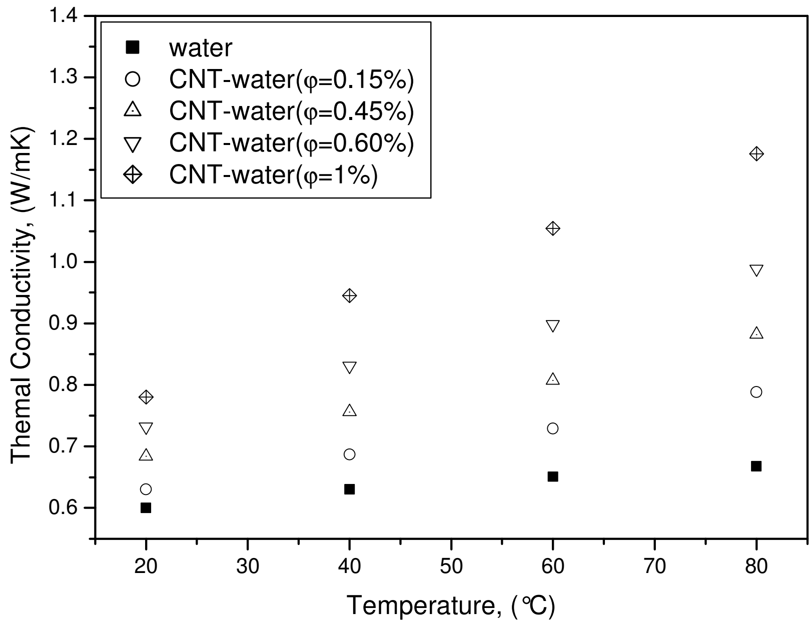

(b)

Figure 2.6: Variation of thermal conductivity of nanofluids with temperature for various nanoparticle concentrations

respectively within $\pm 5\%$ accuracy. Here, 45 ml of nanofluid samples are taken in a vial of 30 mm diameter whose cap is equipped with a septum through which the sensor needle was inserted. The needle was inserted fully into the fluid and oriented vertically and centrally inside the vial without touching the side walls of the vial.

Figure 2.9 (a) and (b) demonstrate the experimentally measured value of thermal conductivity of Al_2O_3/water and CNT/water nanofluids, respectively. The thermal conductivity of nanofluids increases by increasing nanoparticle concentration and temperature. At higher fluid temperature, the Brownian motion of nanoparticles intensifies, consequently the micro convection increases resulting in an enhancement of the thermal conductivity of nanofluids. Figure 4 (a) depicts the enhancement in the thermal conductivity with temperature for Al_2O_3/water nanofluid. For 1 vol.% concentration and 60^0C fluid temperature, Al_2O_3/water nanofluid exhibit 12% enhancement in thermal conductivity compared to water. Similar observations have been made by previous researchers [110, 118-129]. The enhancement in the thermal conductivity with temperature for CNT/water nanofluid is shown in Fig. 4 (b). This shows that at 60^0C, the effective thermal conductivity of CNT/water nanofluids increases by 12% and 38% for 0.15% and 0.60% volume concentration, respectively. Earlier, various authors [120-121] reported similar observations during their experimental investigation.

2.5.2 Viscosity measurements

The viscosity of the fluid is the measure of its resistance to deformation. In case of flow through ducts, the pressure drop and the pumping power requirements depends on the viscosity of the fluids. Although the nanofluids increase the heat transfer performance, these fluids exhibit an enhancement in the viscosity compared to the base fluid. The viscosity of the nanofluid depends on the particle shape, particle size, volume fraction and temperature of the nanofluids.

Nanofluids usually contain lower nanoparticle concentration and therefore the nanofluids are assumed as Newtonian fluids. Here, efforts have been made to study the effects of the temperature and the nanoparticle concentration on absolute viscosity. In this study, the viscosity of the nanofluid was measured by using cone and plate viscometer (Model: Brookfield DV-II+ Pro, Make: Brookfield Engineering Laboratories, USA). The cone is connected to the spindle drive while the plate is mounted in the sample cup. A spindle (CPE-40) is used in this study and can be used for measuring the viscosity in the range 0.15-3065 cP. Cone and plate geometry requires 0.5–2 ml sample for the measurement. The nanofluid under test is poured into the sample chamber of the viscometer. The spindle speed and the shear rate are varied between 0.1–200 rpm and 0–750 s^{-1}, respectively. As the spindle rotates, the viscous drag of the fluid against the spindle is measured by the deflection of the calibrated spring. A data logger records the shear rate, shear strain and viscosity data at room temperature. The viscosity of nanofluid is measured at different temperature by activating the temperature control system. The viscosity values obtained by various fluids such as: water, glycerin and ethylene glycol at room temperature are used to validate with the available values. The measured values of viscosity for distilled water, glycerin and ethylene glycol are found to be 0.83, 10.9 and 356.5 cP, respectively. The results agree well with the literature values of 0.79, 10.7 and 352 cP, for water, glycerin and ethylene glycol, respectively, with ±5% accuracy. Figure 2.10 (a) and (b) indicates the variation of viscosity of Al_2O_3/water and CNT/water nanofluid as a function of temperature for different nanoparticle concentration. It is observed that the viscosity of nanofluids decreases by increasing the temperature. In addition, the absolute viscosity of nanofluid increases with the particle volume concentration and are in close agreement with the values reported by earlier researchers [47, 122-123].

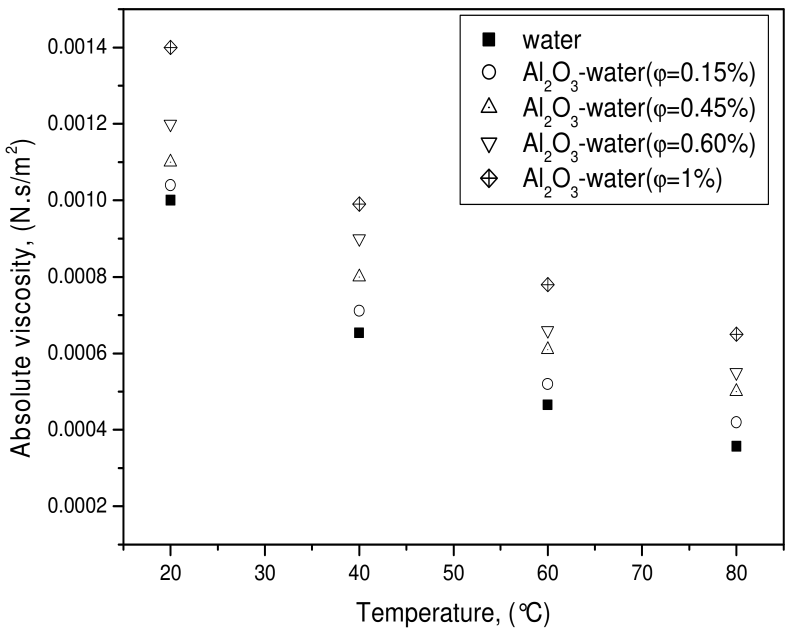

(a)

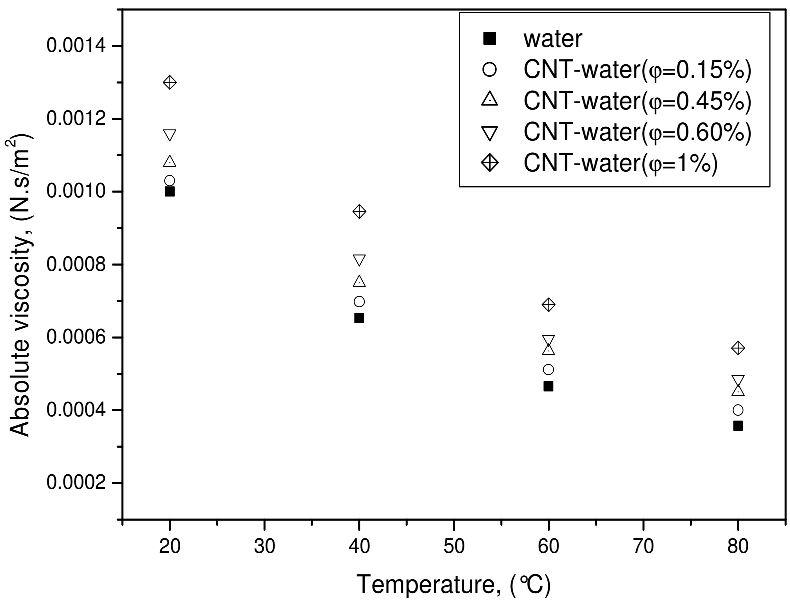

(b)

Figure 2.7: Variation of viscosity of nanofluids with temperature for various nanoparticle concentrations

2.6 Concluding Remarks

In this chapter, the two-step method is used for preparing Al_2O_3/water and CNT/water nanofluids. Various techniques such as: ultrasonic vibration, functionalization and surfactant addition method are adopted to prepare nanofluids. The morphological characterization for two different nanoparticles such as: Al_2O_3 and CNT are obtained by using scanning electron microscopy (Model: SUPRA 55, Make: Carl Zeiss Microscopy, Germany). The dynamic light scattering (DLS) methodology is used to measure the average particle size and particle size distribution of the nanoparticle in the suspension by using a particle sizing system (Model: Nicomp 380, Make: Santa Barbara, USA).

The FCNT nanofluid exhibits lower hydrodynamic diameter compared to SCNT nanofluid. The Al_2O_3/water nanofluid prepared using simple sonication method exhibits better stability. The electrophoresis behavior of individual nanoparticle in the suspension is studied by measuring the zeta potential of the suspension. Here, FCNT exhibit higher value of zeta potential compared to SCNT and Al_2O_3/water nanofluid. Also, the zeta potential value decreases with increasing nanoparticle concentration. The wettability behavior of various nanofluids on the solid surface is studied by measuring the contact angle of the fluid at the solid surface. The addition of nanoparticle to base fluid (water) reduces contact angle leading to an increase in wettability of the surface. The wettability of CNT/water nanofluid is higher compared to water followed by Al_2O_3/water nanofluid.

The effective thermal conductivity of various nanofluids are measured by using the thermal property analyzer (Model: KD2 Pro., Model: Decagon Devices, USA) with isothermal temperature bath. The thermal conductivity of nanofluids (CNT/water, Al_2O_3/water) was found to increase with nanoparticle concentration and temperature. The effective thermal conductivity of CNT/water nanofluid is found to be higher compared to Al_2O_3/water nanofluids for similar conditions. In addition, the viscosity of nanofluids (CNT/water, Al_2O_3/water) was measured by using cone and plate viscometer (Model: Brookfield DV-II+ Pro, Make: Brookfield Engineering Laboratories, USA). The viscosity Al_2O_3/water nanofluids were found to be higher compared to CNT/water nanofluids for similar conditions.

Chapter 3

Heat Transfer Performance of Nanofluids through Uniformly Heated Circular Tube with Helical Twisted Tape Inserts

3.1 Introduction

The enhancement of heat transfer plays a vital role in the heat exchanging equipments. The enhancement in the heat transfer improves the thermal performance, reduces size and cost. In order to improve the thermal performance, several techniques have been employed by various researchers. The heat transfer enhancement techniques are broadly classified into two categories, namely, active method which needs an external power source and passive method which does not need any external power source. Among various passive technique twisted-tapes, helical-screw tapes and wire have been mostly used in ducts because of its increased heat transfer performance [44-56]. The improvement in the heat transfer by using inserts may be due to various reasons, namely, decrease in hydraulic diameter, the increase in the length of the flow path due to helical configuration of inserts, the increase in the shear stress at wall and tube leading to improvement in fluid mixing. Further, it is observed that nanofluids exhibit better thermal performance compared to conventional single phase fluids. Therefore, it is a logical approach that combination of inserts and nanofluids can improve the heat transfer rate compared to values obtained by using any one of these technique. In view of this, an effort has been made to evaluate the combined effect of nanofluid and helical twisted tape inserts on the thermal performance through uniformly heated pipe.

In the present chapter, experimental investigation has been carried out to study the thermal performance of two different nanofluids (Al_2O_3/water and CNT/water) through a uniformly heated tube with helical twisted tape inserts. Three cases are considered for the analysis. Initially, tests are performed to study the heat transfer and friction factor characteristics of Al_2O_3/water and CNT/water nanofluids in laminar flow regime. Later on, the analysis is extended to evaluate the thermal performance of the nanofluids in transition flow regime. In third problem, efforts have been made to study the effect of different nanoparticle concentration on the thermal performance. The effect of twist ratio on thermal performance is studied in each case. In addition, the comparison of thermal performance of nanofluids (Al_2O_3/water and CNT/water) and water is studied for similar operating conditions.

3.2 Test Facility, Experimental Procedure and Data Reduction

3.2.1 Test facility

Figure 3.1 depicts the schematic view of the test facility to study the flow and convective heat transfer characteristics of the Al_2O_3 and CNT nanofluid in a tube with helical tape. The test facility includes the test section, power supply unit, nanofluid supply system, cooling section and instrumentation scheme for measuring temperature. The test section is made of a 1000 mm long copper tube of 10.5 mm ID and 12.5 mm OD. One end of the copper tube is fitted to a 1000 mm long PVC tube of 10.5 mm ID and 12.5 mm OD. The long PVC tube, termed as calming section, is kept long enough to ensure the fully developed flow condition at the entrance of the test section. The inlet and outlet of the test section is connected to the calming section and heat exchanger, respectively. The copper tube is heated uniformly by wrapping two heating elements made of nichrome heating wire (20 gauge, 53.5 Ω, 1 kW). The nichrome heating wire has ceramic bead insulation that prevents the direct contact of nichrome wire with the test section. The terminals of the nichrome heating wires are connected to an auto transformer and the power supply to the test section is varied by varying the voltage. The entire test section is insulated by using glass wool insulation in order to minimize heat loss from the test section to the surroundings. Six calibrated RTD PT100 type temperature sensors with an accuracy of ±0.1^{0}C are placed in the thermo wells mounted on the test section at distances 0.15m, 0.30m, 0.45m, 0.60m, 0.75m and 0.90m from the inlet of the test section to measure the outside wall temperature. Two calibrated RTD PT100 type temperature sensors are located at the inlet (T_1) and outlet (T_8) of the test section to measure the inlet and outlet temperature of the working fluid. The inside wall temperature of the test section were evaluated by calculating the tube wall temperature drop from 1-D radial heat conduction equation. The temperature at various locations was recorded by using a DAS (Model 34970, Make: Agilent Technologies).

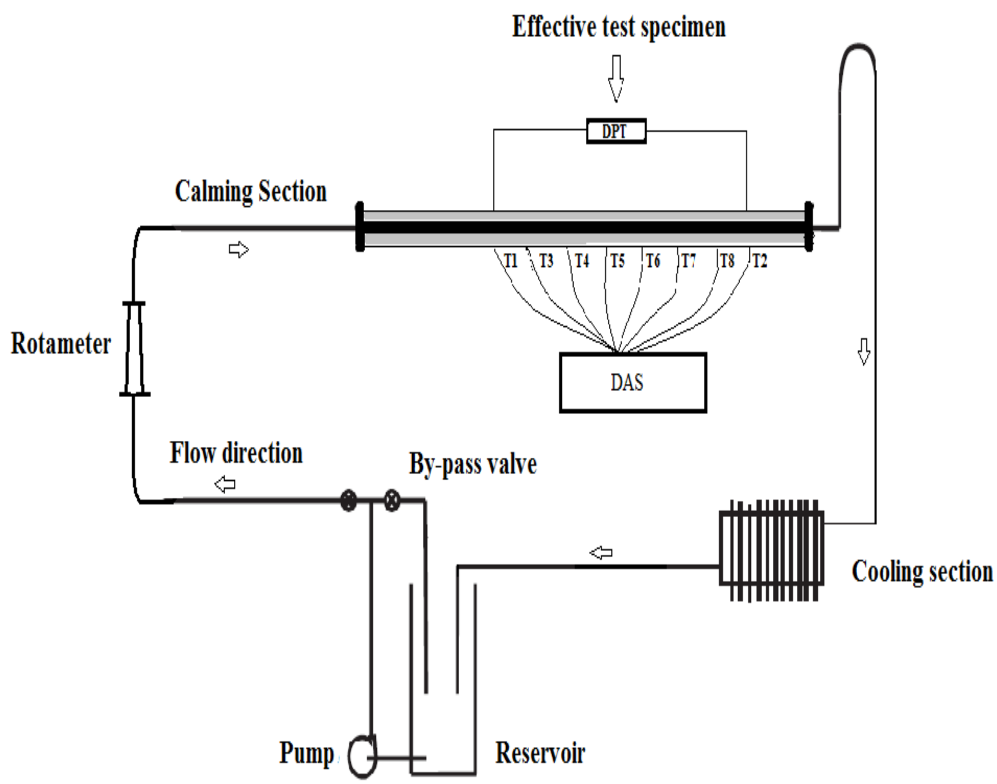

Figure 3.1: Schematic diagram of test facility

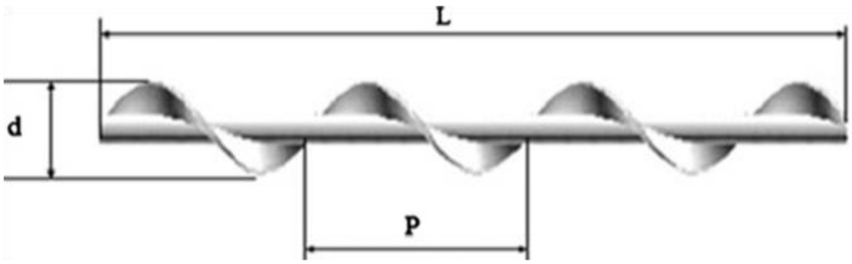

(a)

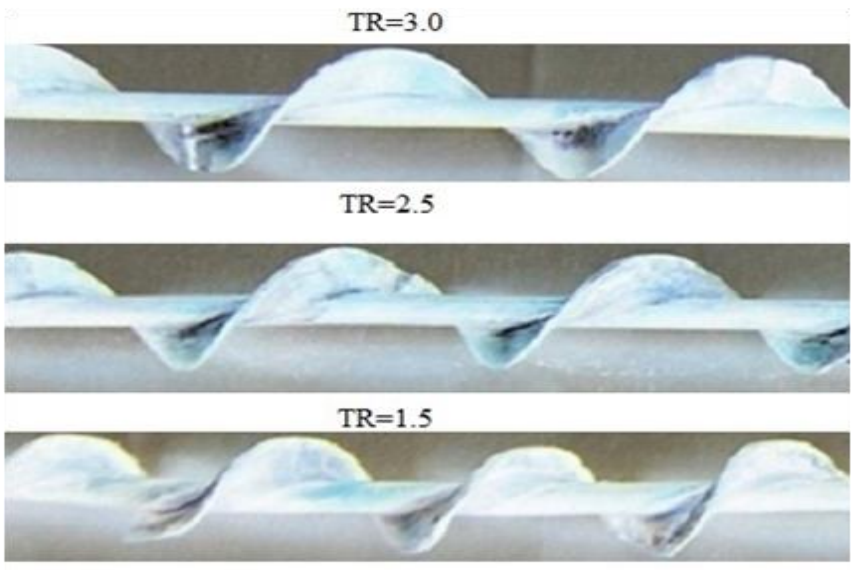

(b)

Figure 3.2: (a) Schematic of helical screw-tape inserts and **(b)** Photographic view of helical twisted tape inserts used in the present study

A peristaltic pump (Model: RH-P1201, Make: Ravel Hiteks Pvt. Ltd.) with a maximum capacity of 2.5 liters/min is used to feed nanofluid from the coolant storage tank to the test section. The coolant flow rate of the peristaltic pump is controlled by varying the rotational speed. The peristaltic pump was calibrated by using a measuring glass jar. This was achieved by collecting the volume of water in the jar for a given time interval and comparing with the volume flow rate calculated from the rotational speed of peristaltic pump. The flow rate of the nanofluid is controlled by the bypass valve arrangement, and the remaining fluid is sent back to the storage tank. The nanofluid, heated in the test section, is allowed to cool by passing through an air cooler. A differential pressure transducer (Model: D9824-6-005BD, Make: Omicron) with an accuracy of ±0.25% mounted across the test section is used to measure the pressure drop across the test section. In addition, a U-tube manometer with Carbon Tetrachloride (CCl_4) as manometer liquid is used to measure the pressure drop during the experimental investigation. The helical screw-tape inserts with various twist ratios (Fig. 3.2) were fabricated by winding uniformly a copper strip of 3.5 mm width over a 2.5 mm copper rod and painted with insulating gel. The twist ratio, TR is defined as the ratio of length of one twist to the diameter of the twist. Three helical screw-tape inserts with twist ratio of 1.5, 2.5 and 3 are used in the present study.

3.2.2 Experimental procedure

Tests were carried out to evaluate the convective heat transfer and friction factor characteristics of water and nanofluids through the tube with helical tape inserts. The storage tank is filled with the working fluid and the circulation pump is turned on to initiate the flow of coolant through the test section. The peristaltic pump is used to measure the coolant mass flow rate. The flow rate is adjusted to obtain the required Reynolds number to carry out the experimental investigation. After adjusting the required flow rate, the electric power is supplied to the heating element to heat the outer surface of tube. During heating, the DAS and a voltmeter monitor the surface temperature and the electric power, respectively. After attaining the steady state condition, the power supply to the heating element and the temperature at various locations of the test tube is noted by using voltmeter and DAS, respectively. Initially, tests were conducted with water and the results obtained from the experimental study were validated with the results of Shah [124] and Gnielinski [125]. Later on, two different working fluids, namely, CNT/water and Al_2O_3/water were used to study the friction factor and heat transfer characteristics in the horizontal tube. Subsequently, the screw tape inserts were inserted in the tube to study its effect on heat transfer and pressure drop characteristics. In order to evaluate the friction factor characteristics during the flow, the electric power supply to the heating coils was switched off and the pressure drop was measured by using a differential pressure transducer (Model: D9824-6-005BD, Make: Omicron). The tube wall temperatures, inlet and outlet temperatures of the working fluid, mass flow rate, electric power input are recorded during each test run. An error analysis is made to evaluate various errors associated in the experimental study following the procedure suggested by Coleman and Steel [126] and ANSI/ASME standard [127]. The uncertainties associated with various parameters namely, flow rate, wall and fluid temperatures, voltage, current and pressure drop were evaluated to estimate the combined uncertainty in Reynolds number, Nusselt number and friction factor on the basis of 95% confidence level. The maximum uncertainty in various parameters, namely, Reynolds number, friction factor and Nusselt number were found to be ±2.5%, ±6%, and ±2%, respectively.

3.3.3 Data reduction

The total heat supplied to the test section and the heat absorbed by the working fluid is estimated from Eq. (3.1) and Eq. (3.2), respectively.

$$Q_1 = VI \quad \text{(energy supplied)} \tag{3.1}$$

$$Q_2 = \dot{m} C_P (T_{out} - T_{in}) \quad \text{(energy absorbed)} \tag{3.2}$$

$$(\mathrm{Q}_1 - \mathrm{Q}_2) \times 100\% / \mathrm{Q}_1 < 3\% \tag{3.3}$$

The heat balance between the heat input *(Q_1)* and heat transfer rate of the water *(Q_2)* is less than 3%, shown by Eq. (3.3).

Here, the Newton's law of cooling Eq. (3.4) is used for estimation of experimental heat transfer coefficient. While, the experimental Nusselt number is evaluated by using Eq. (3.5).

$$h = \frac{Q_2}{A(\bar{T}_w - \bar{T}_f)} \tag{3.4}$$

Here, $\bar{T}_w$ is the average temperature of the wall and $\bar{T}_f$ is the average bulk temperature of fluid.

Where, $A = \pi DL$, $\bar{T}_w = \frac{T_1 + T_2 + T_3 + T_4 + T_5 + T_6}{6}$, $\bar{T}_f = \frac{T_{in} + T_{out}}{2}$

$$Nu_{\exp} = \frac{hD}{k} \tag{3.5}$$

where *D*, *h* and *k* represents the diameter of the test section, average heat transfer coefficient and thermal conductivity of the working fluid, respectively.

The pressure drop (ΔP) measured across the test section is used to determine the friction factor (*f*) using the following relation:

$$f_{\exp} = \frac{\Delta P}{\left(\frac{L}{D}\right)\left(\frac{\rho u^2}{2}\right)} \tag{3.6}$$

Where, *u*, ρ and *D*, *L* represents the fluid velocity, fluid density, the diameter of the test section and length of the test section, respectively.

Thermal performance factor (η) is the parameter usually used to evaluate the effect of enhancement in heat transfer rate and the increase in the pressure drop. This is defined as the ratio between the Nusselt number ratio $\left(Nu/Nu_{pt}\right)$ and friction factor ratio $\left(f/f_{pt}\right)^{\frac{1}{3}}$ for the same pumping power condition [44, 49, 50-51, 52, 56, 128]:

$$\eta = \frac{\left(Nu_i / Nu_{pt} \right)}{\left(f_i / f_{pt} \right)^{\frac{1}{3}}} \qquad (3.7)$$

where Nu_i and f_i denotes the Nusselt number and friction factor with enhancing factor (helical inserts), respectively. While, Nu_{pt} and f_{pt} represents the plain tube Nusselt number and friction factor, respectively

3.3 Results and Discussion

The experiments have been carried out to study the thermal performance of two different nanofluids (Al_2O_3/water and CNT/water) through a uniformly heated tube with helical twisted tape inserts of twist ratio, TR=1.5, 2.5, 3. Three cases are considered for the analysis. Initially, tests are performed using 0.15% concentration of nanofluids (Al_2O_3/water and CNT/water) in laminar flow regime (Re= 840-2280). Subsequently, the analysis is extended to study the thermal performance of nanofluids (Al_2O_3/water and CNT/water) in transition regime (2400-5600). In third case, the investigation has been extended to analyze the effect of nanoparticle concentration (φ=0.15, 0.45, 0.60, 1%) on the thermal performance of nanofluids. The effect of twist ratio on thermal performance of is studied in each case. The heat transfer enhancement and the increase of friction factor of nanofluids are evaluated by using the Nusselt number and friction factor of the basefluid in the plain tube as reference data.

3.3.1 Thermal performance of nanofluids through uniformly heated circular tube with helical twisted tape inserts in laminar flow regime

The experiments were carried out by using 0.15% volume concentration Al_2O_3/water and CNT/water nanofluid with helical tape inserts of twist ratio, TR= 1.5, 2.5 and 3. Reynolds number was varied in the range of 840 to 2280. The test data were used to calculate the Nusselt number, friction factor and thermal performance factor for various Peclet numbers in laminar flow regime with and without helical screw tape inserts. These are detailed below.

Heat transfer study

Initially, tests have been carried out by using pure water in order to validate the test facility. The Nusselt number of single phase fluid reported by Shah [124] is expressed below:

$$Nu = 1.953(\mathrm{Re}\,\mathrm{Pr}\frac{D}{x})^{1/3} \text{ for } \mathrm{Re}\,\mathrm{Pr}\frac{D}{x} \geq 33.33 \tag{3.8}$$

$$Nu = 4.364 + 0.0722(\mathrm{Re}\,\mathrm{Pr}\frac{D}{x}) \text{ for } \mathrm{Re}\,\mathrm{Pr}\frac{D}{x} \leq 33.33$$

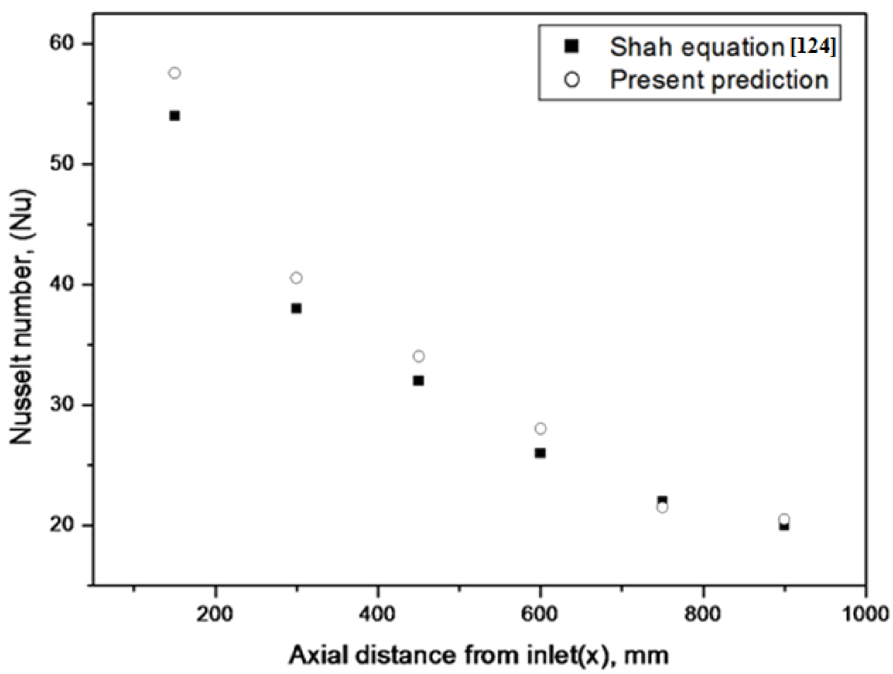

Figure 3.3: Variation of Nusselt number with Peclet number

The Nusselt number obtained from the present experimental study (Eq. 3.5) is compared with the values obtained from Shah Equation [124] and is shown in Fig. 3.3. The deviation between the present prediction obtained from Eq. (3.5) and the values obtained from Eq. (3.8) is found to be less than ± 7%. This indicates that the present test facility is in good condition and can be used to evaluate the heat transfer characteristics of both Al_2O_3/water and CNT/water nanofluid.

Figure 3.4 depicts the variation of Nusselt number with Peclet number for various working fluids and twist ratios. It is observed that Nusselt number increases with Peclet number. Tests have been carried out by using 0.15% volume concentration of Al_2O_3/water and CNT/water nanofluid. For given operating condition, the Nusselt number of both the nanofluids (Al_2O_3/water, CNT/water) was found to be higher compared to pure water. This may be due to the fact that the nanoparticles increase the thermal conductivity. In addition, the collision among nanoparticles and between the nanoparticles and tube wall increases the energy exchange rate leading to an increase in the heat transfer rate. Previous researchers have reported similar observations for Al_2O_3/water nanofluid in their experimental investigation [52]. Recently, Rathnakumar et al. [129] reported the experimental investigation of CNT/water nanofluids in circular tube with helical screw tape inserts in laminar flow regime. Their results exhibited lower heat transfer performance compared to present experimental study. This difference may be due to the use of surface modification method of nanoparticles during the synthesis of CNT/water nanofluids. In addition, the CNT/water nanofluid exhibits enormous enhancement in heat transfer compared to the Al_2O_3/water nanofluid for the similar conditions. This may be due to various reasons. Carbon nanotubes (CNTs) possess higher thermal conductivity, higher aspect ratio, lower specific gravity, larger specific surface area (SSA) and lower thermal resistance compared to Al_2O_3 [4, 103]. The CNT nanoparticles have porous structure and create capillary action leading to enhancement in heat transfer. It may be noted that the higher thermal conductivity and large specific surface area (SSA) of CNT nanoparticles play an important role in the heat transfer enhancement. In addition, the average size of the CNT and Al_2O_3 nanoparticles used in the present investigation is found to be 20 nm and ~100 nm, respectively. Therefore, the enhancement in heat transfer for CNT/water nanofluid is found to be higher compared to Al_2O_3/water nanofluid.

Tests have been carried out in order to evaluate the heat transfer enhancement of pure water and nanofluids with helical screw tape insert. Three different twist ratios (TR=1.5, 2.5 and 3) are considered in the present investigation and the results are depicted in Figs.3.4 and 3.5. The helical screw tape insert exhibits higher Nusselt number in both nanofluids and pure water. The enhancement in Nusselt number was found to increase with the decrease in the twist ratio (TR) for both pure water and nanofluids. The thermal performance of CNT/water nanofluid is found to be higher compared to Al_2O_3/water nanofluid and pure water both in the plain tube and the plain tube with helical screw tape inserts. The Nusselt number of various working fluids such as: CNT/water, Al_2O_3/water and pure water for the plain tube with helical inserts is higher compared to the plain tube for a given value of Peclet number. This may be due to the fact that the plain tube fitted with helical inserts decreases the hydraulic diameter and increases the fluid velocity leading to the increase in the Reynolds number. Therefore, the Nusselt number increases with inserts. In addition, the turbulent intensity of the fluid increases at the tube wall leading to excellent mixing. In such a case, the re-development of thermal and hydraulic boundary layer takes place leading to the enhancement in the heat transfer rate. The average enhancement in Nusselt number of Al_2O_3/water and CNT/water in the plain tube were found to be 10.72% and 20.27%, respectively compared to the water as the working fluid. The enhancement in Nusselt number decreases with the increase in Peclet number (Fig.3.5). In the case of Al_2O_3/water nanofluid, the increase in the average Nusselt number was found to 230.14%, 175.07% and 135.79%, for various twist ratios 1.5, 2.5 and 3, respectively. On the contrary, the enhancement in the Nusselt Number for CNT/water nanofluid was found

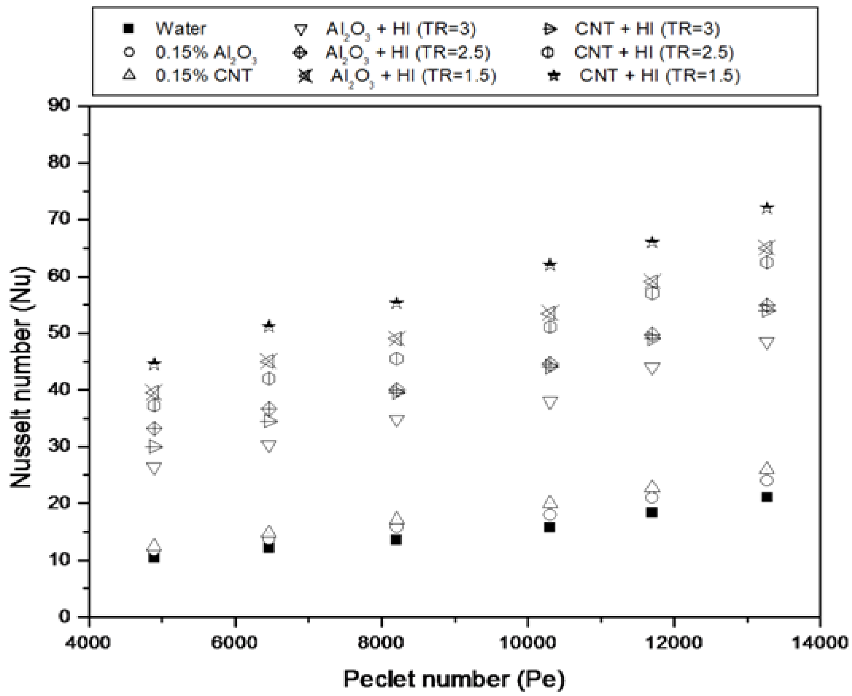

Figure 3.4: Variation of Nusselt number with Peclet number

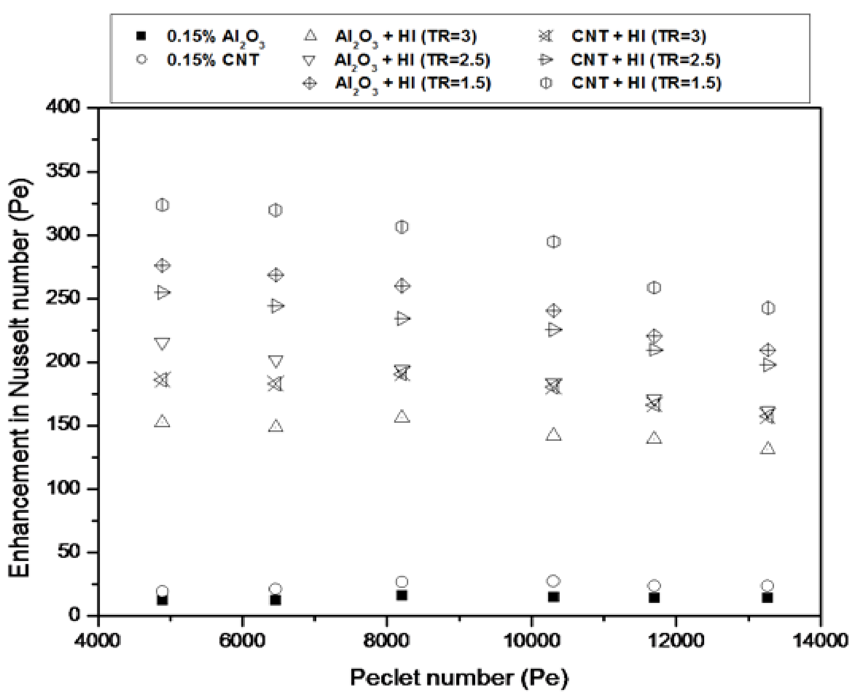

Figure 3.5: Enhancement in Nusselt number at different Peclet number

to be 272.61%, 213.58% and 166.45% for the twist ratios 1.5, 2.5 and 3, respectively. It may be noted that the enhancement in the convective heat transfer is due to the addition of nanoparticles in water and the use of helical screw tape inserts. For given Peclet number, the enhancement of Nusselt number of pure water with helical screw tape insert is larger compared to the enhancement of Nusselt number by using Al_2O_3/water and CNT/water nanofluids in the plain tube. It may be noted that the mechanism of heat transfer rate is different in both the cases. The heat transfer enhancement in the case of nanofluids is due to various reasons such as: improved thermal conductivity of nanofluids compared to pure water, Brownian motion of nanoparticles and particle migration. While, in the case of helical screw tape inserts, the random movement of the fluid particles increases the energy exchange rate leading to the enhancement in heat transfer. The higher turbulence intensity close to the tube wall results in excellent fluid mixing. This leads to redevelopment of thermal and hydraulic boundary layers and the enhancement in the heat transfer rate.

The present experimental results are used to derive the correlation among various parameters, namely, Nusselt number, Reynolds number, Prandtl number and twist ratio by using least square method of regression analysis (Eq. 3.9). The correlations are valid for laminar flow (Re < 2280), various twist ratios (1.5-3) and 0.15% volume concentration of both the nanofluids (Al_2O_3/water and CNT/water). The Nusselt number values predicted by the correlations are in reasonable agreement with the experimental results.

$$Nu = \begin{cases} 0.508(\mathrm{Re}\,\mathrm{Pr})^{0.529}(T.R.)^{-0.438}, & Al_2O_3\text{/water nanofluid} \\ \\ 0.631(\mathrm{Re}\,\mathrm{Pr})^{0.517}(T.R.)^{-0.430}, & \text{CNT/water nanofluid} \end{cases} \tag{3.9}$$

Pressure drop study

Tests have been carried out by using pure water in order to validate the test facility for friction factor. The friction factor values evaluated from the present experimental study are compared with the theoretical values obtained using the Hagen-Poiseuille equation given by:

$$f = \frac{64}{\mathrm{Re}} \tag{3.10}$$

In this study, the friction factor of water is obtained by using Eq. (3.6) and shown in Fig. 3.6. Present test data are found to be in good agreement with the values obtained by using Hagen-Poiseuille correlation (Eq. 3.10). The deviation between the present test data and theoretical values are found to be within ±5%.

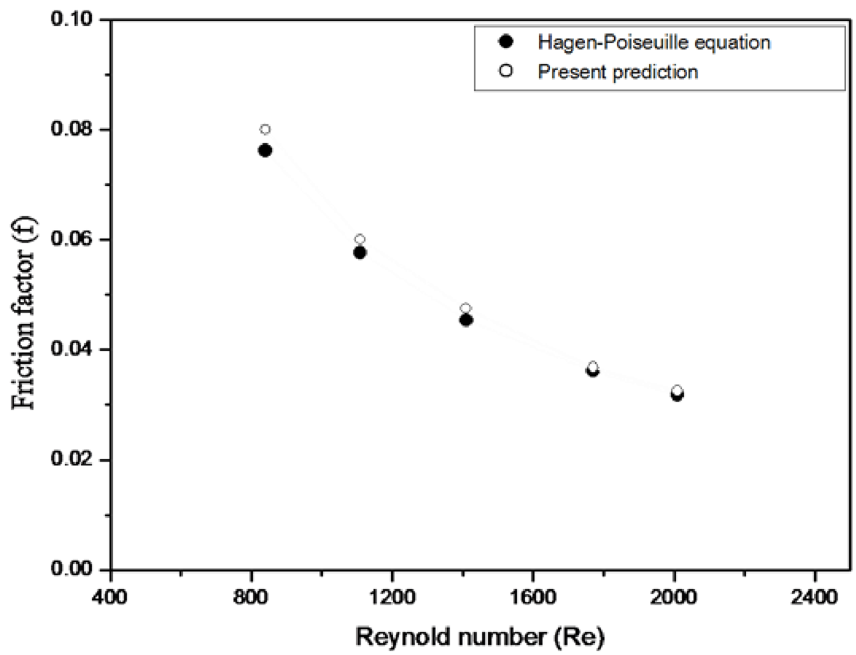

Figure 3.6: Variation of friction factor with Reynolds number

The variation of friction factor of various working fluids (CNT/water, Al_2O_3/water and pure water) with Peclet number for the plain tube and the plain tube with helical screw tape inserts is shown in Fig. 3.7. The increase in the pressure drop of pure water due to the dispersion of nanoparticles (CNT and Al_2O_3) is minimal. However, the pressure drop increases significantly with the use of helical inserts in the plain tube for both nanofluids (Al_2O_3/water and CNT/water). The friction factor found to increase with the decrease in the twist ratio. Compared to the plain tube with water, the maximum friction factor of CNT/water nanofluid with inserts was found to be 19.99, 13.24 and 11.80 times higher for twist ratios of 1.5, 2.5 and 3, respectively. The maximum friction factor of Al_2O_3/water nanofluid with inserts was found to be 20.43, 13.79 and 12.02 times the friction factor of plain tube with water for various twist ratios 1.5, 2.5 and 3, respectively. For a given twist ratio (TR=1.5), the Al_2O_3/water nanofluid exhibits higher pressure drop compared to CNT/nanofluid. This may be due to the fact that the larger size of Al_2O_3 particle (~100 nm) compared to CNT nanoparticle (20 nm). Because of the larger size of the Al_2O_3 particle, the nanofluid (Al_2O_3/water) exhibits higher viscosity and reduces the free flow area in the presence of inserts. Therefore, the pressure drop in the case of Al_2O_3/water nanofluid is higher compared to the CNT/water nanofluid.

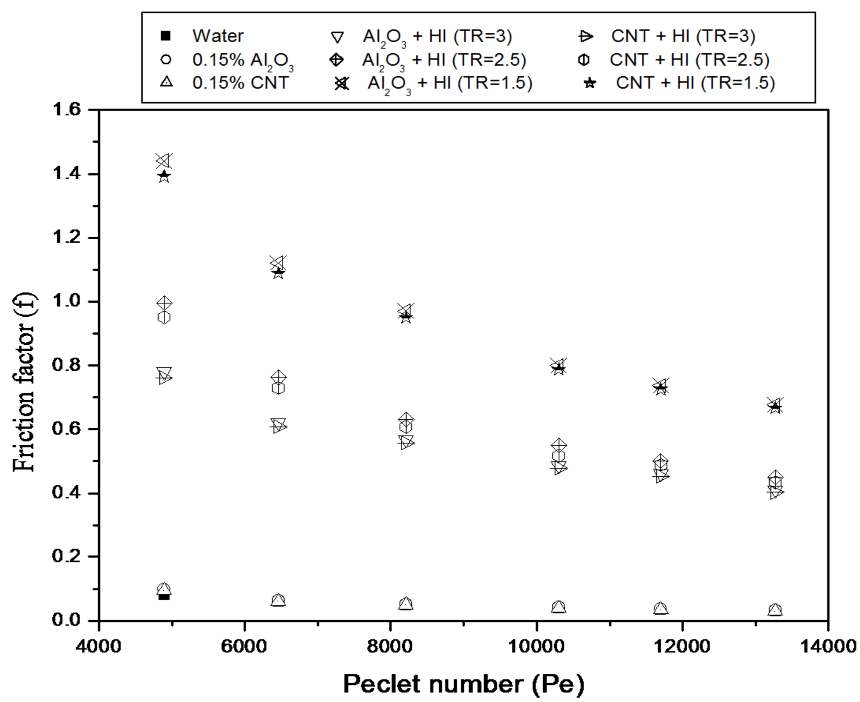

Figure 3.7: Variation of Nusselt number with Peclet number of nanocoolant

$$f = \begin{cases} 289.20(\mathrm{Re})^{-0.743}(\mathrm{T.R.})^{-0.791}, & \mathrm{Al_2O_3/water\ nanofluid} \\ 250.98(\mathrm{Re})^{-0.726}(\mathrm{T.R.})^{-0.796}, & \mathrm{CNT/water\ nanofluid} \end{cases} \quad (3.11)$$

The results obtained from the present experimental study are used to derive the correlations among various parameters such as: friction factor, Reynolds number and twist ratio by using least square method of regression analysis (Eq. 3.11). These correlations are valid for laminar flow (Re < 2280), different twist ratios (1.5-3) and 0.15% volume concentration of both the nanofluids (Al_2O_3/water and CNT/water). The friction factor values predicted by the correlations are in reasonable agreement with the experimental data.

Thermal performance factor

The variation of thermal performance factor (η) of various working fluids such as: Al_2O_3/water and CNT/water nanofluid with Peclet number is shown in Fig. 3.8. The values of η were found to be higher for the low twist ratios irrespective of the working fluid and Peclet number. This may be due to fact that the helical screw inserts with lower twist ratio generates stronger turbulence/swirl in the flow. This indicates that for a given operating condition, the helical screw tape inserts with the lower twist ratios should be considered for energy saving. The thermal performance factor *(η)* decreases with the increase in Peclet number. This may be due to the increase in the pressure drop with the increase in Peclet number. It may be noted that the value of η need to be greater than unity for the net energy gain in the system. The values of η for the CNT/water nanofluid are found to be higher compared to the Al_2O_3/water nanofluid and pure water for all twist ratios (1.5, 2.5 and 3) and for various Peclet number (5,000-13,300). The values of η are found to be higher for low twist ratios irrespective of the working fluid and Peclet number. This may be due to the stronger turbulence/swirl flow generated by the helical screw tape insert in the case of insert with lower twist ratio. For twist ratios of 1.5, 2.5 and 3, the thermal performance factor varies between 2.29-1.69, 2.03-1.55, and 1.69-1.35 respectively by using CNT/water nanofluid. On the contrary, the thermal performance factor of Al_2O_3/water nanofluid (by volume 0.15%) was found to vary between 2.14-1.65, 1.90-1.47 and 1.58-1.31 for the twist ratios of 1.5, 2.5 and 3, respectively.

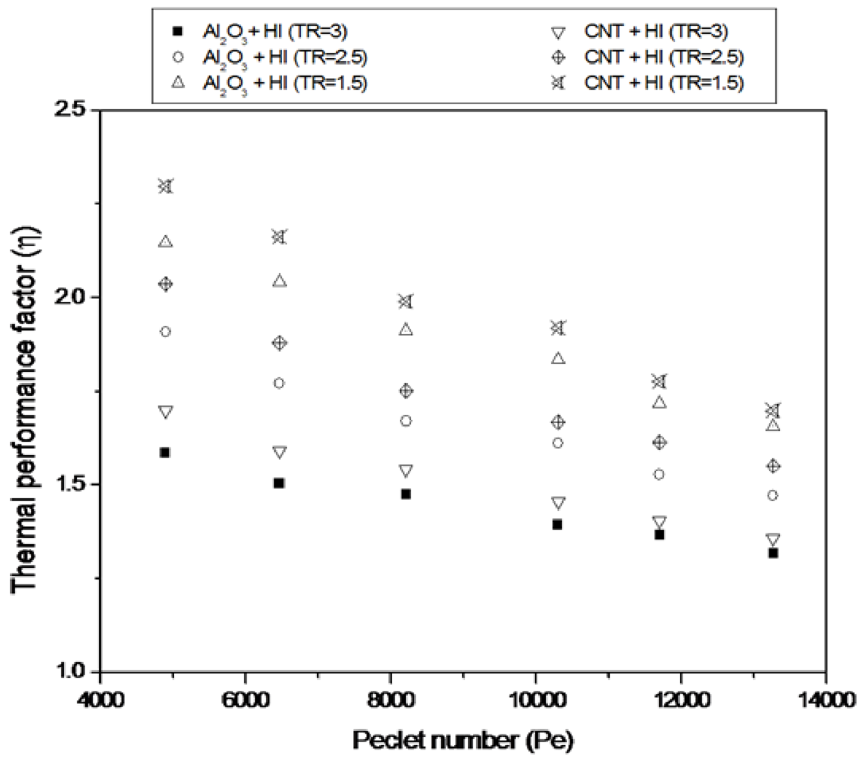

Figure 3.8: Variation of thermal performance factor with Peclet number

3.2.2 Thermal performance of nanofluids through uniformly heated circular tube with helical twisted tape inserts in transition flow

In section 3.2.1, the thermal performance of nanofluids through a uniformly heated tube with helical twisted tape inserts is analyzed in laminar flow regime. The investigation has been extended for transition flow using 0.15% volume concentration of Al_2O_3/water and CNT/water nanofluids. Here, Reynolds number is varied in the range of 2400 to 5600. The test data are used to calculate the Nusselt number, friction factor and thermal performance factor for various Peclet numbers in transition flow regime with and without helical screw tape inserts. These are detailed below.

Heat transfer study

Earlier, the test facility is validated in the laminar flow regime for Nusselt number and friction factor values using water as working fluid (section 3.2.1). Following the earlier analysis (section 3.2.1), here tests have been made with water as the working fluid in transition regime. The Nusselt number of single phase fluid reported by Gnielinski [125] is expressed below:

$$Nu = \frac{\left(\frac{\Gamma}{2}\right)(\mathrm{Re}-1000)\,\mathrm{Pr}}{1+12.7\left(\frac{\Gamma}{2}\right)^{0.5}\left(\mathrm{Pr}^{2/3}-1\right)} \tag{3.12}$$

where, $\Gamma = (1.58 \ln \mathrm{Re} - 3.82)^{-2}$, $2300 < \mathrm{Re} < 5\times10^{6}$ $0.5 < \mathrm{Pr} < 2000$

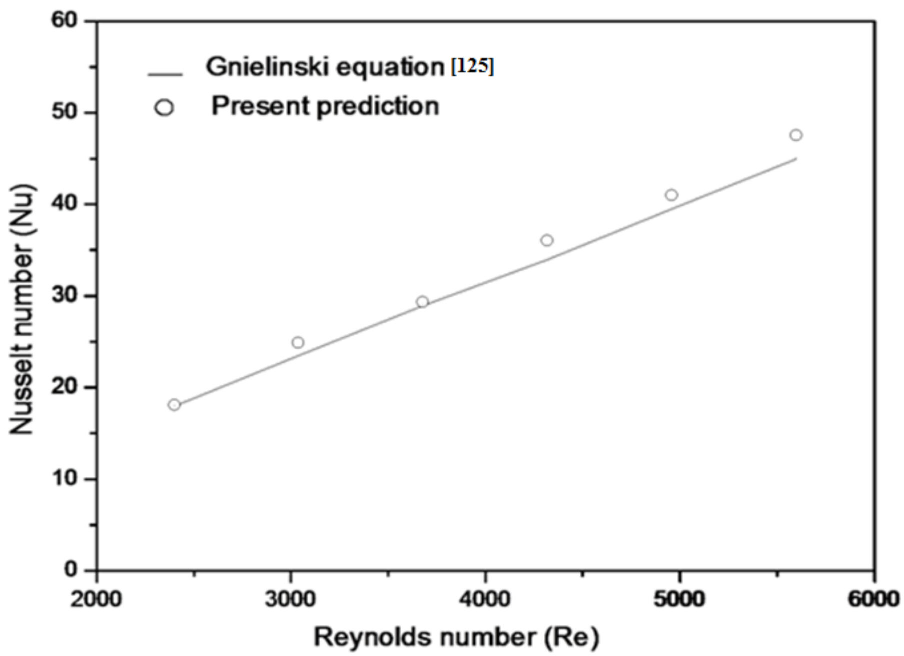

Figure 3.9: Comparison of experimental Nusselt number with Gnielinski equation

The Nusselt number for water obtained by using Eq. (3.5) is compared with the values obtained from Eq. (3.12) of Gnielinski [125] and are shown in Fig. 3.9. The deviation between the present prediction obtained from Eq. (3.12) and the values obtained from Eq. (3.5) is found to be less than ± 3%. This indicates that the present test facility is in good condition and can be used to evaluate the heat transfer characteristics of both Al_2O_3/Water and CNT/water nanofluid.

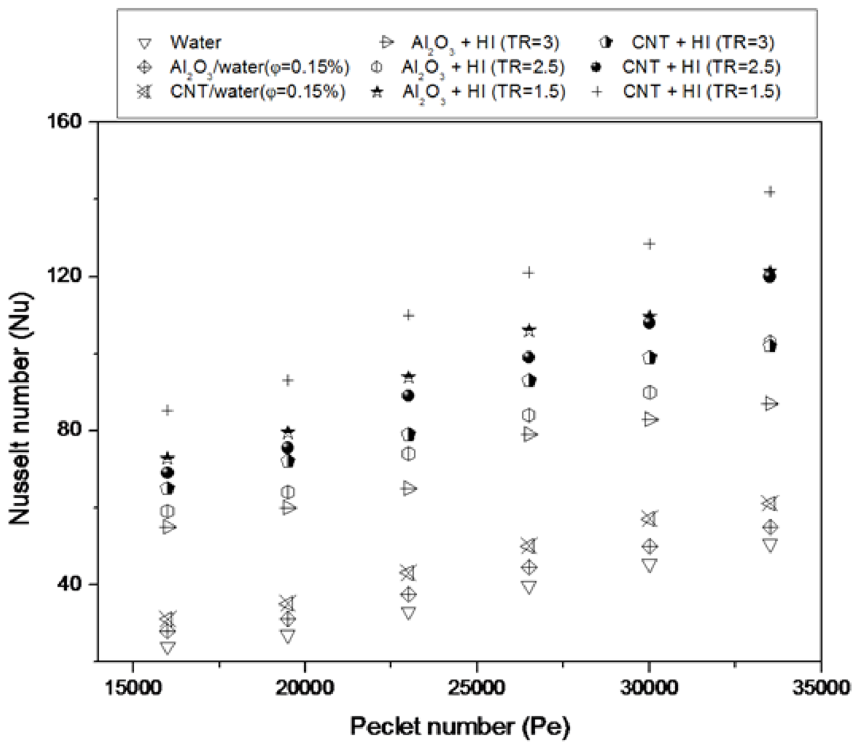

Figure 3.10: Variation of Nusselt number with Peclet number.

Figure 3.10 depicts the variation of Nusselt number with Peclet number. Under similar conditions, the Nusselt number of both the nanofluids (Al_2O_3/water, CNT/water) is higher than that of water. This may be due to the fact that the nanoparticles increase the thermal conductivity. In addition, the collision among nanoparticles and between the nanoparticles and tube wall increases the energy exchange rate leading to an increase in the heat transfer rate. It is observed that Nusselt number increases with Peclet number. Tests have been carried out using 0.15% volume concentration of Al_2O_3/water and CNT/water nanofluid. The heat

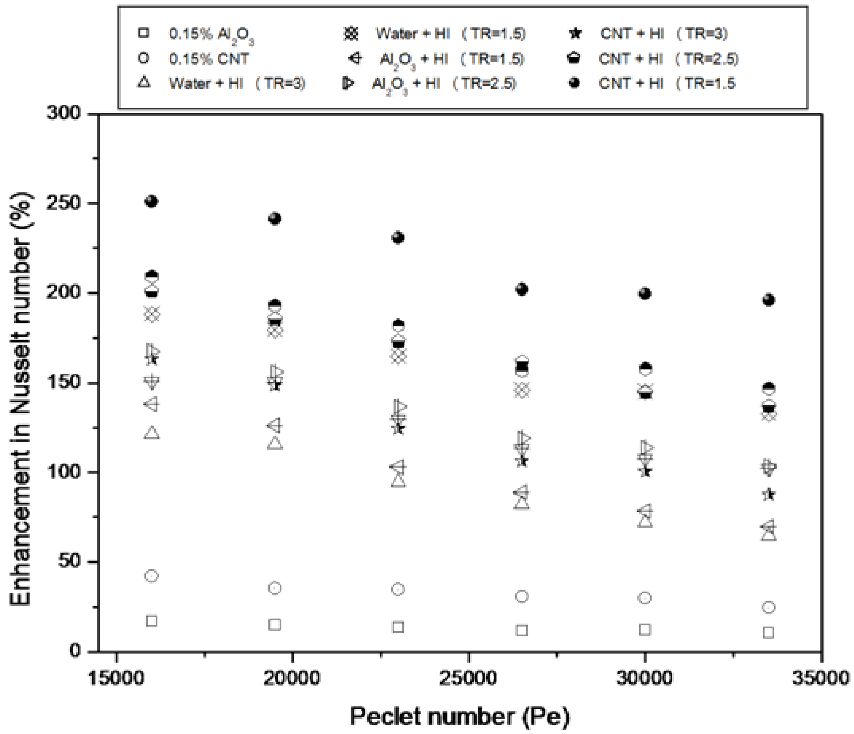

Figure 3.11: Enhancement in Nusselt number at different Peclet number

transfer characteristics of both nanofluids (Al_2O_3/water and CNT/water) were found to be higher compared to the pure water. In addition, the CNT/water nanofluid exhibits enormous enhancement in heat transfer over the Al_2O_3/water nanofluid for the similar conditions. Previous researchers [53] have reported a similar observation for Al_2O_3/water nanofluid in their experimental investigation. This may be due to the following reasons. The size of the CNT and Al_2O_3 nanoparticles used in the present investigation is found to be 20 nm and ~100 nm, respectively. Carbon nanotubes (CNTs) possess higher thermal conductivity, higher aspect ratio, lower specific gravity, larger specific surface area (SSA) and lower thermal resistance compared to Al_2O_3 [4, 103]. The CNT nanoparticle have a porous structure, CNT in water creates capillary action leading to enhancement in heat transfer. It may be noted that the higher thermal conductivity and large specific surface area (SSA) of CNT nanoparticles play an important role in the heat transfer enhancement. Therefore, the enhancement in heat transfer for CNT/water nanofluid is found to be higher compared to Al_2O_3/water nanofluid.

Tests have been carried out in order to estimate the heat transfer enhancement of pure water and nanofluids with helical screw tape insert. Three different twist ratios namely, TR=1.5, 2.5 and 3 are considered in the analysis and the results are depicted in Figs. 3.10 and 3.11. The helical screw tape insert exhibits higher Nusselt numbers in both nanofluids and pure water. It is observed that the enhancement in Nusselt number was found to increase with the decrease in the twist ratio (TR) for both pure water and nanofluids. The thermal performance of CNT/water nanofluid is found to be higher compared to Al_2O_3/water nanofluid and pure water both in the plain tube and the plain tube with inserts. It is observed that the Nusselt number of all the working fluids, namely, CNT/water, Al_2O_3/water and pure water for the plain tube with helical inserts is higher compared to the plain tube for a given Peclet number. This is due to the fact that the plain tube fitted with helical inserts decreases the hydraulic diameter and increases the fluid velocity leading to the increase in the Reynolds number; and therefore the Nusselt number increases with inserts**.** In addition to this, the turbulent intensity of the fluid increases at the tube wall leading to excellent mixing. This leads to the re-development of thermal and hydraulic boundary layer which enhances the heat transfer rate. The average enhancement in Nusselt number of Al_2O_3/water and CNT/water in the plain tube were found to be 12.02% and 26.13%, respectively compared to the water as the working fluid. The enhancement in Nusselt number was found to decrease with the increase in Peclet number and is shown in Fig. 3.11. The enhancement in the Nusselt number of pure water with various twist ratios 1.5, 2.5 and 3 were found to be 159.60%, 125.85% and 91.30%, respectively. In addition, the increase in the average Nusselt number for various twist ratios 1.5, 2.5 and 3 were found to be 172.81%, 131.21% and 99.33%, respectively for Al_2O_3/water nanofluid. While, the CNT/water nanofluid exhibits 215.55%, 173.25% and 120.32%enhancement in the Nusselt Number corresponding to the twist ratios 1.5, 2.5 and 3, respectively. It may be noted that the enhancement in the convective heat transfer is due to the addition of nanoparticles and the use of helical screw tape inserts. It is observed that the enhancement of Nusselt number of pure water with helical screw tape insert is larger compared to the enhancement of Al_2O_3/water and CNT/water nanofluids in the plain tube for a given Peclet number. It may be noted that the mechanism of heat transfer rate is different in both the cases. The heat transfer enhancement in the case of nanofluids is due to various reasons such as: improved thermal conductivity of nanofluids compared to pure water, Brownian motion of nanoparticles and particle migration. While, the enhancement in heat transfer with the helical screw tape inserts is due to the random movement of the fluid particles that increases the energy exchange rate leading to the enhancement in heat transfer. The higher turbulence intensity close to the tube wall results in an excellent fluid mixing and the redevelopment of thermal and hydraulic boundary layers. This essentially enhances the heat transfer rate.

Pressure drop study

Tests have been carried out by using pure water in order to validate the test facility for friction factor in transition flow regime. Blasius [130] developed an expression in order to evaluate the friction factor of pure water valid in the range of $3000 < \mathrm{Re} < 10^5$ and expressed as:

$$f = \frac{0.316}{\mathrm{Re}^{0.25}} \tag{3.13}$$

The experimental friction factor of water is obtained by using Eq. (3.6) and is shown in Fig. 3.13. Present test data is found to be in good agreement with the values obtained by using Blasius [130] correlation (Eq.

3.13). The deviation between the present test data and theoretical values are found to be within ±4%.

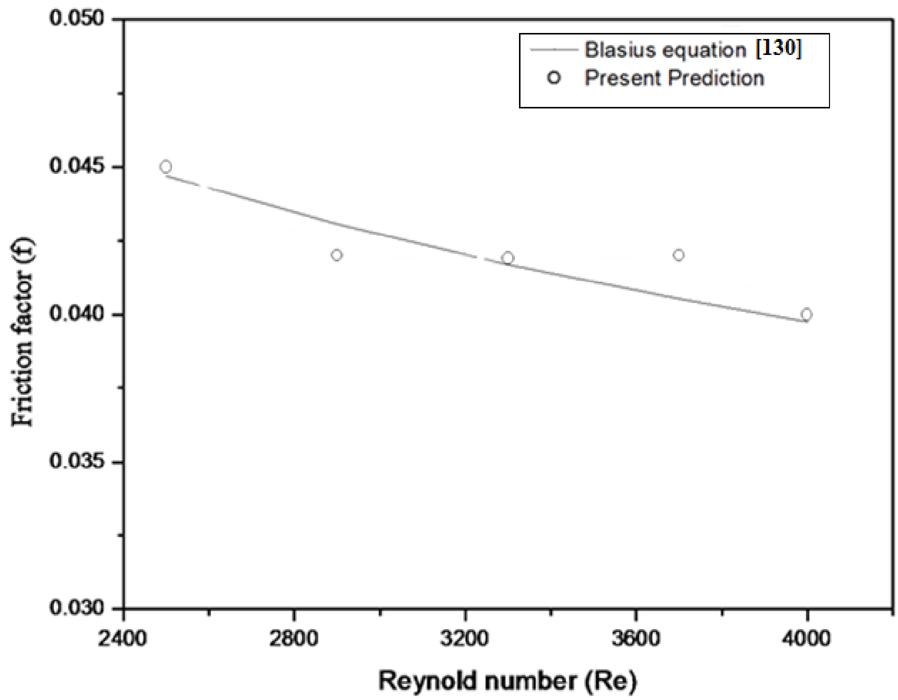

Figure 3.12: Comparison of experimental friction factor with Blasius equation

Figure 3.13 depicts the variation of friction factor of various working fluids, namely, CNT/water, Al_2O_3/water and pure water with Peclet numbers both for the plain tube and the plain tube with helical screw tape inserts. However, the pressure drop was found to increase significantly with the use of helical inserts in the plain tube for both Al_2O_3/water and CNT/water nanofluids. It is observed that the friction factor increases with a decrease in the twist ratio. The maximum friction factor of CNT/water nanofluid with inserts was found to be 7.75, 6.67 and 6.15 times the friction factor of a plain tube with water corresponding to twist ratios of 1.5, 2.5 and 3, respectively at Pe =16000. While, the maximum friction factor of Al_2O_3/water nanofluid with inserts was found to be 8.04, 6.95 and 6.19 times the friction factor of plain tube with water corresponding to twist ratios of 1.5, 2.5 and 3, respectively at Pe =16000. It is observed that at TR=1.5, the Al_2O_3/water nanofluid exhibits higher pressure drop compared to CNT/nanofluid. This may be due to the fact of the larger size of an Al_2O_3 particle (~100 nm) compared to a CNT nanoparticle (20 nm). Because of the larger size of the Al_2O_3 particle, the nanofluid (Al_2O_3/water) exhibits higher viscosity and reduces the free flow area in the presence of inserts. Therefore, the pressure drop in the case of Al_2O_3/water nanofluid is higher compared to the CNT/water nanofluid.

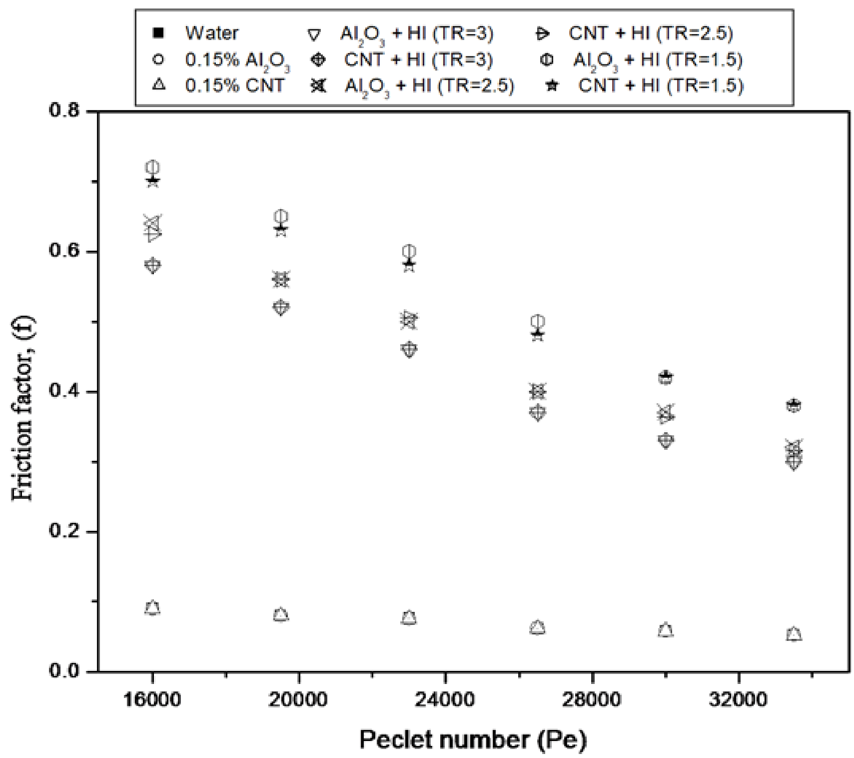

Figure 3.13: Variation of friction factor with Peclet number

Thermal performance factor

Figure 3.14 depicts the variation of thermal performance factor of various working fluids, namely, water, Al_2O_3/water and CNT/water nanofluid with Peclet number. It is observed that the values of η are higher for the low twist ratios irrespective of the working fluid and Peclet number. This may be due to the generation of stronger turbulence/swirl flow by the helical screw inserts with lower twist ratio. This indicates that helical screw tape inserts with the lower twist ratios should be considered for the saving of energy for a given operating condition. In addition, the thermal performance factor (η) was found to decrease with the increase in Peclet number. This may be due to the increase in the pressure drop with the increase in Peclet number.

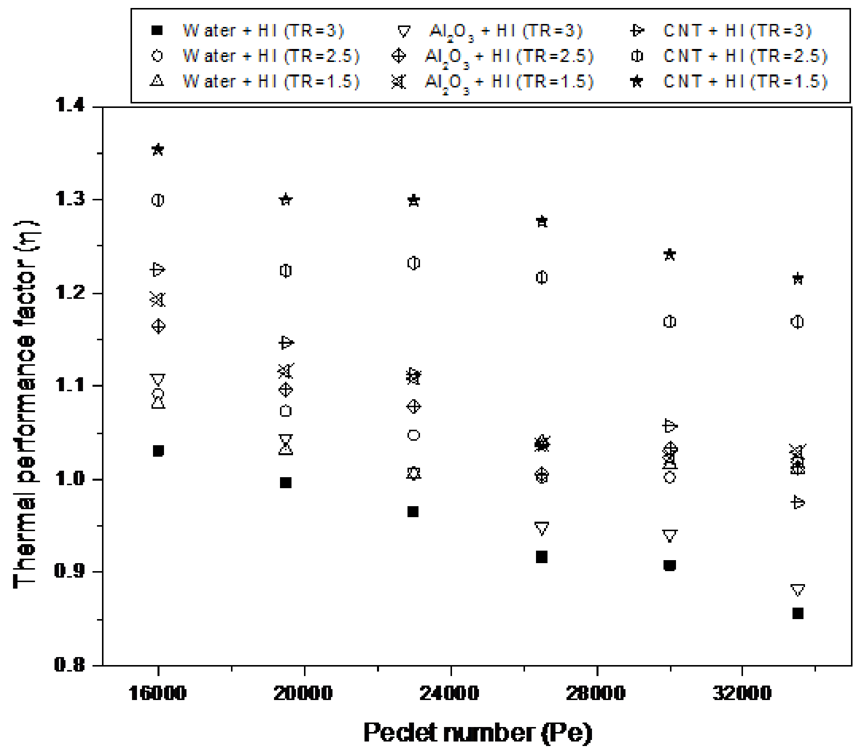

Figure 3.14: Variation of thermal performance factor with Peclet number

It may be noted that the value of η needs to be greater than unity for the net energy gain in the system. The values of η for the CNT/water nanofluid is found to be higher compared to the Al_2O_3/water nanofluid and pure water for all twist ratios (1.5, 2.5 and 3) and for the Peclet number varying between 16,000-33,500. It is observed that the values of η are higher for the low twist ratios irrespective of the working fluid and Peclet number. This is due to the stronger turbulence/swirl flow generated by the helical screw tape insert in the case of insert with the smallest twist ratio. Here, η is found to vary between 1.35-1.16, 1.29-1.21and 1.22-0.97 for twist ratios of 1.5, 2.5 and 3, respectively using CNT/water nanofluid as the working fluid. While, the thermal performance factor of the Al_2O_3/water nanofluid (by volume 0.15%) varies between 1.19-1.02, 1.16-1.01and 1.10-0.88 for the twist ratios of 1.5, 2.5 and 3, respectively.

3.3.3 Thermal performance of nanofluids of varied particle volume fraction through uniformly heated circular tube with helical twisted tape inserts in transition flow regime

The thermal performance of nanofluid for given particle volume concentration (φ= 0.15 %) with helical twisted tape inserts is discussed in previous section (3.2.1 and 3.2.2). It argued that the thermal performance increases with the nanoparticle concentration [4, 19-43, 46-46]. In view of this, experiments were carried out by using Al_2O_3/water and CNT/water nanofluid with varied range of particle volume concentration, φ= 0.15 %, 0.30%, 0.60% and 1% and helical tape inserts of twist ratios, TR= 1.5, 2.5 and 3. Here, Peclet number is varied in the range of 16000 to 33500. The thermal performance factor is evaluated for various Peclet numbers with and without helical screw tape inserts. This is detailed below:

Heat transfer study

Figure 3.15(a-d) depicts the variation of Nusselt number with Peclet number for water and nanofluids with helical tape inserts of various twist ratio (TR= 1.5, 2.5 and 3). Tests have been carried out with varied range of particle volume concentration (0.15, 0.45%, 0.60% and 1%) of Al_2O_3/water and CNT/water nanofluid. It is observed that the Nusselt number increases with the increase in the nanoparticle concentration and Peclet number. For similar operating conditions, the Nusselt number value of both the nanofluids (Al_2O_3/water, CNT/water) is higher compared to water. The increase in the nanoparticle concentration results in an increase in the effective thermal conductivity. The convective heat transfer enhancement of nanofluids may be due to several factors namely, improved effective thermal conductivity of the nanofluid over the base fluid (water), Brownian motion of nanoparticles, and particle migration [19-43, 46-46]. The heat transfer characteristics of both nanofluids (Al_2O_3/water and CNT/water) were found to be higher compared to the pure water. In addition, the CNT/water nanofluid exhibits enormous enhancement in heat transfer compared to Al_2O_3/water nanofluid for the similar operating conditions. Earlier several researchers [53] reported similar observation for Al_2O_3/water nanofluid in their experimental investigation. This may be due to the various factors. The average size of the CNT and Al_2O_3 nanoparticles used in this study is found to be 20 nm and ~100 nm, respectively. Carbon nanotubes (CNTs) possess higher thermal conductivity, higher aspect ratio, lower specific gravity, larger specific surface area (SSA) and lower thermal resistance compared to Al_2O_3 [4, 103]. In addition, the porous structure of CNT creates capillary action resulting in enhancement in heat transfer. It may be noted that the higher thermal conductivity and large specific surface area (SSA) of CNT nanoparticles play an important role in the heat transfer enhancement. Therefore, the enhancement in heat transfer for CNT/water nanofluid is found to be higher compared to Al_2O_3/water nanofluid.

Tests were performed to evaluate the heat transfer enhancement of pure water and nanofluids with helical screw tape insert. Three different twist ratios namely, TR=1.5, 2.5 and 3 and varied range of particle volume concentration (0.15%, 0.45%, 0.60% and 1%) of Al_2O_3/water and CNT/water nanofluid are considered in the analysis and the results are depicted in Figs. 3.15 (a-d). The helical screw tape insert exhibits higher Nusselt number in both nanofluids and pure water. The enhancement in Nusselt number is found to increase with the increase in particle volume concentration. The Nusselt number increases with the decrease in the twist ratio (TR) for nanofluids of various particle volume concentrations. The thermal performance of CNT/water nanofluid is found to be higher compared to Al_2O_3/water nanofluid and pure water both in the plain tube

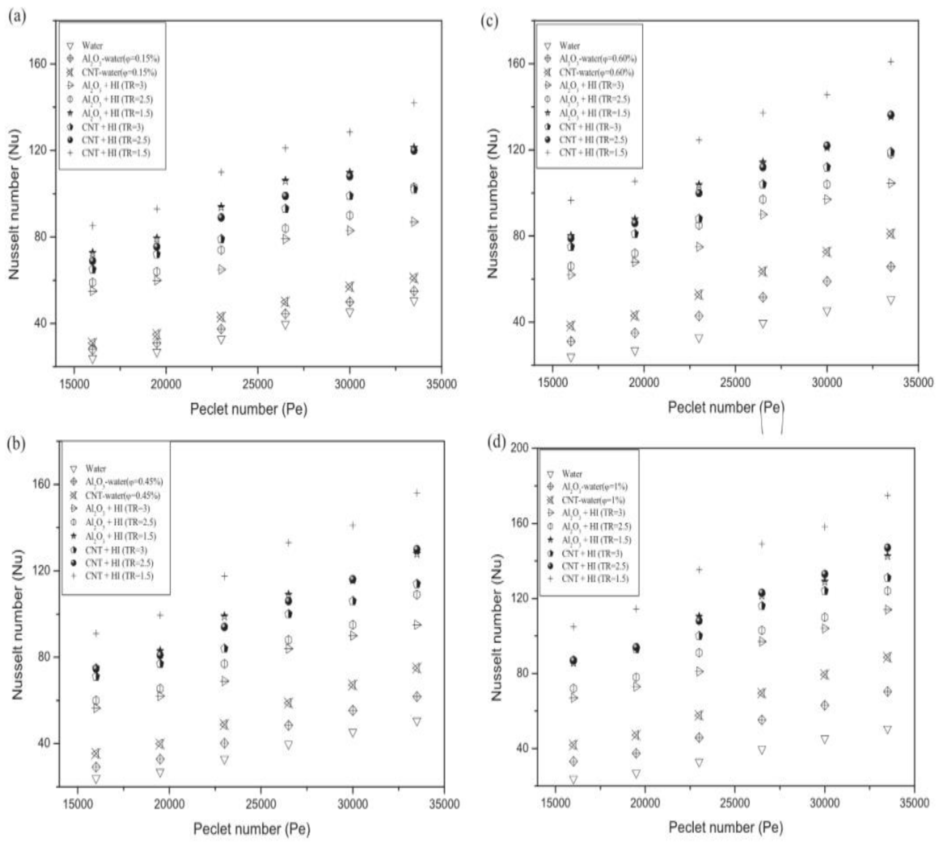

Figure 3.15: Variation of Nusselt number with Peclet number for particle volume fraction: (a) φ=0.15%, (b) φ=0.45%, (d) φ=0.60% and (d) φ=1%

and the plain tube with inserts. For a given Peclet number, the Nusselt number of various working fluids (CNT/water, Al_2O_3/water and pure water) with tube with helical inserts is higher compared to the plain tube. This is due to the fact that the tube fitted with helical inserts decreases the hydraulic diameter and increases the fluid velocity leading to the increase in the Reynolds number and therefore the Nusselt number increases with inserts**.** In addition, the helical insert increases the random movement of the nanoparticles and the energy exchange rates in the nanofluid. The higher turbulence intensity of the fluid close to the tube wall and the helical insert is responsible to promote thorough mixing of nanofluid. This leads to an efficient redevelopment of the thermal or hydrodynamic boundary layer which consequently results in the improvement of convective heat transfer.

Fig. 3.15 (a-d) depicts the variation in Nusselt number with Peclet number and particle volume concentration. The enhancement in Nusselt number was found to increase with the increase in particle volume concentration. It is observed that, Nusselt number decreases with increase in Peclet number. The average increase in Nusselt number were found to be 39.03% and 75.02% by using Al_2O_3/water (φ=1%) and CNT/water nanofluid (φ=1%), respectively compared to the pure water results. The average increase in the Nusselt number of pure water for twist ratios 1.5, 2.5 and 3 were found to be 156.71%, 123.49% and 90.30%, respectively. In case of pipe fitted with helical inserts both nanofluids (Al_2O_3/water and CNT/water nanofluid) exhibit maximum enhancement in Nusselt number at 1% particle volume concentration. The increase in the average Nusselt number for various twist ratios 1.5, 2.5 and 3 were found to be 210.74%, 163.20% and 144.08%, respectively for Al_2O_3/water nanofluid with 1% particle volume concentration.

While, the CNT/water nanofluid (φ=1%) exhibits 280.91%, 215.11% and 196.44% average increase in Nusselt number corresponding to the twist ratios 1.5, 2.5 and 3, respectively. It may be noted that the enhancement in the convective heat transfer of water is due to the addition of nanoparticles and the use of helical screw tape inserts. For a given Peclet number, pure water with helical screw tape insert exhibits higher enhancement various nanofluids (Al_2O_3/water and CNT/water) in the plain tube. It may be noted that the mechanism of heat transfer rate is different in both the cases. The heat transfer enhancement in the case of nanofluids is due to various reasons such as: improved thermal conductivity of nanofluids compared to pure water, Brownian motion of nanoparticles and particle migration. While, the enhancement in heat transfer with the helical screw tape inserts is due to the random movement of the fluid particles that increases the energy exchange rate leading to the enhancement in heat transfer. The higher turbulence intensity close to the tube wall results in an excellent fluid mixing and the redevelopment of thermal and hydraulic boundary layers. This essentially enhances the heat transfer rate.

Pressure drop study

Fig. 3.16 (a-d) shows the friction factor variations with Peclet number. The friction factor increases with the increase in particle volume concentration for various nanofluids (CNT/water and Al_2O_3/water). This may be due to the fact that viscosity of nanofluids increases with nanoparticle concentration. While friction factor found to decrease with the increase in Peclet numbers. In addition Figure 3.16 (a-d) depicts the variation of friction factor with Peclet numbers for various working fluids, namely, CNT/water, Al_2O_3/water and pure water for the plain tube with helical screw tape inserts. The pressure drop was found to increase significantly with the use of helical inserts in the plain tube for both Al_2O_3/water and CNT/water nanofluids. It is observed that the friction factor increases with the decrease in the twist ratio. The maximum friction factor values obtained for CNT/water nanofluid (φ=1%) were found to be 14.96, 13.40 and 12.51 times compared to the water results at twist ratios 1.5, 2.5 and 3, respectively. While, the maximum friction factor of Al_2O_3/water nanofluid(φ=1%) with inserts was found to be 19.62, 16.58 and 15.57 times the friction factor for plain tube with water for twist ratios of 1.5, 2.5 and 3, respectively. It is observed that at TR=1.5, the Al_2O_3/water nanofluid exhibits higher pressure drop compared to CNT-nanofluid. This may be due to the larger size of a Al_2O_3 particle (~100 nm) compared to a CNT nanoparticle (20 nm). It may be noted that larger size of the Al_2O_3 particle exhibits higher viscosity for Al_2O_3/water nanofluid and resulting in the reduction in the free flow area in the presence of inserts. Therefore, the pressure drop in the case of Al_2O_3/water nanofluid is higher compared to the CNT/water nanofluid.

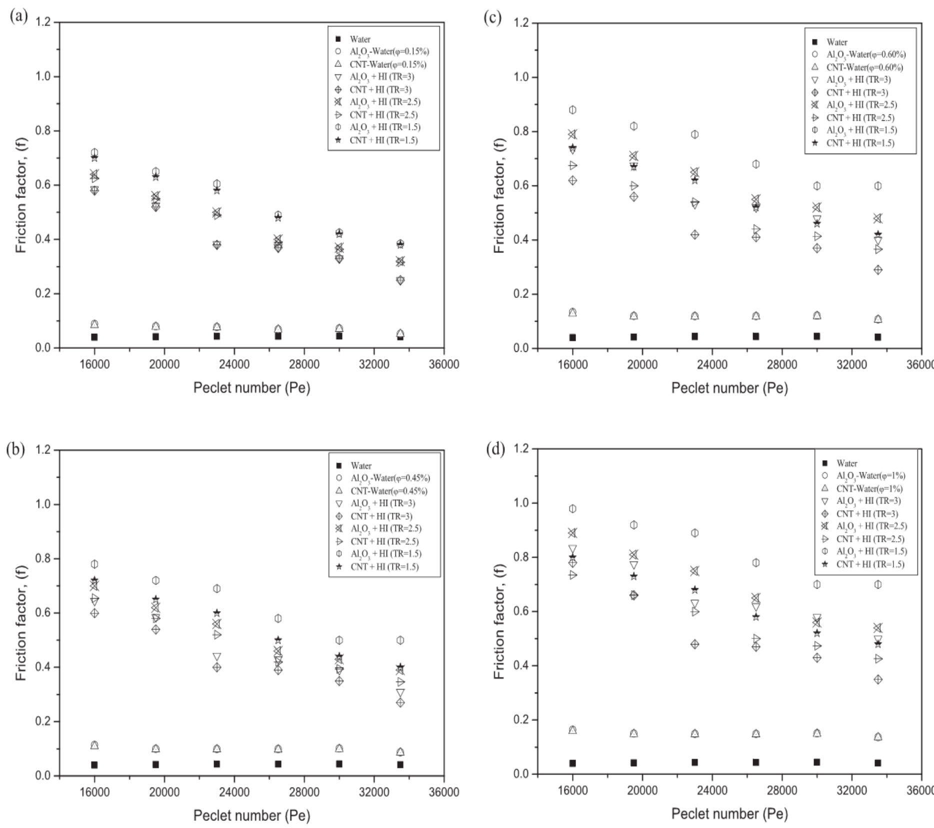

Figure 3.16: Variation of friction factor with Peclet number for particle volume fraction: (a) φ=0.15%, (b) φ=0.45%, (d) φ=0.60% and (d) φ=1%

Thermal performance factor

Thermal performance factor (η) or overall enhancement ratio (OER) is the parameter usually used to evaluate the effect of enhancement in heat transfer rate and the increase in the pressure drop. This parameter involves the Nusselt number as heat transfer performance parameter and the friction factor as pumping power or pressure drop parameter. Figure 3.17 (a-d) depicts the variation of thermal performance factor of various working fluids, namely, Al_2O_3/water and CNT/water nanofluid with Peclet number. It is observed that the values of η are higher for the low twist ratios irrespective of the working fluid and Peclet number. This may be due to the generation of stronger turbulence/swirl flow by the helical screw inserts with lower twist ratio. This indicates that helical screw tape inserts with the lower twist ratios should be considered for the saving of energy for a given operating condition. In addition, the thermal performance factor (η) was found to decrease with the increase in Peclet number. This may be due to the increase in the pressure drop with the increase in Peclet number. Moreover, increase in particle volume concentration for Al_2O_3/water and CNT/water nanofluid increases thermal performance factor for all Peclet number.

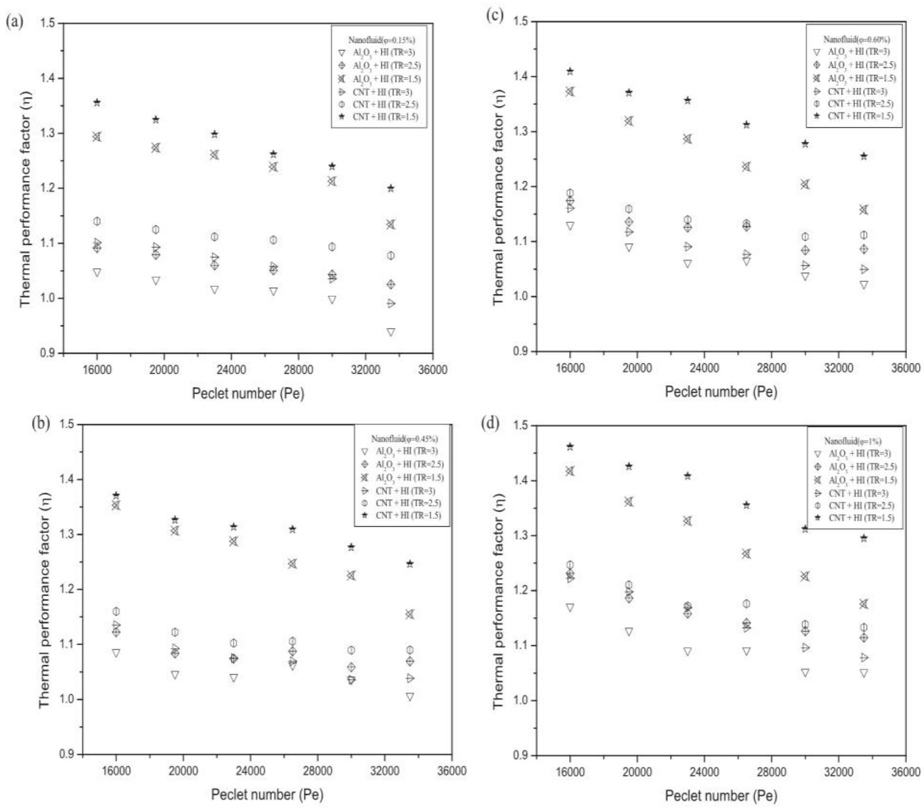

Figure 3.17: Variation of thermal performance factor with Peclet number for particle volume fraction: (a) φ=0.15%, (b) φ=0.45%, (d) φ=0.60% and (d) φ=1%

It may be noted that the value of η needs to be greater than unity for the net energy gain in the system. The thermal performance factor of CNT/water nanofluid is found to be greater than unity for varied range of Peclet number (16000-33500), twist ratio (T.R. = 1.5, 2.5 and 3) and particle volume concentration (φ= 0.15%, 0.45%, 0.60% and 1%). Here, Al_2O_3/water nanofluid exhibits lower thermal performance factor only

(η <1) for TR=3, φ=0.15% and Pe >30000. While the thermal performance factor different twist ratio (T.R. = 1.5, 2.5 and 3) and with particle volume concentration (φ= 0.15%, 0.45%, 0.60% and 1%) are found to be greater than unity. Previous researchers [53] have reported a similar observation for Al_2O_3/water nanofluid in their experimental investigation. The values of η for the CNT/water nanofluid is found to be higher compared to the Al_2O_3/water nanofluid and pure water for various twist ratios (1.5, 2.5 and 3) and different volume concentrations (φ= 0.15%, 0.45%, 0.60% and 1%) at all Peclet number. It is observed that the values of η are higher for the lower twist ratios irrespective of the working fluid and Peclet number. This is due to the stronger turbulence/swirl flow generated by the helical screw tape insert with the smallest twist ratio. For φ=1% and TR=1.5, Pe=16000, both of nanofluids (Al_2O_3/water and CNT/water nanofluid) exhibits maximum value of thermal performance factor (η). The maximum value of thermal performance factor (η) found to be 1.46 and 1.41 for Al_2O_3/water nanofluid and CNT/water nanofluid, respectively.

3.4 Concluding Remarks

This chapter reports study of the thermal performance of two different nanofluids (Al_2O_3/water and CNT/water) through a uniformly heated tube with helical twisted tape inserts. It includes thermal performance evaluation of nanofluids in the laminar regime, transition regime and varied range of nanoparticle concentration.

In the first problem, thermal performance of water and nanofluids with 0.15 % volume concentration is analyzed for twist ratio (TR= 1.5, 2.5, 3) and Reynolds number (840-2280). The test data are used to evaluate the Nusselt number, friction factor and thermal performance factor of various nanofluids for varied range of Peclet number. In addition, efforts have been made to prepare to propose a correlation for the friction factor as a function of Reynolds number and twist ratio for both nanofluids. Also, based on the test data a correlation for Nusselt number is proposed as a function of Reynolds number, Prandtl number and twist ratio.

Next, the analysis is extended to evaluate the thermal performance of various nanofluids (Al_2O_3/water and CNT/water) with 0.15 % volume concentration for several twist ratio (TR= 1.5, 2.5, 3) and Reynolds number (2400-5600). The enhancement in heat transfer, friction factor of nanofluid compared to pure water is reported. In addition, the thermal performance factor of various nanofluids is discussed. Based on the analysis, Nusselt number and friction factor of nanofluids is found to be higher in laminar flow regime compared to transition regime for given twist ratio and working fluid.

In the last problem, the effect of nanoparticle concentration on the thermal performance is studied for the transition flow regime. Four different concentrations are used in the investigation. The enhancement in the heat transfer and friction factor of nanofluids for various nanoparticle concentrations is studied through experimental investigation. The Nusselt number increases with increase in Peclet number and nanoparticle concentration. The thickness of boundary layer gets thinner at higher Reynolds number and adding nanoparticles to base fluid enhances the thermal conductivity. The friction factor increases with the increase in particle volume concentration for various nanofluids (CNT/water and Al_2O_3/water). This may be due to the fact that viscosity of nanofluids increases with nanoparticle concentration. While the friction factor is found to decrease with the increase in Peclet numbers.

The Nusselt number for the tube fitted with helical inserts is found to be higher compared to the plain tube for a given Peclet number. The tube fitted with helical tapes decreases the hydraulic diameter leading to the increase in the fluid flow and swirl generation. The enhancement in Nusselt number decreases with the increase in Peclet number and increases with the decrease in the twist ratio (TR). The experimental results reveal that CNT/water nanofluid gives enormous enhancement in heat transfer compared to Al_2O_3/water nanofluid. The value of friction factor increases with the decrease in twist ratio. The increase in the friction factor by the addition of Al_2O_3 and CNT nanoparticle in base fluid is minimal because of the low volume concentration of nanoparticles. The experimental results show that helical screw tape inserts give better thermal performance for CNT/water nanofluid compared to Al_2O_3/water nanofluid. For a given operating condition, the thermal performance factor for CNT/water nanofluid is higher compared to Al_2O_3/water for all twist ratios.

This experimental study shows the enhancement is heat transfer of various nanofluids through uniformly heated tube with helical screw tape inserts. Seeing the better heat transfer capability of nanofluids, the analysis is extended to analyze the thermal performance in an automobile radiator and is discussed in the next chapter.

Chapter 4

Thermal Performance of Nanofluids through an Automobile Radiator

4.1 Introduction

A steady-state heat exchanger consists of a fluid flowing through a pipe or system of pipes, where heat is transferred from one fluid to another. Hot (cold) fluid flows through a system of pipes and cold (hot) fluid flows over the pipes resulting in the exchange of heat from the hot (cold) fluid to the cool (hot) fluid. The automobile engine utilizes a heat exchanger device, termed as a radiator, in order to remove the heat from the cooling jacket of the engine. In case of radiators, the addition of fins is one of the approaches to increase the cooling rate. It provides greater heat transfer area and enhances the air convective heat transfer coefficient. However, this traditional approach of increasing the cooling rate by using fins and microchannel has already reached their limit. In addition, heat transfer fluids at fluid side such as: water and ethylene glycol exhibit very low thermal conductivity. In view of this, the new technique is needed to improve the existing cooling performance of heavy vehicle engines. It may be noted that use of nanofluid in an automobile radiator can enhance the heat removal rate leading to the reduction in size of the cooling system. In addition, the smaller size could reduce the drag and leading to lesser fuel consumption.

In the present chapter, the thermal performance is evaluated by using nanofluids through an automobile radiator with the varied range of particle volume concentration (φ= 0.15 %, 0.30%, 0.60% and 1%). Two different cases are considered for the analysis. Initially, tests are conducted to study the thermal performance of CNT/water nanofluid. Later on, the analysis is extended to evaluate the thermal performance of Al_2O_3/water nanofluids through a radiator. Subsequently, the thermal performance of CNT/water nanofluid and Al_2O_3/water nanofluids is compared for same operating conditions. The effect of various parameters such: flow rate, pH, particle volume fraction and the synthesis method of nanofluid on the thermal performance of the radiator are discussed.

4.2 Test Facility, Experimental Procedure and Data Reduction

4.2.1 Test facility and experimental procedure

Fig. 4.1 depicts the schematic view of the test facility in order to study the heat transfer performance on the thermal performance of the CNT/water nanofluid in an automobile radiator. The test facility includes a test section, AC-power supply, coolant supply system, cooling section and instrumentation scheme for measuring the temperature. An automobile radiator which is a cross flow heat exchanger is used as the test section for the present investigation. The radiator consists of 30 serpentine finned tubes with stadium shape made of Aluminum. Each tube is of 310 mm length, 20 mm width and 3mm height (Fig. 4.2 a-b). The total effective heat transfer area of the tube and fins are 0.445 m^2. A closed storage tank of 15 liters capacity is used to store the coolant. The coolant is supplied to the test section by using a centrifugal pump and the outlet supply from the test section is sent back to the storage tank for recirculation in the test section. A bypass valve arrangement is used to control the coolant flow rate into the test section. Flow rate was measured by using a calibrated rotameter with the precision of 0.1 lit/min. An electrical power supply (220V, 15A, AC) is provided to the heating elements (2kW, 4 Nos.) in order to heat the coolant in the storage tank. The inlet temperature is maintained at a constant temperature of 90^0C in all the test runs. A temperature controller is used to maintain the constant temperature of the coolant. Eight calibrated RTD PT100 type temperature sensors with an accuracy of ± 0.1 ^{0}C are mounted on the test section to measure outside wall temperature. Three calibrated RTD PT100 type temperature sensors

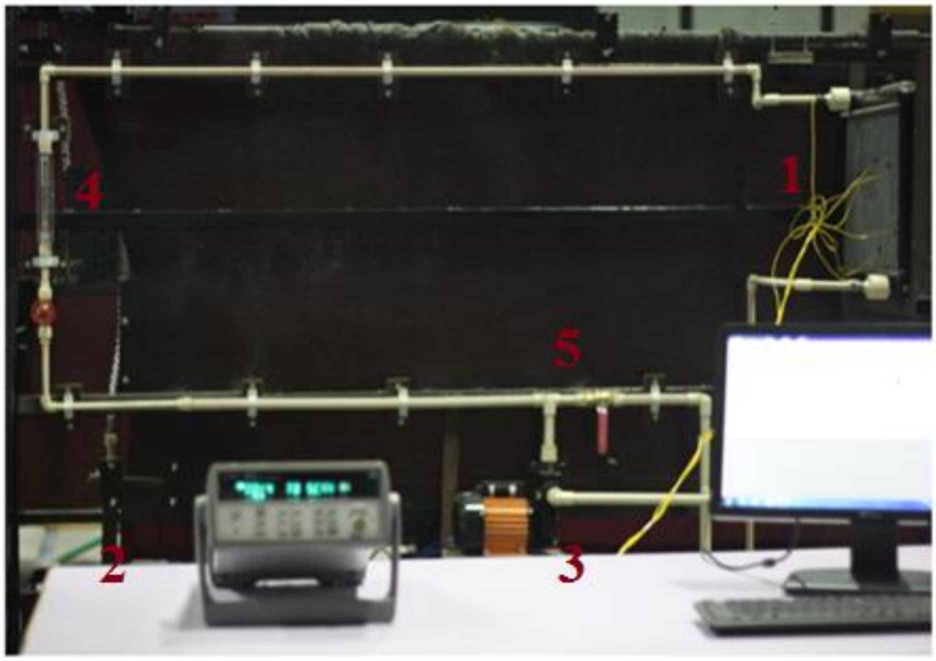

1. Radiator and cooling fan
2. Data acquisition sytem
3. Pump
4. Flow meter
5. By pass valve

(a)

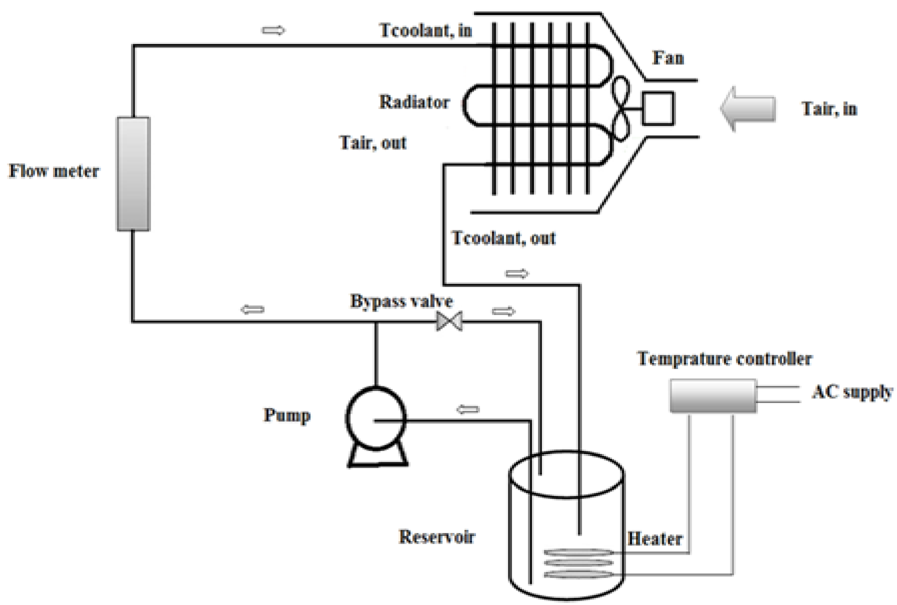

(b)

Figure 4.1: (a) Photographic view of radiator test facility and **(b)** Schematic of test facility

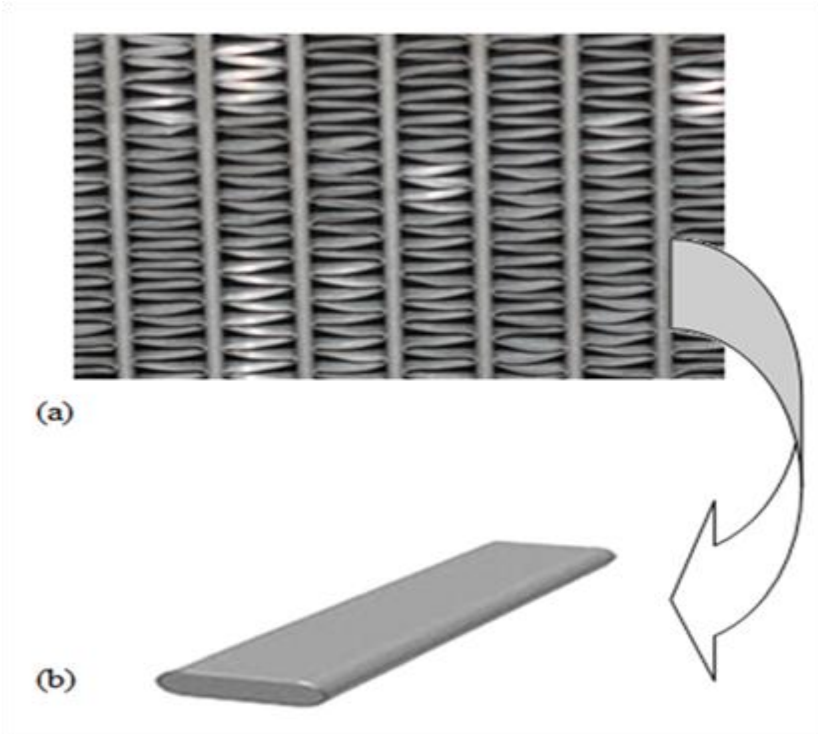

Figure 4.2: (a) The photographic view of fin and flat tube of the automobile radiator and **(b)** Schematic of stadium shape of the radiator flat tube

are located at inlet and outlet of the test section to measure the temperature of the working fluid, while the other one is used to measure the inlet air temperature. In addition, one RTD PT100 type temperature sensor was used to measure the temperature of the coolant in the storage tank. Subsequently the required temperature in the feeding tank is maintained by controlling the power supply to the heating element. A data acquisition system (DAS) (Model: 34972A, Make: Agilent Technologies) was used to measure the temperatures. In addition to this a fan that provides constant air supply is used to cool the coolant through the radiator. The temperature and velocity of the air kept constant for all test runs.

A thermal property analyzer (Model: KD2 Pro., Model: Decagon Devices, USA) with an accuracy of ±5.0% and cone and plate viscometer (Model: Brookfield DV-II+ Pro, Make: Brookfield Engineering Laboratories, USA) with an accuracy of ±1.0% were used to measure the thermal conductivity and viscosity of the nanocoolant at various volume fractions and sample temperatures. Tests were performed at ambient temperature 35 ± 1^0C with a relative humidity of 65 ± 5%. The errors associated in various parameters were evaluated by following the procedure reported by Coleman and Steele method [126] and ANSI/ASME standard [127]. The uncertainties associated in various parameters namely, flow rate, wall and fluid temperatures, voltage and current were evaluated to calculate the total uncertainty in Nusselt number on the basis of 95% confidence level. A maximum uncertainty in Reynolds number and Nusselt number were found to be ±5% and ±6%, respectively.

4.2.2 Data reduction

The heat transfer coefficient and corresponding Nusselt number was obtained by following procedure detailed as below:

According to Newton's cooling law, one can write:

$$Q = hA\Delta T = hA(T_b - T_w) \tag{4.1}$$

Where, A is the surface area of the tube and T_b is the bulk temperature of the fluid and T_w is the average wall temperature. The bulk temperature is assumed to be the average values of inlet and outlet temperature of the fluid moving through the radiator.

$$T_b = \frac{T_{in} + T_{out}}{2} \tag{4.2}$$

Where, T_{in} and T_{out} are inlet and outlet temperatures, respectively. While, average wall temperature is derived as below:

$$T_w = \frac{T_1 + T_2 + \ldots.. + T_8}{8} \tag{4.3}$$

Here, T_1 to T_8 denote the temperature of tube wall at various longitudinal and transverse locations of the radiator.

The heat transfer rate can be calculated as,

$$Q = \dot{m}C_P\Delta T = \dot{m}C_P(T_{in} - T_{out}) \qquad (4.4)$$

Where, $\dot{m}$ is mass flow rate and C_p specific heat capacity of the fluid.

Utilizing Eqs. (4.1) and (4.4) one can obtain:

$$Nu_{\exp} = \frac{hD_{hy}}{k} \qquad (4.5)$$

Where, $Nu_{\exp}$, k and D_{hy} denote the average Nusselt number, the thermal conductivity of fluid and hydraulic diameter of the tube, respectively. The physical properties are measured at the bulk temperature of the fluid.

4.3 Results and Discussion

Tests are performed to evaluate the thermal performance of two different nanofluids (Al_2O_3/water and CNT/water) through an automobile radiator with varied range of particle volume concentration (φ= 0.15 %, 0.30%, 0.60% and 1%). Initially, tests are conducted to study the thermal performance of CNT/water nanofluid. Later on, the analysis is extended to evaluate the thermal performance of Al_2O_3/water nanofluid through the radiator. Subsequently, the thermal performance of CNT/water nanofluid and Al_2O_3/water nanofluids is compared for same operating conditions. The effect of various parameters such: flow rate, pH, particle volume fraction and the synthesis method of nanofluid on the thermal performance of the radiator are discussed.

4.3.1 Thermal performance of CNT/water nanofluid through radiator

In this study, tests are performed by using water and CNT/water nanofluid with the varied range of concentration (0.15%, 0.45%, 0.60%, and 1% by volume). Tests were conducted at ambient temperature 35 ± 1^0C with a relative humidity of 65 ± 5%. For all the test runs, the inlet temperature of the coolant is maintained at 90^0C. The flow rate of coolant is varied between 2-5 lit/min. The observation obtained from the present investigation is summarized below.

Heat transfer with water

Initially, the tests are conducted with water in order to validate the test facility. The Nusselt number of single phase fluid reported by Dittus Boelter [131] and is expressed below:

$$Nu = 0.0236 \ \mathrm{Re}^{0.8} \, \mathrm{Pr}^{0.3} \tag{4.6}$$

Where, $0.6 \leq \mathrm{Pr} \leq 160, \ \mathrm{Re} \geq 10000$

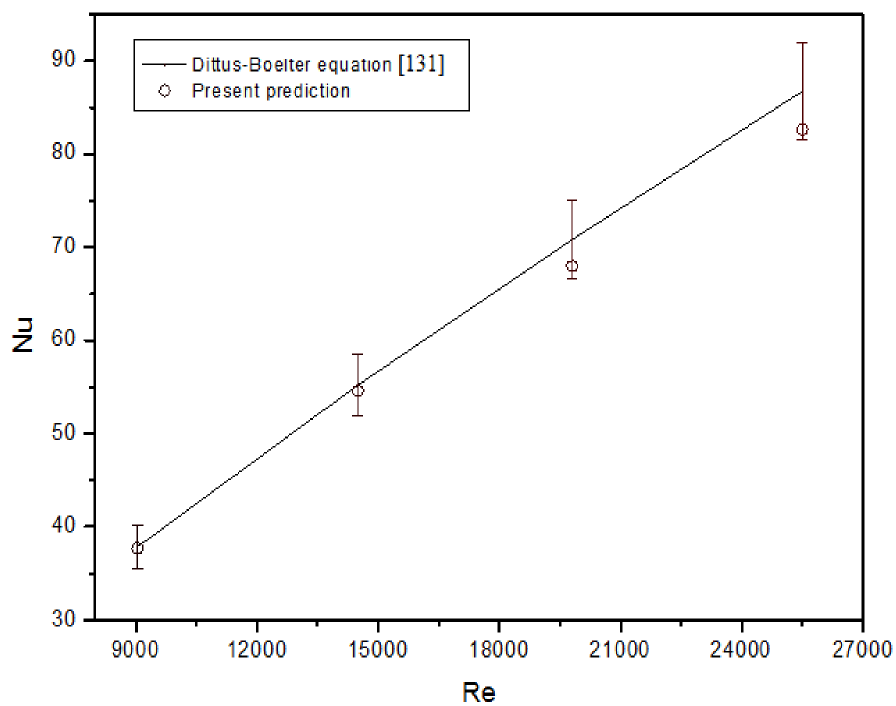

Figure 4.3: Variation of Nusselt number for pure water with existing correlations

The results obtained from the present experimental study are compared with the empirical correlation suggested by Dittus Boelter [131]. The variation of the Nusselt number with Reynolds number is shown in Fig. 4.3. The test data exhibited good agreement with Dittus Boelter equation [131]. The results show that the Nusselt number increases with the increase in the Reynolds number. The experimental results show the average deviation of 6% from theoretical results.

Effect of pH variation

Figure 4.4 depicts the variation of Nusselt number for water and CNT/water nanocoolant prepared by functionalization method with various pH value. For functionalized CNT/water nanocoolant (FCNT), the value of pH is varied in the range of 5.5 to 9.0. The nanocoolant is found to exhibit enormous heat transfer performance compared to water. This may be due to the fact that the effective thermal conductivity of the CNT suspension increases leading to an increase in heat transfer. In addition, the turbulence effect, due to random motion (Brownian motion) of CNT in the base liquid becomes significant with the increase in the coolant flow rate.

The maximum enhancement in thermal performance was observed at 5 lit/min coolant flow rate. The enhancement in heat transfer of functionalized CNT/water nanocoolant compared to pure water was found to be 90.76%, 65.79% and 80.31% for 5.5, 6.5 and 9.0 pH values, respectively. The thermal performance of nanocoolant for 5.5 pH was found to be higher compared to 6.5 and 9.0 pH nanocoolants. The reason may be due to the fact that the pH of an isoelectric point for CNT is 7.4 [132]. An isoelectric point (IEP) is the concentration of potential controlling ions at which the zeta potential is zero. Thus, at the IEP, the surface charge density equals the charge density, which is the starting point of the diffuse layer. Therefore, the charge density in this layer is zero. As the pH of the solution departs from the IEP of nanoparticles, the colloidal particles get more stable and ultimately modify the thermal conductivity of the fluid. The surface charge state is a basic feature which is mainly responsible for increasing thermal conductivity of the nanofluids. As the nanofluids become more acidic (lower pH value), more charges are accumulated on the particle surface, leading to lower agglomeration of nanoparticles in the suspension. Consequently the effective thermal conductivity of the nanofluid increases. In addition, with the increase in pH of the nanofluid, the surface charge of the CNT increases leading to the increase in thermal conductivity and stability of nanofluid [132]. It may be observed (Fig.5) that the performance in heat transfer increases with the increase in the coolant flow rate. This shows that the enhancement in Nusselt number is lower for 2 lit/min compared to 5 lit/min (Fig. 4.4).

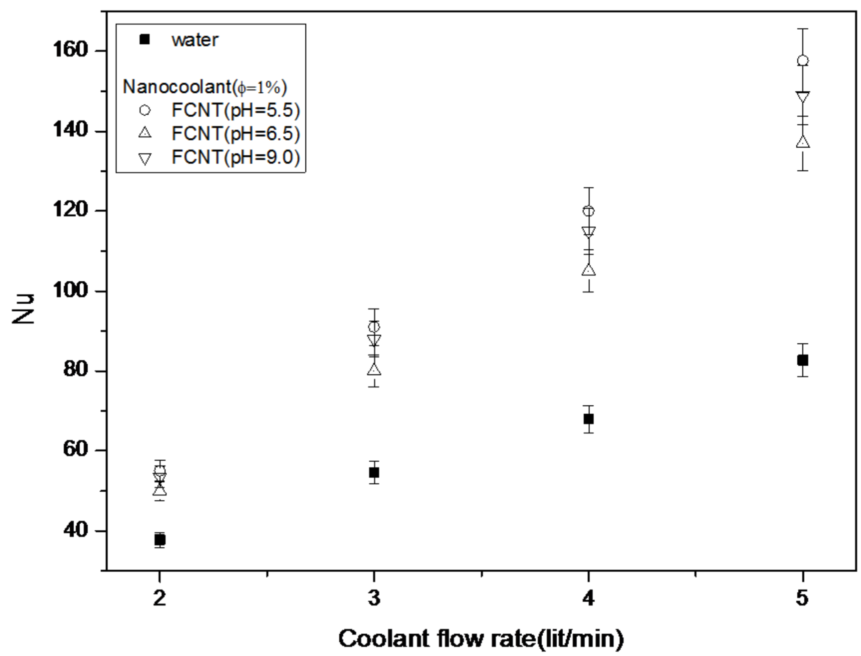

Figure 4.4: Effect of pH variation on nanocoolant heat transfer performance

Effect of synthesis method

The thermal performance of both the fluids, namely, functionalized CNT/water (FCNT) nanocoolant and surfactant treated CNT/water (SCNT) nanocoolant is depicted in Fig. 4.5. For the given coolant temperature of 90 ^{0}C, the functionalized CNT/water (FCNT) nanocoolant exhibits better thermal performance compared to the surfactant treated CNT/water (SCNT) nanocoolant for all coolant flow rate. The SCNT nanocoolant was synthesized by using sodium dodecyl sulfate (SDS) as the surfactant for proper dispersion of CNT in water base fluid. It is argued that the bonding strength between the surfactant and nanoparticle becomes weak at the higher temperature for the SCNT nanofluids [118, 133]. In such a case, the nanofluid will lose its stability and sedimentation of nanoparticles could occur. This may be the possible reason for the deterioration in heat transfer performance of SCNT nanocoolant at the higher temperature. This is observed in the present investigation and depicted in Fig. 4.5.

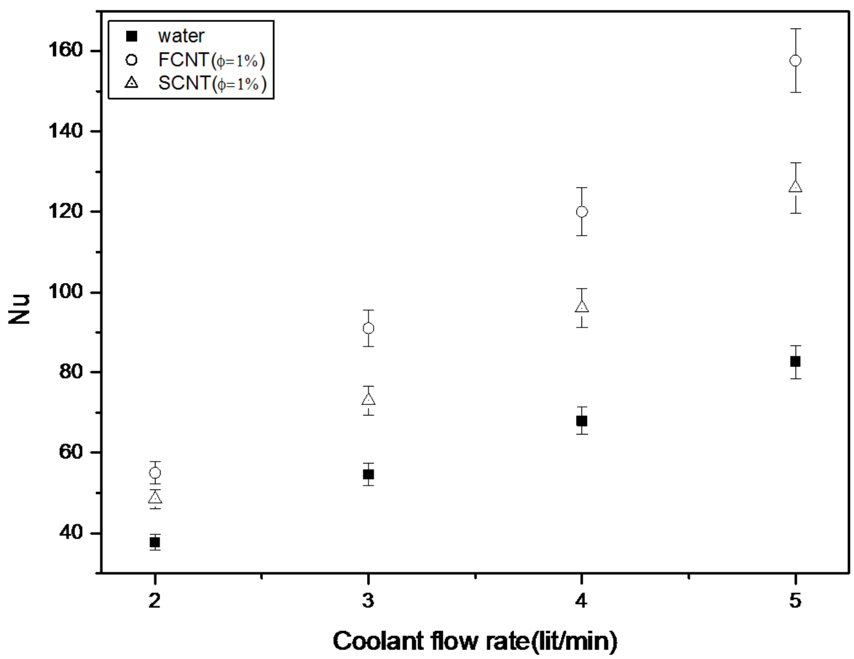

Figure 4.5: Effect of synthesis method on nanocoolant heat transfer performance

Effect of nanoparticle concentration

Figure 4.6 depicts that the variation of Nusselt number with the nanoparticle concentration and flow rate of the coolant. It is observed that the Nusselt number increases with the increase in the nanoparticle concentration and coolant flow rate. The increase in the nanoparticle concentration results in an increase in the effective thermal conductivity. In addition, the heat transfer enhancement is associated with the collision among nanoparticles and between the nanoparticles and the tube wall of the automobile radiator. This leads to an increase in the Brownian motion and the energy exchange rate of nanoparticles. The effective thermal conductivity, the Brownian motion of nanoparticles, particle migration increases with the increase in the nanoparticle concentration resulting in an increase in heat transfer.

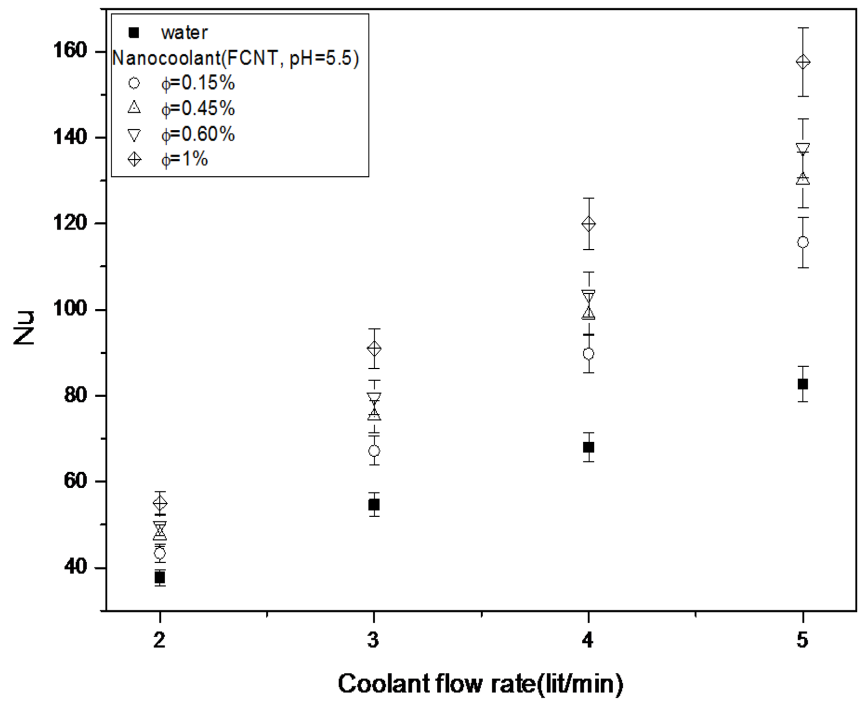

Figure 4.6: Nusselt number variation for different nanoparticle concentration

In this study, an effort has been made to evaluate the enhancement in heat transfer rate. This can be calculated as:

$$Percentage\ Enhancement = \frac{Nu_{nf} - Nu_{bf}}{Nu_{bf}} \tag{4.7}$$

The enhancement in Nusselt number for CNT/water nanofluid compared with water for various nanoparticle concentration (φ= 0.15%, 0.45%, 0.60% and 1%) is shown in Fig. 4.6. The enhancement in heat transfer for FCNT/water nanofluid at 0.15% nanoparticle volume concentration is found to be 15.30%, 22.09%, 32.18% and 39.95 for 2 lit/min, 3 lit/min, 4 lit/min and 5 lit/min, respectively. While, the enhancement in heat transfer of FCNT/water nanofluid at 1% nanoparticle volume concentration is found to be 45.87%, 66.64%, 76.55% and 90.76% for 2 lit/min, 3 lit/min, 4 lit/min and 5 lit/min, respectively. The Maximum enhancement in Nusselt number was found to be 90.76% by using FCNT/water nanofluid of 1% volume concentration with 5 lit/min coolant flow rate compared with the pure water results. It may be noted that the addition of nanoparticles to the water could effectively remove the heat in an automobile radiator. This improvement in heat transfer could reduce the size of radiators in an automobile engine leading to an improved fuel economy.

4.3.2 Comparative thermal performance of CNT/water and Al_2O_3/water nanofluids

In the previous section 4.3.1, the heat transfer of nanofluids through radiator is analyzed using CNT/water nanofluid. Here, the effort has been made to evaluate the heat transfer characteristics of Al_2O_3/water. Also, the comparative heat transfer characteristics of water, CNT/water and Al_2O_3/water are reported for varied range of concentration (0.15%, 0.45%, 0.60%, and 1% by volume). These tests were performed at ambient temperature 35 ± 1^{0}C with a relative humidity of 65 ± 5%. The inlet temperature of the coolant is maintained at 90^{0}C for all the test runs and the flow rate is varied between 2-5 lit/min. The observation obtained from the present investigation is summarized below.

Heat transfer study

Figure 4.7 shows the variation in Nusselt number with different coolant flow rate of various nanofluids (CNT/water and Al_2O_3/water) at 0.15% volume concentration. While, the variation in Nusselt number with different coolant flow of various nanofluids (CNT/water and Al_2O_3/water) at 1% volume concentration is shown in Fig. 4.8. It is observed that the

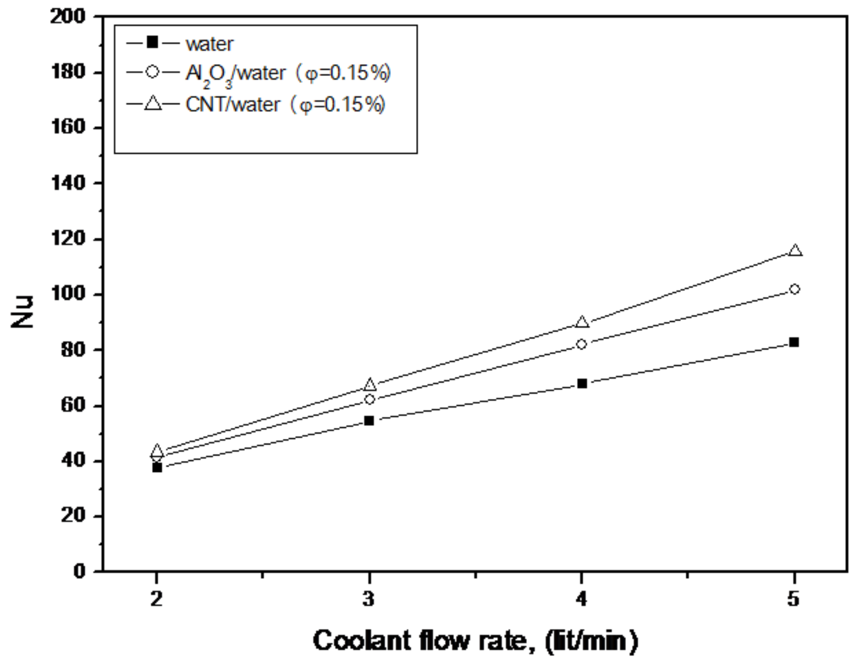

Figure 4.7: Comparison of Nusselt number variation for nanocoolant at 0.15 vol. %

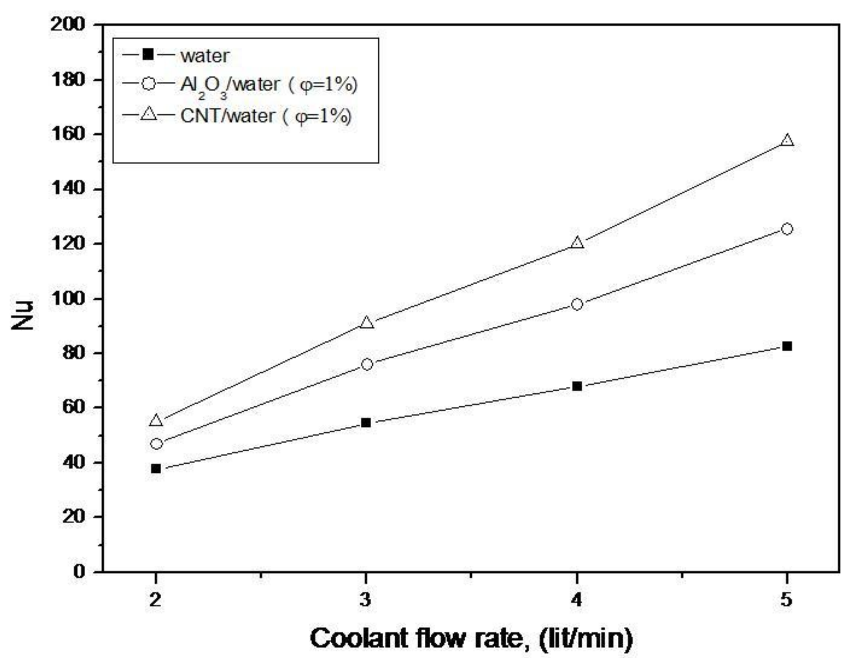

Figure 4.8: Comparison of Nusselt number variation for nanocoolant at 1 vol. %

Nusselt number increases with the increase in the coolant flow rate, thereby increases the heat transfer. This may be due to the fact that the enhanced thermal conductivity of nanofluids increases the heat transfer performance. CNT/water nanofluid was found to exhibit enormous heat transfer performance compared to Al_2O_3/water nanofluid for any value of coolant flow rate and nanoparticle concentration. Compared to water, CNT/water nanofluid (1% by volume) exhibited 45.87%, 66.64%, 76.55% and 90.76% increase in the Nusselt number at flow rates 2lit/min, 3lit/min, 4lit/min and 5lit/min, respectively. On the contrary, Al_2O_3/water nanofluid (1% by volume) exhibited 24.66%, 39.17%, 44.18% and 52.03% increase in the Nusselt number at coolant flow rates 2lit/min, 3lit/min, 4lit/min and 5lit/min, respectively compared to the results with water as a coolant. The increase in the Nusselt number of CNT/water nanofluid (0.15% by volume) compared to water was found to be 15.30%, 22.09%, 32.18% and 39.95% for the flow rates of 2 lit/min, 3 lit/min, 4 lit/min and 5 lit/min, respectively. While, Al_2O_3/water nanofluid (0.15% by volume) exhibited 10.21%, 13.63%, 20.83% and 23.07% enhancement in Nusselt number at coolant flow rate 2 lit/min, 3lit/min, 4lit/min and 5lit/min, respectively compared to the pure water. Compared to water, the maximum enhancement in Nusselt number for CNT/water and Al_2O_3/water nanofluid are found to be 90.76% and 52.03%, respectively. The experimental result shows that CNT/water nanofluid gives enormous enhancement in heat transfer compared to the Al_2O_3/water nanofluid. CNT nanoparticles of 20-30 nm diameter, 3-8 µm length and Al_2O_3 nanoparticles with <100 nm diameter are used in the present experimental investigation. Carbon nanotubes (CNTs) have higher thermal conductivity, higher aspect ratio, lower specific gravity, large specific surface area (SSA) and lower thermal resistance compared to Al_2O_3/water nanofluid. The higher thermal conductivity and larger specific surface area (SSA) of CNT nanoparticles compared to Al_2O_3 nanoparticles play an important role for the better heat transfer enhancement of CNT/water nanofluid [4]. Therefore, greater enhancement is shown by CNT/water compared to Al_2O_3/water nanofluid.

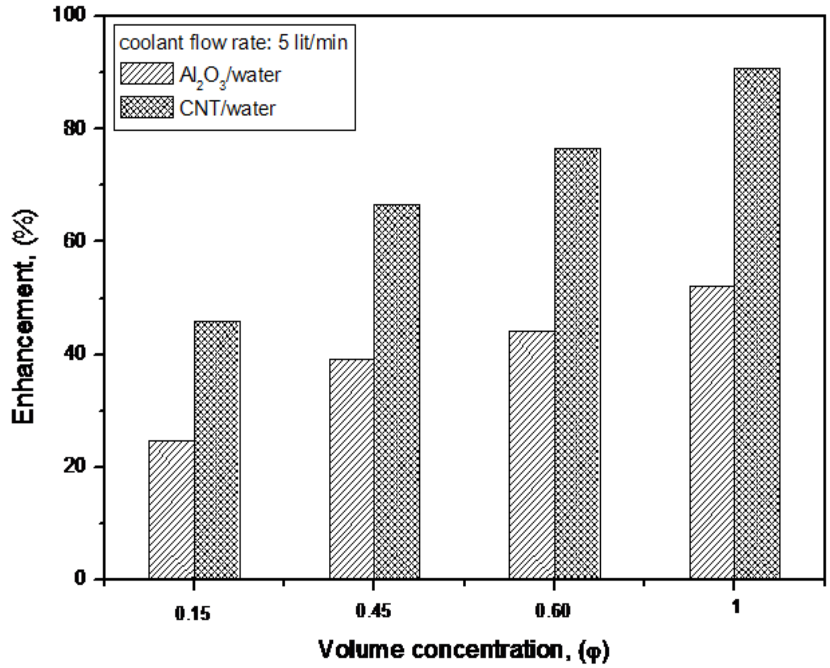

Figure 4.9: Variation of thermal performance for different nanoparticle concentration.

Effect of nanoparticle concentration

Following the previous analysis (Eq. 4.7), here efforts have been made to evaluate the enhancement in heat transfer rate. Figure 4.9 depicts the percentage of enhancement in Nusselt number for two different nanofluids namely, CNT/water and Al_2O_3/water for different nanoparticle concentration (φ = 0.15%, 0.45%, 0.60% and 1%) compared with water.

It can be seen from Fig. 4.9 that with the increase in nanoparticle concentration, the percentage enhancement in heat transfer increases for both CNT/water and Al_2O_3/water nanofluid. The nanoparticle concentration results in an increase in the effective thermal conductivity. Besides, the heat transfer enhancement is associated with the collision among nanoparticles and between the nanoparticles and the tube wall of the automobile radiator. This leads to an increase in the Brownian motion and the energy exchange rate of nanoparticles. The effective thermal conductivity, the Brownian motion of nanoparticles, particle migration increases with the increase in the nanoparticle concentration resulting in an increase in heat transfer. The heat transfer enhancement of Al_2O_3/water nanofluid at nanoparticle concentration 0.15%, 0.45%, 0.60% and 1% are found to be 23.07%, 33.12%, 40.38% and 52.03%, respectively compared with water. While, the enhancement in heat transfer for CNT/water nanofluid is found to be 39.95%, 57.32%, 69.42% and 90.76% for the nanoparticle concentration of 0.15%, 0.45%, 0.60% and 1%, respectively compared with water. The increase in heat transfer leads to higher thermal performance because of higher heat transfer coefficients obtained by utilizing nanofluid in automobile radiator compared to water as a coolant. The increase in heat transfer rate causes an improvement in cooling performance of the automotive engine.

4.4 Concluding Remarks

This chapter reports the thermal performance of nanofluids through an automobile radiator with the varied range of particle volume concentration (φ = 0.15%, 0.30%, 0.60% and 1%). Initially, tests are conducted to study the thermal performance of CNT/water nanofluid. Subsequently, the analysis is extended to compare the thermal performance of CNT/water nanofluid and Al_2O_3/water nanofluids for same operating conditions. The effect of various parameters such: flow rate, pH, particle volume fraction and the synthesis method of nanofluid on the thermal performance of the radiator are discussed

In the first study, the thermal performance is evaluated by using CNT/water nanofluids in the varied range of particle volume concentration 0.15- 1 vol.% and coolant flow rate of 2 lit/min to 5 lit/min. The CNT nanocoolants are synthesized by functionalization (FCNT) and surface treatment (SCNT) method. The effects of various parameters, namely synthesis method, variation in pH values and nanoparticle concentration on the Nusselt number are examined through the experimental investigation. The test data are used to evaluate the Nusselt number of CNT/water nanofluids for the varied range of coolant flow rate. The thermal performance nanofluids are compared with water in terms of percentage enhancement in heat transfer for similar conditions. Results demonstrate that CNT/water nanocoolant exhibit enormous change Nusselt number compared with water. The results of functionalized CNT nanocoolant with 5.5 pH exhibits better performance compared to the nanocoolant with the pH value of 6.8 and 9. The surface treated CNT nanocoolant exhibits the deterioration in heat transfer performance. In addition, Nusselt number found to increase with the increase in the nanoparticle concentration and nanofluid velocity.

Next, an effort has been made to evaluate the thermal performance of automobile radiator by using Al_2O_3/water nanofluid. The forced convective heat transfer performance of two different nanofluids, namely, Al_2O_3/water and CNT/water has been studied experimentally. Four different concentrations of nanofluid in the range of 0.15- 1 vol. % were prepared by the additions nanoparticles (Al_2O_3 and CNT) into the water as base fluid. The coolant flow rate is varied in the range of 2 lit/min to 5 lit/min. Both nanocoolants exhibit an enormous change in the heat transfer compared with the pure water. The heat transfer performance of CNT/water nanofluid was found to be better compared to Al_2O_3/water nanocoolant. Furthermore, the Nusselt number is found to increase with the increase in the nanoparticle concentration and nanofluid velocity.

Present study exhibits the heat transfer performance of various nanofluids (Al_2O_3/water and CNT/water) through an automobile radiator. Further, efforts have been made to evaluate the heat transfer performance of nanofluid charged heat pipe in various thermal devices including solar water heating and electronics cooling. These are discussed in next chapter.

Chapter 5

Thermal Performance of Nanofluid Charged Heat Pipes in Solar Flat Collector and Electronics Cooling

5.1 Introduction

Heat pipes are high-efficient heat transfer devices and have been widely used in various thermal systems. Heat pipes usually utilize the phase change of the working fluid to transport the heat. Therefore, the selection of working fluid is of great importance to promote the thermal performance of heat pipes. The significant enhancement in heat transfer is observed using nanofluids in heat pipes as the working fluids. Heat pipes transfer heat by evaporating the working fluid in a heating zone through the capillary structure which lies in the inner wall of the heat pipe. Heat pipes also work under gravity with the condenser above the evaporator does not require external power or capillary action to return the working fluid from the condenser to the evaporator. The later one is termed as thermosyphon or wickless gravity assisted heat pipe. Heat pipes can be integrated with the flat plate of solar heating system to improve its thermal performance. It is observed that with the increasing demand for higher power and smaller size of electronics components, an efficient cooling system is needed to remove heat. The existing cooling system that utilizes air as a coolant may not be adequate to remove the excess heat of electronics components. In such a case, one can select a suitable working fluid in the heat pipe that can transfer maximum heat energy.

In view of this, an attempt has been made to study the thermal performance of the heat pipe using CNT with water as the working fluid for solar heating applications. Various concentrations of nanoparticles are used to find the optimal concentration for the maximum performance. The effect of the tilt angle, filling ratio and coolant flow rate on the solar collector has been discussed in the study. The thermal performance of the thermosyphon with nanofluid is compared with operation with water. Later on, the experiments are conducted to study the nanofluid charged heat pipe module with PCM for electronics cooling. The study compares the thermal performance of heat pipe module with CNT/water nanofluid and water as the working fluid. The effectiveness of PCM as ESM was tested by using different fan speed and heating powers. The results obtained by the cooling module with heat pipe and paraffin wax as ESM was compared with the cooling module that utilities only a heat pipe and water as the ESM.

5.2 Thermal Performance of Two-Phase Thermosyphon Flat Plate Collector by using Nanofluids

An experimental study is carried out to investigate the thermal performance of solar heat pipe collector at outdoor test condition. The thermal performance of wickless heat pipe solar collector was investigated by using CNT/water nanofluid. The optimal value of CNT nanofluid concentration for better performance is obtained from the investigation. The thermal performance of the heat pipe solar collector with CNT nanofluid is compared to that of pure water.

5.2.1 Test facility, experimental procedure and data reduction

Test facility

The schematic of the solar collector test facility is shown in Fig. 5.1 (a). The schematic of the solar collector with the wickless heat pipes is depicted in Fig. 5.1 (b). An attempt has been made to evaluate the performance of two phase thermosyphon for various volume concentration of CNT (0.15%, 0.45%, 0.60% and 1%). In view of this, five same size identical collectors have been fabricated for the investigation. Each collector consists of three absorber plate and each absorber plate contains one heat pipe filled with the working fluid. Table 5.1 summarizes the design parameters of various components of the heat pipe solar collector.

Table 5.1: Specifications of the different components of the collector

Gross dimensions Length 0.63 m Width 0.36 m Depth 0.1 m **Transparent cover** Material: white glass **Absorber plate** Material: copper Length 0.51m Pitch distance 0.1m Thickness 0.001m Coating: black **Insulation** Material: glass wool Thickness 0.05 m Position: Back and sides **Box material** Frame: aluminum Base: galvanized iron	**Wickless heat pipes** Material: copper Outer diameter 0.012 m Inner diameter 0.010 m Evaporator length 0.51 m Condenser length 0.085 m Adiabatic length 0.030m Total length 0.625 m Number of Heat pipes in each collector 3 Working fluid: Collector No.1:- D.I. water Collector No.2:- CNT Nanofluid (φ=0.15%) Collector No.3:- CNT Nanofluid (φ=0.45%) Collector No.4:- CNT Nanofluid (φ=0.60%) Collector No.5:- CNT Nanofluid (φ=1%)

The wickless heat pipes were made of copper tubes with an outer diameter of 12 mm and a length of 625 mm. The thickness, width and length of each copper absorber plate are 1 mm, 100mm, and 510 mm, respectively. The absorber plates were painted dull black to enhance the ability to absorb solar radiation. Each individual wickless heat pipe was brazed to the absorber plate at 120 mm pitch. The heat energy was absorbed by the heat pipes and was transferred to the coolant at the heat exchanger. The heat exchanger consists of three interconnected steel collars with an OD of 40 mm, ID 36 mm and 90 mm long attached around the condensing section of the heat pipes. Three absorber plate associated with the heat pipe and the heat exchanger were housed in a collector case of 630 mm length and 360 mm breadth and 100 mm thickness. The collector consists of galvanized steel sheet case and 50 mm thick insulation glass wool behind the absorber plate. This was used to avoid any loss of energy to the surrounding. Ordinary white glass was chosen as the upper glazing for the collector. The glass was secured at the top of the frame by using rubber gasket. This arrangement prevents the collector from the dust particle.

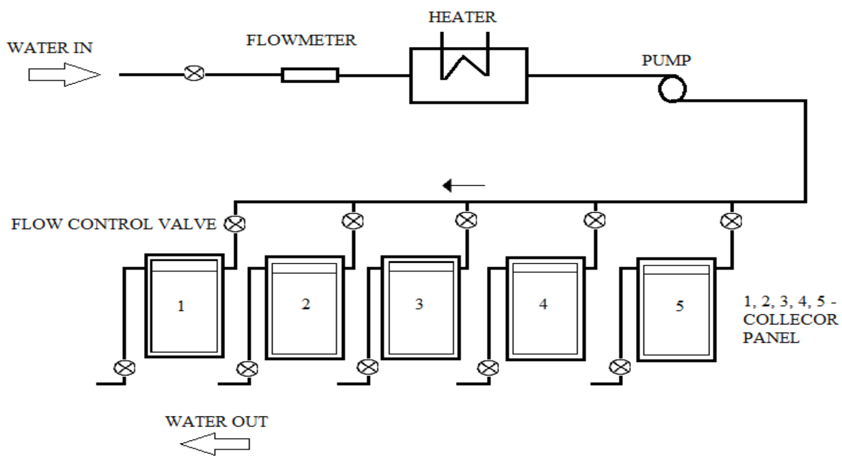

(a)

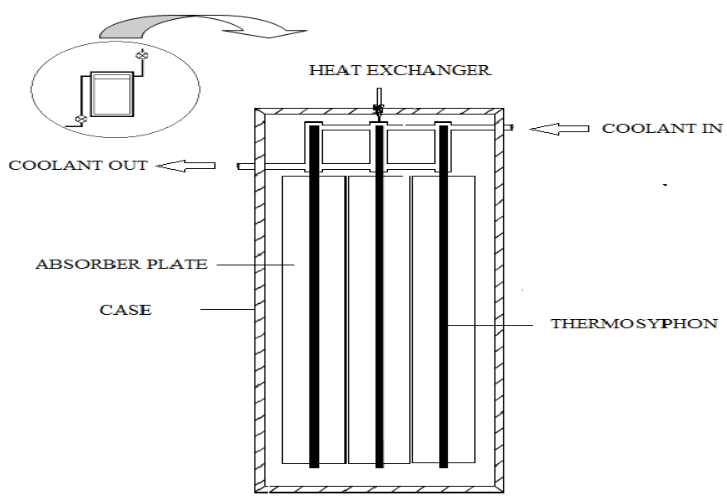

(b)

Figure 5.1: (a) Schematic diagram of solar collector test facility and **(b)** Thermosyphon solar collector

Experimental procedure

The measuring system used in the present study includes T-type thermocouples, pyranometer, ambient air sensor and flow meter. The mass flow rate of cooling water in the main line was measured by using a rotameter with an accuracy ±0.1 l/min. While, the quantity of cooling water was passing through the heat exchanger of each collector adjusted by using flow control valve and measured by using a stopwatch of ±0.01 second accuracy and a graduated glass bottle of tolerance ±1 cm^3. The temperature of the inlet and outlet cooling water, plate and ambient air were measured by using copper-constantan (type-T) thermocouples with an accuracy of $\pm 0.1^0C$. Temperatures were recorded using a computer based data logger. A pyranometer (Model-DWR 8101, Make-DynaLab) was used to measure the instantaneous value of global solar radiation intensity.

The two-phase thermosyphon solar collectors were installed on a tiltable stand and tested under outdoor field conditions of Karad, India (latitude 17.28^0 N; longitude 74.20^0E). The collector was set at a tilt from horizontal with 32.28^0 (Karad latitude + 15^0) facing south [134]. Day long experiments were carried out from 8:00 a.m. to 4:00 p.m. and values were recorded at half hour intervals. During each test run the solar radiation intensity (I_t), ambient air temperature (T_a), inlet cooling water temperature (T_i) and outlet cooling water temperature (T_o) of each collector were recorded for fixed mass flow rate.

The experiments were carried in following groups:

1. Firstly, the tests were carried out on five collectors with water and nanofluids (0.15%, 0.45%, 0.60% and 1% by volume concentration) as the working fluid for the wickless heat pipe. All five collectors were kept in the same climatic conditions throughout the day. The inlet temperature of the coolant and the ASHRAE standard mass flow rate ($0.02A_{coll}$, kg/s) was same for each collector in their test runs [134]. These tests were carried out to study the effect of CNT

nanofluid and its different concentration on the instantaneous performance of the wickless heat pipe solar collectors.

2. The experiments were carried out on two collectors with water and nanofluid (0.15% volume) as the working fluid to study the effect of collector tilt angle on the thermal performance.
3. Also, experiments were performed on three collectors with various filling ratio (50%, 60%, 70%) of CNT/water nanofluid as working fluid for wickless heat pipe. All three collectors were kept in same climatic conditions throughout the day. During test runs, the inlet temperature of the coolant and the ASHRAE standard mass flow rate ($0.02A_{coll}$, kg/s) is kept same for each collector [134]. These tests were carried out to study the effect of working fluid (CNT/water nanofluid) filling ratio on the instantaneous performance of the wickless heat pipe solar collectors.
4. In addition, tests were performed for three different mass flow rates and various inlet cooling water temperatures, to study the effect of the coolant mass flow rate on the thermal performance of collector.

Data reduction

The instantaneous thermal efficiency of a solar collector is defined as the ratio of the amount of energy removed by the coolant to the total solar radiation incident on the collector during the specified time period under the steady-state condition. The rate of thermal energy input (Q_{in}), the rate of thermal energy gain (Q_g) and the instantaneous efficiency (η_{coll}) of each collector were evaluated as below:

$$Q_{in} = I_t A_{coll} \tag{5.1}$$

$$Q_g = \dot{m} C_w (T_0 - T_i) \tag{5.2}$$

$$Q_g = A_{coll} F_R [I_t (\tau\alpha) - U_L (T_i - T_a)] \tag{5.3}$$

$$\eta_{coll} = \frac{Q_g}{Q_{in}} = \frac{\dot{m} C_w (T_o - T_i)}{I_t A_{coll}} \quad (5.4)$$

$$\eta_{coll} = F_R(\tau\alpha) - F_R U_L \frac{(T_i - T_a)}{I_t} \quad (5.5)$$

Here, the energy gain *(Q_g)* and the efficiency *(η_{coll})* were evaluated by using the basic quantities such as: mass flow rate of coolant, temperature of inlet and outlet coolant and solar radiation intensity. Considering the errors involved in the basic quantities, the maximum uncertainty of the energy gain *(Q_g)* and the instantaneous efficiency *(η_{coll})* of the collector were found to be less than 2% and 3%, respectively.

5.2.2 Results and discussion

Experiments were carried out with water and CNT nanofluid with the varied range of concentration (0.15%, 0.45%, 0.60% and 1% by volume) and tilt angles. The test data have been collected from several test runs under quasi-steady state condition. In the present investigation, the ambient temperature, fluid temperature and wall temperature were found to vary within the range of 18^0C-39^0C, 35^0C-54.5^0C and 52.5^0C -83^0C, respectively. The maximum variation in ambient, inlet and outlet temperature in each test period are found to be 0.5^0C, 0.2^0C and 0.4^0C, respectively. The above data satisfies the necessities presented in AHSRAE standard 93-86. The observations from the experimental investigation are summarized below.

Effect of nanoparticle

Five collectors with water and CNT nanofluids with different concentration (0.15%, 0.45%, 0.60% and 1% by volume) as the working fluid for heat pipes were tested under similar climatic conditions. Figure 5.2 (a) depicts the daily variation of various parameters, namely, solar energy input, ambient air temperature, inlet cooling water temperature, outlet cooling water temperature of the wickless heat pipe flat plate solar collectors. It is observed that the solar intensity increases with time and attains a maximum value during 12-13 hour. The maximum ambient temperature and solar radiation throughout the day were found to be 39^0C and 1080 W/m^2, respectively. The maximum water temperature rises up to 52^0C, 53.5^0C, 54.5^0C and 53^0C for 0.15%, 0.45%, 0.60% and 1% volume concentration, respectively. The inlet temperature of the coolant is found to increase with time and the ambient air temperature increases with time and attains the maximum value at 13 hour and gradually decreases during 14-16 hour.

Figure 5.2 (b) depicts the variation of instantaneous efficiencies of solar heat pipe collector throughout the day for the various concentration of CNT nanofluid. It is observed that the instantaneous efficiency follows the same trend as that of solar intensity. The efficiency of the solar heat pipe collector that utilize the CNT/water nanofluid as the working fluid is found to be higher compared to the heat pipe that uses water as the working fluid. This may be due to various reasons. Firstly, the thermal conductivity of the CNT/water nanofluid increases due to the addition of CNT nanoparticles resulting in an increase in heat transfer. Secondly, the cylindrical porous tube structure of the CNT increases the surface roughness and enhances the heat transfer. In addition, the turbulence effect is initiated due to the random motion (Brownian motion) of the CNT in the base liquid. The turbulence effect enhances the heat transfer rate. The efficiency of solar heat pipe collector is found to increase with the increase in the concentration level of CNT nanoparticles in water (0.15%, 0.45% and 0.60%). However, when the concentration level of CNT nanoparticles in water were increased from 0.60% to 1%, the thermal performance decreases. The maximum instantaneous efficiency was found to be 73% for 0.60% volume concentration of nanofluid at 12.00 noon. Similar results were obtained by the previous researcher as well [66]. It has been reported that with the increase in the nanoparticle concentration, the thermal the thermal resistance of the heat pipe decreases leading to

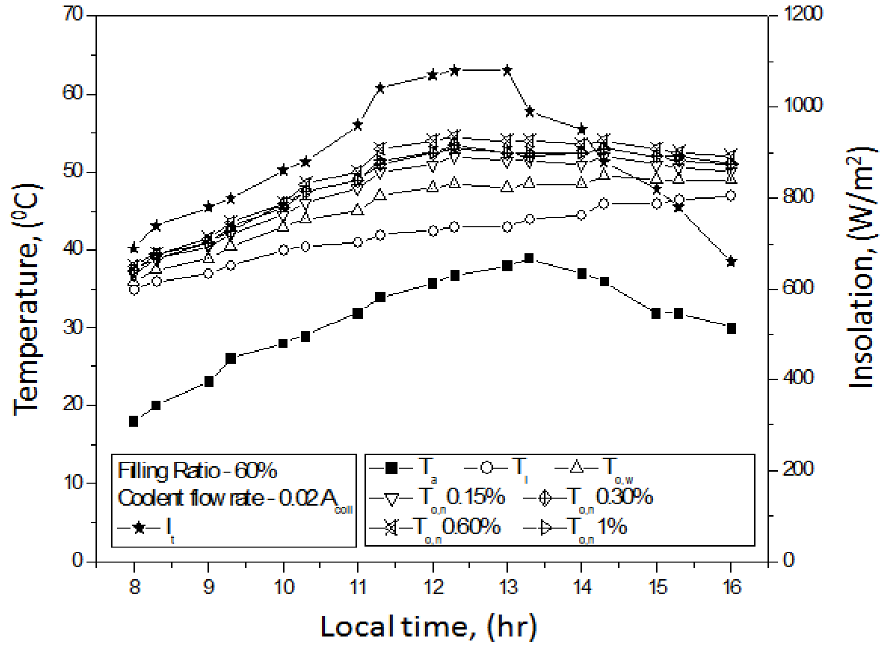

(a)

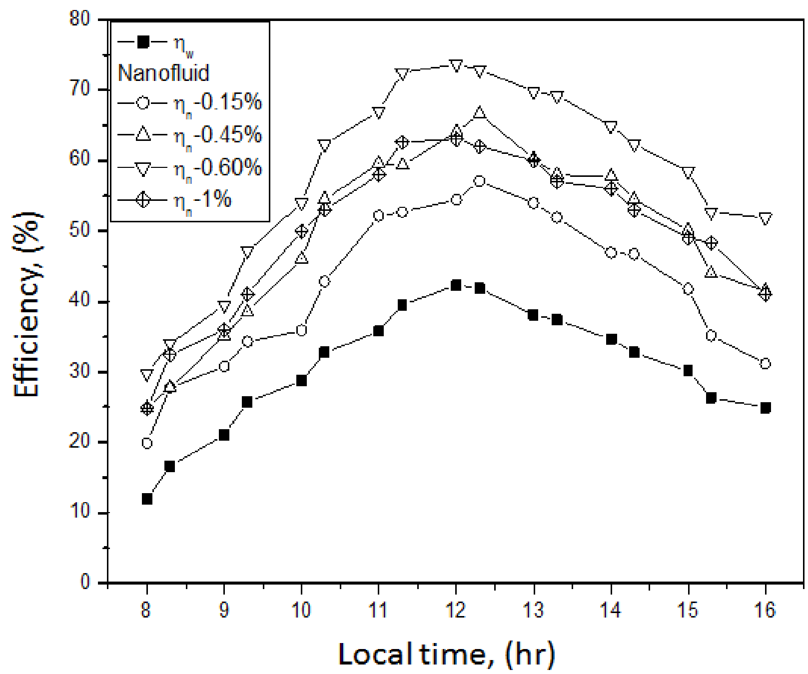

(b)

Figure 5.2: (a) Daily variation of ambient temperature (T_a), inlet temperature (T_i), solar radiations (I_t) and effect of nanoparticle concentration on outlet temperature (T_o) and **(b)** Effect of concentration of nanoparticle on collector efficiencies

increase in the heat transfer rate [67-70]. The thermal resistance of the heat pipe is caused because of the formation of vapour bubble at the solid liquid interface. However, the suspended nanoparticles tend to break the vapour bubble leading to the decrease in the thermal resistance of the heat pipe. Moreover, with the increase in concentration various parameters, namely, thermal conductivity and heat capacity of the fluid are increased leading to an increase in heat transfer. It is observed that the average collector efficiencies for nanofluid collectors with CNT volume concentration 0.15%, 0.45%, 0.60%, 1% are 42.36%, 49.77%, 57.31% and 50.26%, respectively. On the contrary, with the use of pure water the collector efficiency was obtained as 29.86%.

Effect of tilt angle

It is observed that the thermal performance of the heat pipe mainly depends on its tilt angle [67, 135-137]. Tests have been carried out for various tilt angles in two different solar heat pipe collectors under the same climatic conditions. One utilizes nanofluid (0.15% by volume) and the other uses pure water as the working fluid. The variation of collector instantaneous efficiency and the energy gain for various tilt angles is depicted in Fig. 5.3. Experiments were conducted for the fixed value of input radiation (660 kW/m^2) and ASHRAE standard flow rate ($0.02A_{coll}$, kg/s) for each tilt angle. These values are considered in the present analysis following the ASHRAE standard 93-86. The efficiencies of both the collectors that use nanofluid and pure water as the working fluid are found to be lower at smaller tilt angles and it increases with an increase in the tilt angle. However, when the heat pipe tilt angle exceeds a value of 50^0 for both pure water and nanofluid, the efficiency tends to decrease. The variation of energy gain is found to follow the same trend of the instantaneous efficiency for both pure water and nanofluid. The heat gain by heat pipes using water as the working fluid at 20^0, 32^0, 40^0, 50^0 and 60^0 tilt angles are found to be 30.25 W, 38.72 W, 48.40 W, 70.18 W and 57.82 W, respectively. While, by utilizing nanofluid as working fluid, the heat gain of the collector at 20^0, 32^0, 40^0, 50^0 and 60^0 tilt angles are found to be 38.72 W, 48.40 W, 55.66 W, 77.44 W and 62.92 W, respectively. The enhancement in heat transfer rate because of nanofluid is found to be 26%, 25%, 15%, 11% and 9% at tilt angle 20^0, 32^0, 40^0, 50^0 and 60^0, respectively. It is observed that at lower tilt angles the enhancement of heat transfer of heat pipe with nanofluid is higher compared with that of pure water. The significance of higher tilt angle performance of solar heat pipe collector can be found by locating them at high latitude regions. So, solar heat pipe collectors are recommended for high latitude regions where the angle of getting maximum solar radiation matches with the higher performance tilt angle of solar heat pipe collector for enormous performance.

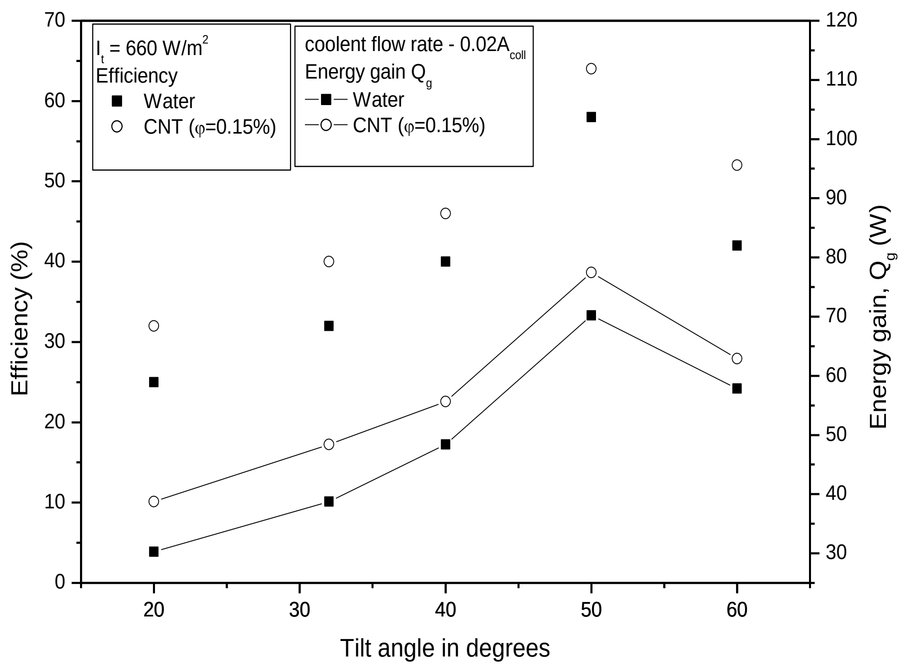

Figure 5.3: Effect of tilt angle on collector instantaneous experimental efficiencies

Effect of filling ratio

Figure 5.4 depicts the instantaneous variation of solar energy input, ambient air temperature, inlet cooling water temperature during test period from 8 am to 4 pm. The variation of thermal energy gain of heat pipe flat plate solar collectors with various CNT/water working fluid filing ratio (50%, 60% and 70%) is shown in Fig. 5.4. Solar radiation input is found to increase with time and attains maximum value during 12 noon to 1.00pm.

It is observed that inlet temperature of coolant increases with time and the ambient temperature increases with time attains the maximum value at 14 hour and gradually decreases during 14 hour to 16 hour. The heat pipe with filling ratio (F.R.) of 60% is found to provide the higher rate of instantaneous thermal energy gain throughout the day. Experimental studies [138-139] report that the heat pipes with 40–60% liquid filling ratio exhibits maximum thermal performance. Similar observation has been made in this study. The heat pipe with 50% CNT/water nanofluid filling ratio was found to provide better thermal energy gain during 11.30 hour to 13.30 hour.

The comparison among various efficiency curves obtained from the wickless solar collectors with three different filling ratio (50%, 60%, 70%) and at ASHRAE standard mass flow rate ($0.02A_{coll}$ kg/s) is shown in Fig. 5.5. By utilizing a curve fitting technique, a straight line fit between instantaneous efficiency and heat loss parameter $(T_i - T_a)/I_t$ is obtained and shown in Fig. 5.5. It may be noted that by extrapolating the straight line fit one can obtain the value of $F_R(\tau\alpha)$ at the point of intersection of straight line fit to the vertical axis and this is supported by Eq. (5.5). At this point, the temperature of the fluid entering to the collector becomes equal to the ambient temperature and collector efficiency attains the maximum value. This value is termed as absorbed energy parameter $F_R(\tau\alpha)$.

At the same time, one can evaluate the slope of the straight line fit and is found to be $F_R U_L$. This slope essentially indicates the amount of energy removed from the solar collector. At the intersection of straight line fit with the horizontal axis, the collector efficiency becomes zero and

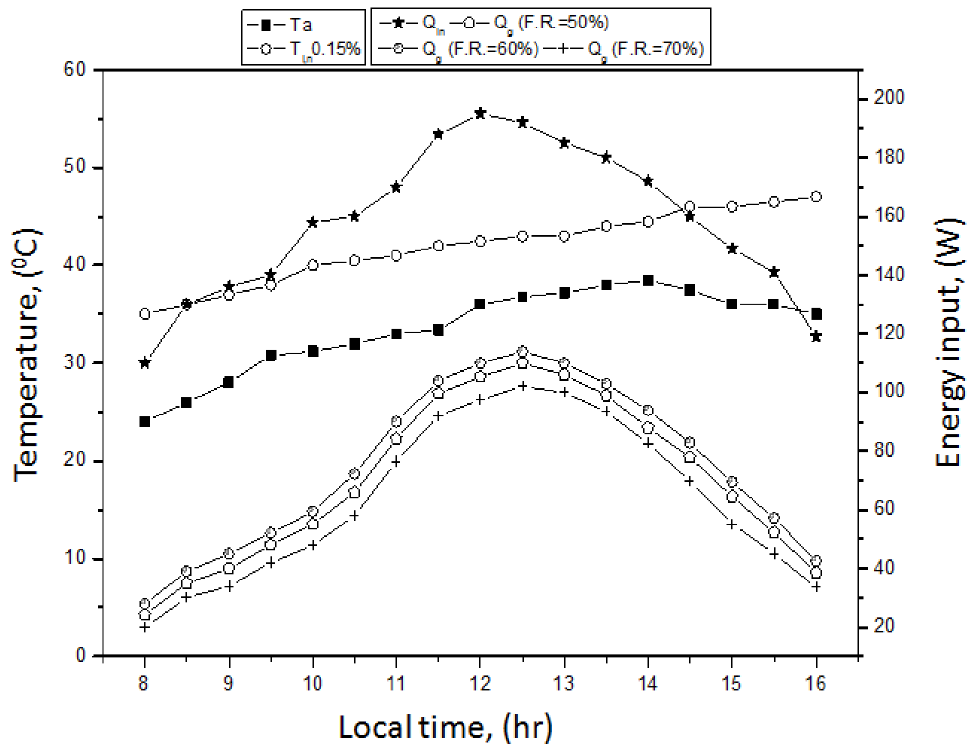

Figure 5.4: Effect of filling ratio on heat gain (Q_g) of wickless solar heat pipe collector

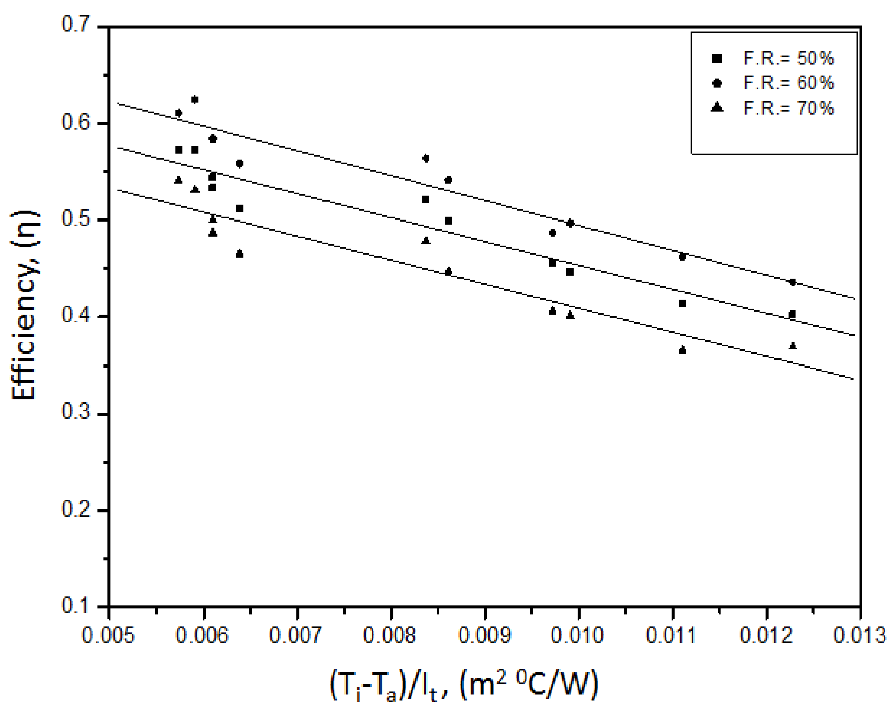

Figure 5.5: Comparison between efficiency curves with different filling ratio

Table 5.2: $F_R U_L$ and $F_R(\tau\alpha)$ values of wickless solar heat pipe collector at different filling ratio

Coolant flow rate (kg/sec)	Filling Ratio (%)	$F_R U_L$	$F_R(\tau\alpha)$
$0.02A_{coll}$	50	25.83	0.57
	60	24.20	0.63
	70	25.52	0.52

this point is referred as the stagnation condition. This situation occurs when no fluid flows in the collector. The efficiency of the solar collector is found to be higher by using 60% filling ratio heat pipe solar collector. The thermal performance of heat pipe collector found to increase with the increase in the CNT/water working fluid filling ratio from 50% to 60%. Based on the investigation the maximum thermal performance was obtained at 60% CNT/water working fluid ratio. The intercept value ($F_R(\tau\alpha)$) and the slope ($F_R U_L$) of the straight line fit for various filling ratio as obtained from Figs. 5.5 are summarized in Table 5.2. These data includes for various filling ratio (50%, 60% and 70%) at ASHRAE standard mass flow rate (0.02 $A_{coll,}$ kg/s). The value of $F_R(\tau\alpha)$ and $F_R U_L$ was found to be highest and lowest, respectively at 60% filling ratio.

Effect of coolant flow rate

Figure 5.6 depicts the effect of coolant flow rate on the thermal efficiency of the solar heat pipe collector. The collector efficiency was found to be maximum at a mass flow rate of $0.02A_{coll}$ kg/s. This mass flow rate commonly termed as the ASHRAE standard mass flow rate for the testing solar collector. Following the similar procedure of curve fitting technique as explained in the previous section, experimental results of present investigation can be represented linearly as a function of the measured parameter [$(T_i - T_a)/I_t$]. Further, following the similar technique,

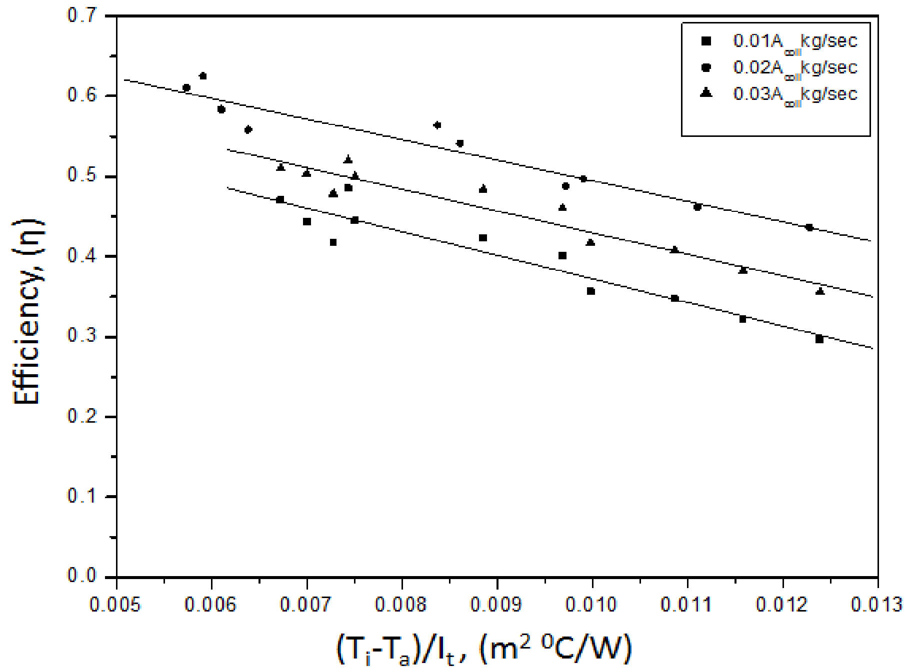

Figure 5.6: Comparison between efficiency curves at different cooling mass flow rate

one can evaluate the value of energy absorbed parameter ($F_R(\tau\alpha)$) and heat removed parameter ($F_R U_L$) of the collector and are summarized in Table 5.3. This includes the results obtained by using various coolant flow rates (0.01A$_{coll}$ kg/s, 0.02A$_{coll}$ kg/s and 0.03A$_{coll}$ kg/s). The value of $F_R(\tau\alpha)$ and $F_R U_L$ is found to be highest and lowest, respectively at the mass flow rate of 0.02A$_{coll}$ kg/s. The performance of solar wickless heat pipe collector was found to be lowest at 0.01Acoll kg/sec coolant flow rate. It is observed that the heat loss values are higher at lower coolant flow rate and higher coolant flow rate compared to ASHRAE standard coolant flow rate 0.02Acoll kg/sec. The variation in heat loss parameter is obtained by varying the filling ratio from 50% to 70% (Table 5.2). In addition, the variation in heat loss parameter for various coolant flow rate (0.01A$_{coll}$ kg/sec to 0.03 kg/sec) is summarized in Table 5.3. Based on the investigation, it is observed that the variation in heat loss parameter is higher by varying coolant flow rates from 0.01A$_{coll}$ kg/sec to 0.03 kg/sec.

Table 5.3: $F_R U_L$ and $F_R(\tau\alpha)$ values of wickless solar heat pipe collector at different coolant flow rate

Filling Ratio (%)	Coolant flow rate, (kg/sec)	$F_R U_L$	$F_R(\tau\alpha)$
60	0.01Acoll	29.43	0.54
	0.02Acoll	24.20	0.63
	0.03Acoll	27.06	0.58

5.3 Thermal Performance of Nanofluid Charged Heat Pipe with Phase Change Material for Electronics Cooling

Section 5.2, discusses the thermal performance of CNT/water nanofluid charged solar heat pipe collector for water heating. Here, efforts have been made to utilize CNT/water nanofluid charged heat pipes for electronics cooling module. An integrated thermal performance of nanofluid charged heat pipe cooling modules with PCM is investigated. Three different concentration of CNT/water nanofluids (1wt. %, 2wt. % and 3wt %) is used in this investigation. The tests are performed for various operating conditions, namely, heating powers (10 W, 20 W, and 30 W), fan voltage (3.15 V and 5.8 V), different working fluid of heat pipes, and different energy storage material (ESM).

5.3.1 Test facility, experimental procedure and data reduction

Test facility and experimental procedure

The heat pipe cooling modules are fabricated to investigate the integrated thermal performance of both phase change material (PCM) and CNT/water nanofluid charged heat pipe. In this study, Paraffin (PCM) and water were used as energy storage material. The nanofluid charged heat pipe was used to enhance the thermal performance of heat pipe cooling module by increasing heat transfer rate. The schematic and photographic view of the heat pipe cooling module test facility is shown in Fig. 5.7 (a) and (b), respectively.

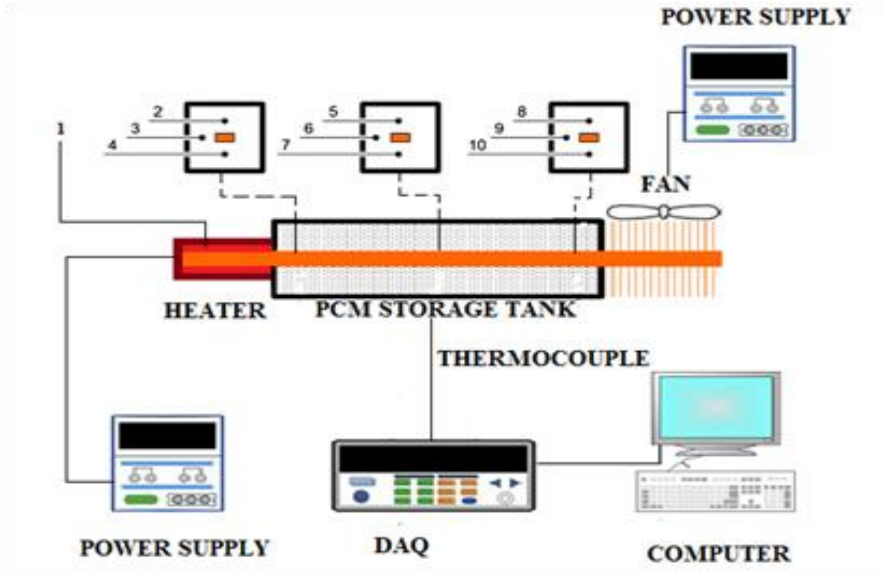

(a)

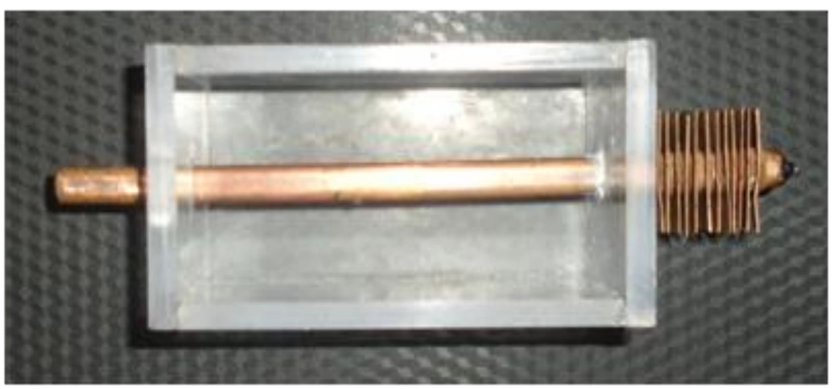

(b)

Figure 5.7: (a) Schematic diagram of heat pipe cooling module test facility and thermocouple location and **(b)** Photographic view of heat pipe cooling module.

An attempt has been made to evaluate the thermal performance of flat heat pipe cooling modules for various weight concentration of CNT

(1 wt.%, 2 wt.% and 3 wt.%) in water as base fluid. In view of this, four same size identical heat pipe cooling modules have been fabricated for the investigation. Here, heat pipes were fabricated by using two different fluids such as: DI water and CNT/water nanofluid. The heat pipe with CNT/water nanofluid comprises three different nanofluid concentration by weight (1 wt.%, 2 wt.% and 3 wt.%). Each cooling module consists of flat heat pipe filled with the working fluid, energy storage tank, and energy storage material, heat sink, cooling fan, heater, a power supply unit and computer. The heat pipes are made of copper tubes with an outer diameter of 6 mm and a length of 120 mm. The heat sink has 15 fins and the size of each fin is 10 mm in height, 20 mm in width and 0.5 mm in thickness. The energy storage tank is made up of acrylic material with the maximum volume of 120 cc.

Data reduction

Energy balance equation of the heat pipe-PCM cooling module during a time interval Δt, from initial time t_i to final time t_e, can be expressed as:

$$Q_{in} = Q_{EST} + Q_{ESM} + Q_{loss} \tag{5.6}$$

Here, Eq. 5.6 provides the balance between heat supplied (Q_{in}), energy stored in the tank (Q_{EST}), energy stored in phase change material (Q_{ESM}) and Heat loss parameter (Q_{loss}). The value of various parameters such as: Q_{in}, Q_{EST}, Q_{ESM} can be calculated from experimental conditions. The energy input by power supply (Q_{in}) is equal to the summation of energy storage in the PCM (Q_{ESM}), the energy storage in the tank body (Q_{EST}), and the total heat loss, Q_{loss}. Here, the heat loss (Q_{loss}) includes various parameters such as: forced convection cooling at the heat pipe fins, heat loss to ambient at the evaporator and the PCM tank.

The energy storage in the PCM is related to the mass and the temperature difference between initial and final temperature of PCM in the storage tank. It can be shown as:

$$Q_{ESM} = M_{ESM} C_{P,\,ESM} (T_e - T_i) \qquad (5.7)$$

where,

$$T_i = \frac{(T_1 + T_2 + \ldots\ldots + T_8)_i}{8} \qquad (5.8)$$

$$T_e = \frac{(T_1 + T_2 + \ldots\ldots + T_8)_e}{8}$$

The energy storage in the acrylic tank can be written as:

$$Q_{EST} = M_{EST} C_{P,\,EST} (T_e - T_i) \qquad (5.9)$$

The thermal performance of the cooling module is determined by the measured temperature evolutions of the storage tank under different charge and discharge processes.

5.3.2 Results and discussion

The tests are performed for various operating conditions, namely, heating powers (10 W, 20 W, and 30 W), fan voltage (3.15 V and 5.8 V), different working fluid of heat pipes, and different ESM (water and paraffin).The filling volumes in EST are kept as 90 cc in all the test runs. The temperature distributions in PCM are obtained during the experimental study. The results obtained from this study are elaborated below.

PCM simultaneous charging process

Figure 5.8 (a) shows the transient temperature distribution of heat pipe for different working fluids such as: DI water and CNT/water nanofluid without ESM (traditional heat pipe) in the energy storage tank. The heat pipe with CNT/water nanofluid involves three different nanofluid concentration by weight (1 wt%, 2 wt. % and 3 wt.%). Tests were conducted for a given heater power (20 W). It is observed that during 100-

250s, the rise in temperature in the nanofluid charged heat pipe is significantly higher compared to the heat pipe that utilizes the DI water as the working fluid. The transient temperature distribution of water and nanofluid charged heat pipe cooling modules with water as ESM is depicted in Fig. 5.8 (b). This indicates that water can be used as ESM for storing heat energy. Results demonstrate that the growth of temperature with time is gradual by using water as ESM compared to the cooling module without PCM. The transient temperature distribution for different working fluid charged heat pipe cooling module with paraffin wax as PCM is depicted in Fig. 5.8 (c). It is observed that the time required to achieve temperature from 20^0C to 80^0C is lower for the heat pipe cooling module with paraffin wax as PCM compared to the cooling module that uses water as ESM. Further, it is noticed that the CNT/water nanofluid charged heat pipe cooling modules exhibit better heat transfer performance compared to the water charged heat pipe cooling module. This shows that lesser time is required to achieve temperature from 20^0C to 80^0C for nanofluid charged heat pipe compared to water charged heat pipe for both the cases that use

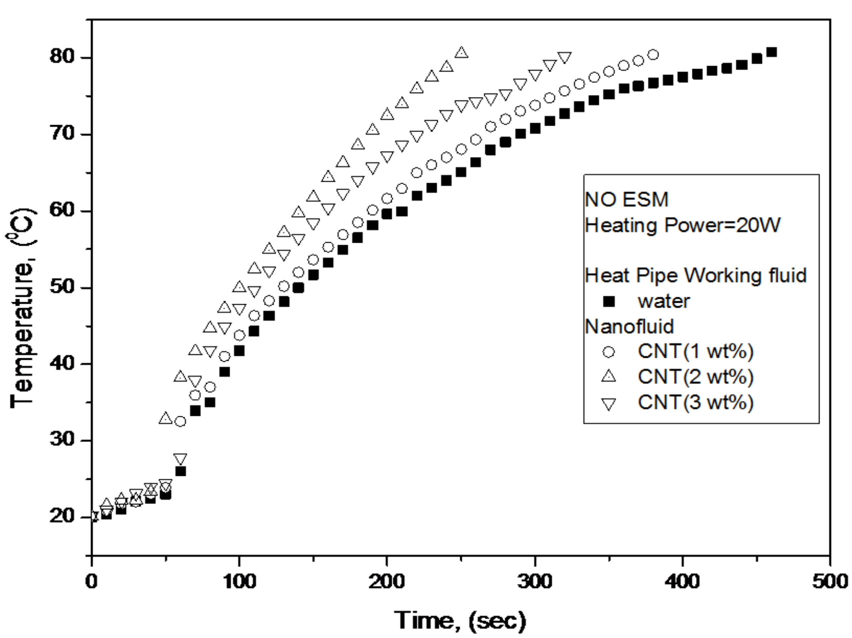

(a)

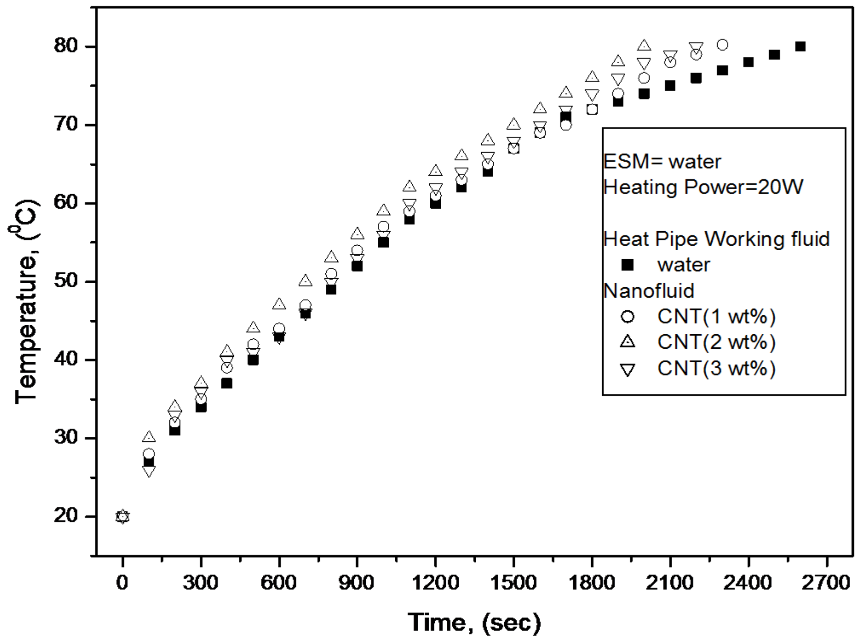

(b)

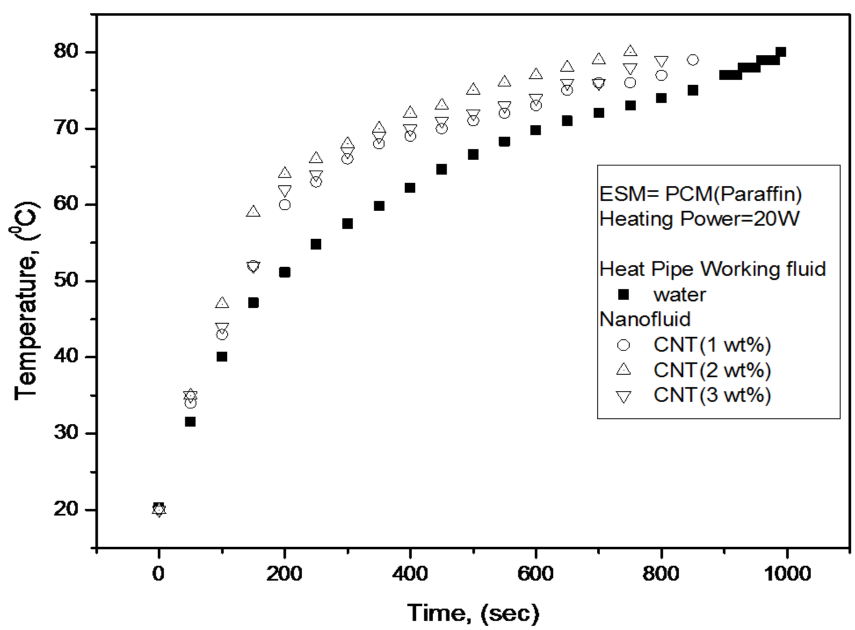

(c)

Figure 5.8: Temperature growth in charge process for different ESM **(a)** without ESM **(b)** water and **(c)** PCM (paraffin)

water and paraffin as energy storage material. It is observed that the CNT/water nanofluid (2 wt.%) charged heat pipe cooling module requires lesser time to achieve 80^0C temperature for all the cases (Fig. 3a-c). In order to achieve the temperature from 20^0C to 80^0C, CNT/water nanofluid (2 wt.%) charged heat pipe cooling module needs 2000 s and 780 s for water and paraffin as ESM, respectively

Figure 5.9 shows the comparison of the thermal performance of various heat pipes cooling module. Here, two different working fluids such as: water, and CNT/water nanofluids (1 wt.%, 2 wt.% and 3 wt.%) are used as working fluid in the heat pipe of heat pipe cooling module. Two different ESM (water and Paraffin) and at two different heater powers (10 W and 20 W) are used in the analysis. Figure 5.9 shows that for both the heating powers, the amount of energy stored in the water as ESM is lower compared to paraffin. Also, the nanofluid charged heat pipe cooling module exhibits higher energy storage performance compared to the cooling module that uses water as the working fluid for heat pipe. This may be due to various reasons. Firstly, the thermal conductivity of the CNT/water nanofluid increases due to the addition of CNT nanoparticles resulting in an increase in heat transfer. Secondly, the cylindrical porous tube structure of the CNT increases the surface roughness and enhances the heat transfer. In addition, the turbulence effect is initiated due to the random motion (Brownian motion) of the CNT in the base liquid. The turbulence effect enhances the heat transfer rate. In both the cases of energy storage material, it is noticed that the thermal performance of nanofluid charged heat pipe module increases with the increase in the CNT nanoparticles concentration in water (1 wt.% and 2 wt.%). However, with the increase in the concentration level of CNT nanoparticles in water from 2 wt.% to 3 wt.%, the thermal performance decreases. Similar results were obtained by the previous researcher as well [66]. This indicates that the rise in the concentration of added nanoparticles reduces the thermal efficiency of the heat pipe. This may be due to the fact that the addition of

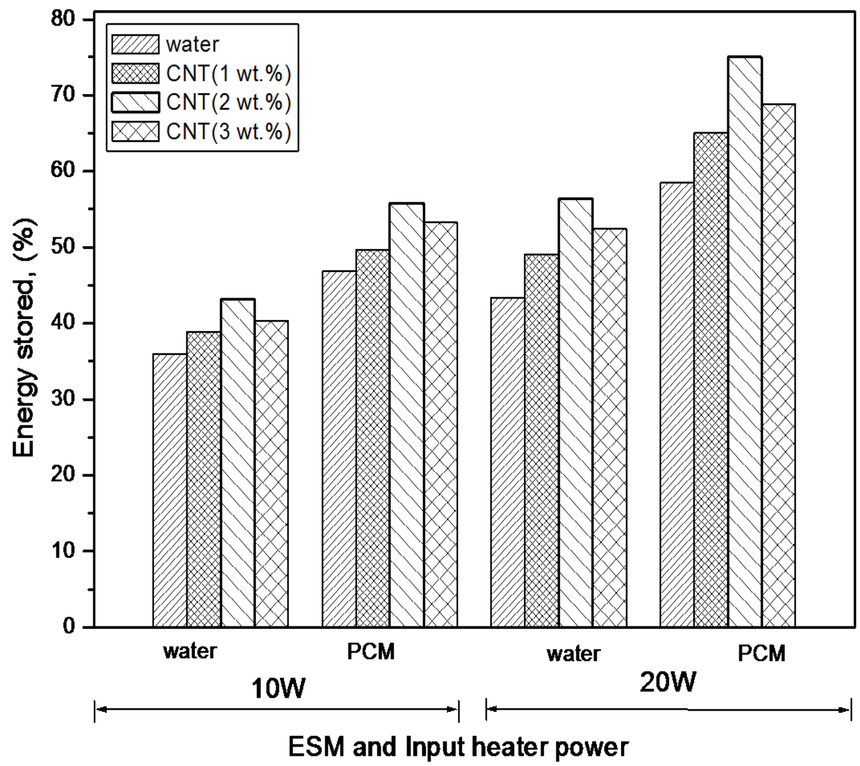

Figure 5.9: Comparison between efficiency curves at different cooling mass flow rate

too many nanoparticles to fluid reduces the rate of vaporization of nanofluid inside the evaporator resulting in a lesser heat transfer rate. Beyond certain concentration, the thermal performance of heat pipe does not increase. The maximum energy stored in paraffin is found to be 75% of the input power for the cooling heat pipe module that uses CNT/water nanofluid with 2 wt. % concentration. The enhancement in energy storage of nanofluid charged heat pipe cooling module with paraffin as ESM compared to water as ESM is found to be 13% at 10 W. While, for the 20W heating power, The enhancement in energy storage of nanofluid charged heat pipe cooling module with paraffin as ESM compared to water as ESM is found to be 20 %. This indicates that enhancement in energy storage of nanofluid used heat pipe cooling module increases with increase in input power from 10W to 20W. It may be noted that at higher input power (20W) heat transfer rate of nanofluid increases due to increase in thermal conductivity of nanofluid with temperature.

PCM simultaneous charge and discharge process

The primary purpose of this study is to simulate the temperature distribution for a fluctuating heating power that changes with time. Here, we are providing power at the heating section of the heat pipe for 300 sec and subsequently switching off the power supply for the duration of 300 sec to simulate the temperature distribution with fluctuating heating power. Figure 5.10 (a-b) depicts temperature variation in water and PCM for simultaneous charge and discharge process for different fan voltage and heating power. Here, CNT/water nanofluid (2 wt.%) charged heat pipe is used in cooling module for test runs. It is observed that in all the cases the temperature of ESM (water, paraffin) changes in synchrony with heating power [140].

The Fig. 5.10 (a-b) shows the transient temperature variation in different ESM (water and Paraffin) for various fan voltages (3.15 V and 5.8 V) with heating power of 10W and 30W, respectively. It is noticed that the water as energy storage material (ESM) with 30 W heating power and 5.8 V fan on cooling sides of heat sink stores same amount of energy when paraffin is used as ESM with 10 W heating power and 3.15 V fan on cooling sides of heat sink. This indicates that water as energy storage material (ESM) needs higher heating power (30 W) and higher fan voltage (5.8 V) to store same amount of energy compared to PCM as energy storage material (ESM). It is observed that utilizing paraffin (PCM) as ESM can save 66% in heating power and reduction in fan voltage. The reduction in fan voltage leads to save fan power consumption. This means that the PCM can absorb the heat energy at the higher rate and discharge lower amount of heat energy to the heat pipe and heat sink to reach the goal of energy management.

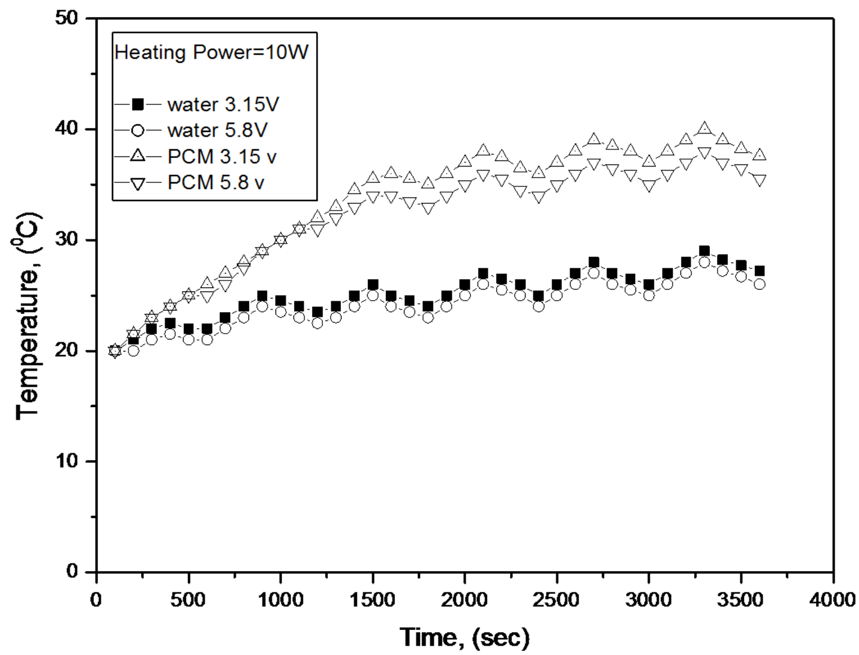

(a)

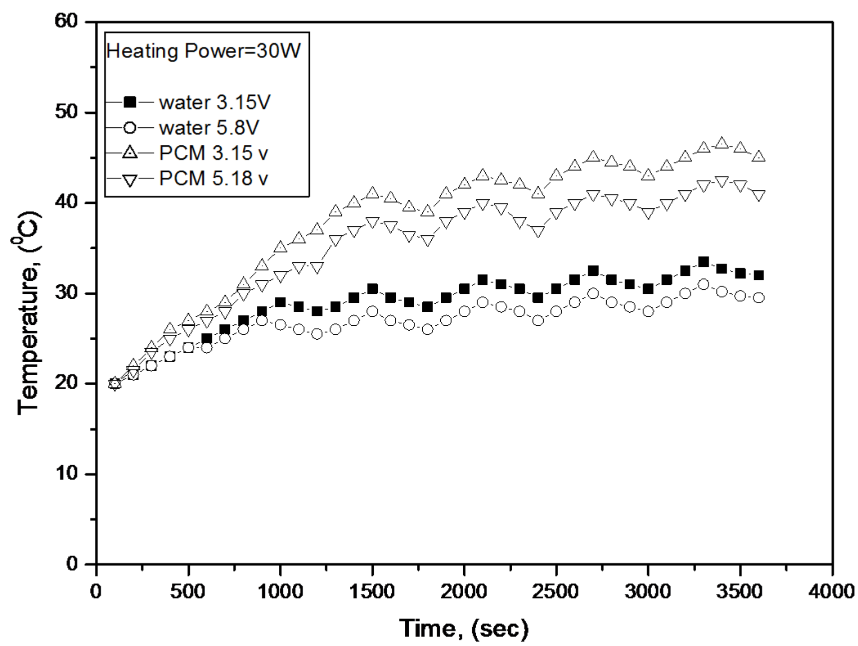

(b)

Figure 5.10: Temperature growth in different ESM for simultaneous charge and discharge process for different heating power: **(a)** 10W and **(b)** 30W.

5.4 Concluding Remarks

This chapter reports the study of thermal performance of solar flat plate collectors and electronics cooling module using nanofluid (CNT/water) charged heat pipes.

Firstly, the experimental investigation has been carried out to study the thermal performance of thermosyphon heat pipe using CNT nanofluid and pure water as working fluid. Tests have been conducted for the varied range of CNT concentration (0.15%, 0.45%, 0.60% and 1% by volume), collector tilt angle, filling ratio and coolant flow rate. Solar heat pipe collector that uses CNT nanofluid as working fluid is found to be more efficient compared to the heat pipe that uses pure water. The efficiency of the solar heat pipe collector is found to increase with the increase in the concentration level of CNT nanoparticles in water, the performance decreases when the CNT concentration exceeds 0.60%. The maximum instantaneous efficiency was found to be 73% for 0.60% volume concentration of nanofluid. The efficiency of the heat pipe collectors for both water and nanofluids increases with the tilt angle and decreases when the tilt angle exceeds 50^0. The increase in working fluid (CNT/water) filling ratio from 50 % to 60 % improves the thermal performance of wickless heat pipe collector. However, with further increase in filling ratio from 60 % to 70% deteriorates the thermal performance. The optimum filling ratio of circular wickless heat pipe collector is found to be 60%. The value of $F_R(\tau\alpha)$ is found to be highest at 60% filling ratio. While, the lowest value of $F_R U_L$ is obtained for this filling ratio. For 60% filling ratio of working fluid, the heat losses are found to higher for both the cases such as: lower coolant flow rate and higher coolant flow rate compared to ASHRAE standard coolant flow rate $0.02A_{coll}$ kg/sec.

In next problem, the thermal performance of a nanofluid (MCNT/water) charged heat pipe with phase change material (PCM) as energy storage material (ESM) for electronic cooling. Tests are conducted to obtain the thermal performance of heat pipe cooling module. The thermal performance of the cooling module is determined by the measured the temperature evolutions of the storage tank under different charge and discharge processes. Present study utilizes two different ESM (water and paraffin), different fan speeds and heating powers in the PCM cooling module. The nanofluid charged heat pipe cooling module enhances the thermal performance compared to water charged heat pipe cooling module. The heat pipe cooling module that uses paraffin (PCM) as ESM is found to be more efficient compared to the heat pipe that uses pure water as ESM. The thermal performance of the heat pipe cooling module is found to increase with the increase in the CNT nanoparticles concentration in water, the performance decreases when the CNT concentration exceeds 2 wt.%. The study demonstrates that the heat pipe module with paraffin as PCM can reduce fan power consumption up to 66% compared with heat pipe module that uses water as energy storage material. The cooling module that uses heat pipe charged with nanofluid (2 wt.%) and paraffin (PCM) as ESM exhibits maximum thermal performance. The heat pipe cooling module automatically adjusts the heat transfer rate that depends on the fan voltage, heater temperature and mass of the PCM. This can be useful for designing the cooling of electronics components.

Chapter 6

Summary and Conclusions

6.1 Introduction

The present study analyzes the thermal performance of various nanofluids such as: Al_2O_3/water and CNT/water for several practical applications including heat exchanging equipment, automobile radiators, flat plate solar collector and cooling of electronics components. The important outcomes of the present study are listed and the conclusions are highlighted in this study.

The stable nanofluids (Al_2O_3/water and CNT/water) are synthesized by using the two-step methods. Various techniques such as: ultrasonic vibration, functionalization and surface modification, are adopted to prepare nanofluids. Various methods have been employed to inspect the stability of nanofluids. The thermophysical properties of nanofluids are measured after preparing stable nanofluid. After preparing stable nanofluid, tests have been performed to study the forced convective heat transfer characteristics of Al_2O_3/water and CNT/water nanofluids through uniformly heated horizontal circular pipe with helical twisted tape inserts (HI). Next, an experimental study has been carried out to evaluate the convective heat transfer characteristics of CNT/water and Al_2O_3/water and nanofluids in an automobile radiator. Efforts have been made to compare thermal performance for CNT/water nanofluid with Al_2O_3/water nanofluid in automobile radiator. Here, nanofluid (CNT/water) charged heat pipes were integrated into the flat plate solar collector to evaluate the thermal performance. The effect of the tilt angle, filling ratio, nanoparticle concentration and coolant flow rate on the thermal performance of the solar collector has been discussed in the study. Further, an attempt has been made to evaluate the thermal performance of a nanofluid (CNT/water) charged heat pipe with phase change material (PCM) as energy storage material (ESM) for electronic cooling. The significant findings obtained from the present study are detailed below.

6.2 Synthesis and Characterization of Nanofluids

Nanofluids are considered as a better medium to transfer heat in various devices. However, the preparation of nanofluids needs special attention since the preparation methods affect various important thermophysical properties and stability of the dispersion. The selection of the proper synthesis method is an important task that ensures the stability of nanofluids over a longer period with negligible agglomeration [104]. In view of this, efforts have been made to prepare nanofluids by employing various methods. Here, CNT/water and Al_2O_3/water nanofluids have been prepared by adopting the two-step technique. The important points are mentioned here.

1. The morphological characterization for two different nanoparticles such as: Al_2O_3 and CNT are obtained by using scanning electron microscopy (Model: SUPRA 55, Make: Carl Zeiss Microscopy, Germany). The shape of Alumina nanoparticle and CNT is found to be spherical and cylindrical, respectively. The size and shape are confirmed as per specification provided by the manufacture of nanopowders.
2. The dynamic light scattering (DLS) methodology is used to measure the average particle size and particle size distribution of the nanoparticle in the suspension by using a particle sizing system (Model: Nicomp 380, Make: Santa Barbara, USA).The FCNT nanofluid exhibits lower hydrodynamic diameter compared to SCNT nanofluid. The Al_2O_3/water nanofluid prepared by using simple sonication method exhibits enough stability (Fig. 2.4).
3. The electrophoresis behavior of individual nanoparticle in the suspension is studied by measuring the zeta potential of the

suspension. Here, FCNT exhibit higher value of zeta potential compared to SCNT and Al_2O_3/water nanofluid. Also, the zeta potential value decreases with increasing nanoparticle concentration (Table 2.2).

4. The wettability behavior of various nanofluids on the solid surface is studied by measuring the contact angle of the fluid at the solid surface. The addition of nanoparticle to base fluid (water) reduces contact angle leading to an increase in wettability of the surface. The wettability of CNT/water nanofluid is higher than water followed by Al_2O_3/water nanofluid (Fig. 2.5).
5. The effective thermal conductivity of various nanofluids are measured by using the thermal property analyzer (Model: KD2 Pro., Model: Decagon Devices, USA) with isothermal temperature bath. The thermal conductivity of nanofluids (CNT/water, Al_2O_3/water) was found to increase with nanoparticle concentration and temperature. The effective thermal conductivity of CNT/water nanofluid is found to be higher compared to Al_2O_3/water nanofluids for similar conditions.
6. In addition, the viscosity of nanofluids (CNT/water, Al_2O_3/water) was measured by using cone and plate viscometer (Model: Brookfield DV-II+ Pro, Make: Brookfield Engineering Laboratories, USA). The viscosity of Al_2O_3/water nanofluids was found to be higher compared to CNT/water nanofluids for similar conditions.
7. Finally, it is observed that CNT/water nanofluid have better thermal and fluid properties to enhance heat transfer compared to Al_2O_3/water nanofluid. The *functionalization* of CNT's is the best method to prepare stable CNT/water nanofluids.

6.3 Thermal Performance of Nanofluids

The heat transfer capacity of coolant (nanofluids) is considered to be a useful technology to enhance the cooling capacity. The synthesis and characterization are important tasks for its use in heat transfer devices. After successful preparation of stable nanofluids, efforts have been made to study the heat transfer characteristics of nanofluids through uniform heated pipes with and without inserts, automobile radiator, solar collectors and nanofluid assisted heat pipe for electronics cooling. The experiments are performed by using nanofluid in various thermal devices. The key findings are presented here.

Convective heat transfer performance of low volume concentration of nanofluids in laminar regime using helical screw tape inserts

Experiments were carried out by using Al_2O_3/water (φ = 0.15%) and CNT/water (φ = 0.15%) nanofluid with helical tape inserts of twist ratio, TR= 1.5, 2.5 and 3. Reynolds number is varied in the range of 840 to 2280. The test data were used to calculate the Nusselt number, friction factor and thermal performance factor for various Peclet numbers in laminar flow regime with and without helical screw tape inserts. The conclusions are detailed below:

1. The use of helical screw tape inserts in the plain tube causes intensification in heat transfer with the significant increase in pressure drop. The Nusselt number for the tube fitted with helical inserts is found to be higher compared to the plain tube for a given Peclet number.
2. The average enhancement in Nusselt number of Al_2O_3/water and CNT/water nanofluid in the plain tube were found to be 10.72% and 20.27%, respectively compared to the water as the working fluid. The enhancement in Nusselt number decreases with the increase in Peclet number. In the case of Al_2O_3/water

nanofluid, the increase in the average Nusselt number was found to be 230.14%, 175.07% and 135.79%, for various twist ratios 1.5, 2.5 and 3, respectively. On the contrary, the enhancement in the Nusselt Number for CNT/water nanofluid was found to be 272.61%, 213.58% and 166.45% for the twist ratios 1.5, 2.5 and 3, respectively (Fig.3.5).

3. The tube fitted with helical tapes decreases the hydraulic diameter leading to the increase in the fluid flow and swirl generation. The enhancement in Nusselt number decreases with the increase in Peclet number and increases with the decrease in the twist ratio (TR).
4. The experimental results reveal that CNT/water nanofluid gives enormous enhancement in heat transfer compared to Al_2O_3/water nanofluid. This is because the CNTs offer a higher thermal conductivity, higher aspect ratio, lower specific gravity, and larger specific surface area (SSA) and lower thermal resistance compared Al_2O_3/water nanofluid.
5. The value of friction factor obtained by using the helical screw inserts were higher compared to the plain tube. The value of friction factor increases with the decrease in twist ratio.
6. The increase in the friction factor by the addition of Al_2O_3 and CNT nanoparticle in the base fluid is minimal because of the low volume concentration of nanoparticles.
7. The maximum friction factor of CNT/water nanofluid with inserts was found to be 19.99, 13.24 and 11.80 times the friction factor of plain tube with water for twist ratios of 1.5, 2.5 and 3, respectively. The maximum friction factor of Al_2O_3/water nanofluid with inserts was found to be 20.43, 13.79 and 12.02 times the friction factor of plain tube with water for twist ratios 1.5, 2.5 and 3, respectively (Fig. 3.13).

8. The experimental results show that helical screw tape inserts give the better thermal performance for CNT/water nanofluid compared to Al_2O_3/water nanofluid. For a given operating condition, the thermal performance factor for CNT/water nanofluid is higher compared to Al_2O_3/water for all twist ratios.
9. The values of thermal performance factor (η) was found to be higher for low twist ratios irrespective of the working fluid and Peclet number. This may be due to the stronger turbulence/swirl flow generated by the helical screw tape insert in the case of insert with lower twist ratio.
10. For the twist ratios of 1.5, 2.5 and 3, the thermal performance factor varies between 2.29-1.69, 2.03-1.55 and 1.69-1.35 respectively by using CNT/water nanofluid. On the contrary, the thermal performance factor of Al_2O_3/water nanofluid (by volume 0.15%) was found to vary between 2.14-1.65, 1.90-1.47 and 1.58-1.31 for the twist ratios of 1.5, 2.5 and 3, respectively.
11. The Nusselt number increases with the volume concentration of nanoparticles because adding nanoparticles to base fluid enhances the thermal conductivity.

Convective heat transfer performance of low volume concentration of nanofluids in transition regime using helical screw tape inserts

Here, the tests are extended for transition flow regime using 0.15% volume concentration Al_2O_3/water and CNT/water nanofluid with helical tape inserts of twist ratio, TR= 1.5, 2.5 and 3. The Reynolds number is varied in the range of 2400 to 5600. The test data were used to calculate the Nusselt number, friction factor and thermal performance factor for various Peclet numbers in transition flow regime with and without helical screw tape inserts. In this study, similar observations (point 1, 3-4 and 8-9) were obtained as discussed in the laminar flow regime.

Apart from previous observations, following conclusions are made from the analysis and elaborated below:

1. The average enhancement in Nusselt number of Al_2O_3/water and CNT/water nanofluid in the plain tube were found to be 12.02% and 26.13%, respectively compared to the water as the working fluid. The enhancement in the Nusselt number of pure water with various twist ratios 1.5, 2.5 and 3 were found to be 159.60%, 125.85% and 91.30%, respectively. In addition, the increase in the average Nusselt number for various twist ratios 1.5, 2.5 and 3 were found to be 172.81%, 131.21% and 99.33%, respectively for Al_2O_3/water nanofluid. While, the CNT/water nanofluid exhibits 215.55%, 173.25% and 120.32% enhancement in the Nusselt Number corresponding to the twist ratios 1.5, 2.5 and 3, respectively.
2. The maximum friction factor of CNT/water nanofluid with inserts was found to be 7.75, 6.67 and 6.15 times the friction factor of a plain tube with water corresponding to twist ratios (TR) of 1.5, 2.5 and 3, respectively at Pe =16000. While, the maximum friction factor of Al_2O_3/water nanofluid with inserts was found to be 8.04, 6.95 and 6.19 times the friction factor of plain tube with water corresponding to twist ratios of 1.5, 2.5 and 3, respectively at Pe =16000.
3. It is observed that the values of η are higher for the low twist ratios irrespective of the working fluid and Peclet number. This is due to the stronger turbulence/swirl flow generated by the helical screw tape insert in the case of insert with the smallest twist ratio (TR). Here, η is found to vary between 1.35-1.16, 1.29-1.21 and 1.22-0.97 for twist ratios of 1.5, 2.5, and 3, respectively using CNT/water nanofluid as the working fluid. While, the thermal performance factor of the Al_2O_3/water

nanofluid (φ = 0.15%) varies between 1.19-1.02, 1.16-1.01 and 1.10-0.88 for the twist ratios of 1.5, 2.5 and 3, respectively.

Convective heat transfer performance of varying concentration (φ = 0.15%, 0.45%, 0.60% and 1%) in transition regime using helical screw tape inserts

The thermal performance of nanofluids for given particle volume concentration (*φ* = 0.15 %) with helical screw tape inserts is discussed in the previous study. The effect of nanoparticle concentration on the thermal performance is studied for the transition flow regime. Four different concentrations are used in the investigation. Here, efforts have been made to test thermal performance of Al_2O_3/water and CNT/water nanofluids with varied range of nanoparticle concentration (*φ* = 0.15%, 0.30%, 0.60% and 1%) and helical tape inserts of twist ratios, TR= 1.5, 2.5 and 3. Here, Peclet number is varied in the range of 16000 to 33500. The thermal performance factor is evaluated for various Peclet numbers with and without helical screw tape inserts. This is detailed below.

1. The Nusselt number increases with the increase in Peclet number and nanoparticle concentration. This may be due that the in thickness of boundary layer gets thinner at higher Reynolds number. Also, the addition of nanoparticles to base fluid enhances the thermal conductivity.
2. The enhancement in the heat transfer and friction factor of nanofluids for various nanoparticle concentrations is studied through experimental investigation. The friction factor increases with the increase in particle volume concentration for various nanofluids (CNT/water and Al_2O_3/water). This may be due to the fact that the viscosity of nanofluids increases with nanoparticle concentration. While the friction factor is found to decrease with the increase in Peclet numbers.

3. The thermal performance factor of CNT/water nanofluids is found to be greater than unity for varied range of Peclet number (16,000–33,500), twist ratio (TR = 1.5, 2.5 and 3) and nanoparticle concentration (φ = 0.15%, 0.45%, 0.60% and 1%).
4. Here, Al_2O_3 nanofluid exhibits lower thermal performance factor ($\eta < 1$) for TR = 3, φ = 0.15% and Pe > 30000. While, the thermal performance factor with different twist ratio (TR = 1.5, 2.5 and 3) and with particle volume concentration (φ = 0.15%, 0.45%, 0.60% and 1%) are found to be greater than unity (Fig. 3.17).
5. The values of η for the CNT/water nanofluid is found to be higher compared to the Al_2O_3/water nanofluid and pure water for various twist ratios (TR = 1.5, 2.5 and 3) and different nanoparticle concentrations (φ = 0.15%, 0.45%, 0.60% and 1%) at all Peclet number. It is observed that the values of η are higher for the lower twist ratios irrespective of the working fluid and Peclet number. This may due to the stronger turbulence/swirl flow generated by the helical screw tape insert with the smallest twist ratio.
6. For φ =1% and TR=1.5, Pe=16000, both of nanofluids (Al_2O_3/water and CNT/water nanofluid) exhibits the maximum value of thermal performance factor (η). The maximum value of thermal performance factor (η) is found to be 1.46 and 1.41 for Al_2O_3/water nanofluid and CNT/water nanofluid, respectively.

Thermal performance of CNT/water nanofluids through an automobile radiator

Tests are performed to evaluate the thermal performance of various fluids (water and nanofluids) through an automobile radiator. Experiments were carried out by using water and CNT/water nanofluid with varied range of concentration (0.15%, 0.45%, 0.60%, and 1% by volume), coolant flow rate, pH and synthesis method of nanofluid. Tests were conducted at ambient temperature 35±1^{0}C with a relative humidity of 65±5%. For all the test runs, the inlet temperature of the coolant is maintained at 90^{0}C. The flow rate of coolant is varied between 2-5 lit/min. The observation obtained from the present investigation is summarized below.

1. The heat transfer performance of various coolants, namely, water, SCNT/water and FCNT/water nanofluid increases with the increase in coolant flow rate.
2. The thermal performance of automobile radiator was found to increase with the use of nanocoolant compared to water.
3. The functionalized CNT (FCNT) nanocoolant exhibits better enhancement in the heat transfer rate compared to surface treated CNT nanocoolant and water. The performance of surface treated CNT nanocoolant (SCNT) is found to deteriorate at the higher temperature. This may be due to the lower bonding strength between nanoparticles and surfactant.
4. The thermal performance of the acidic nanocoolant with the pH 5.5 was found to be better compared to the nanocoolant with pH value of 6.5 and 9.0.

Comparative thermal performance of CNT/water and Al_2O_3/water nanofluids through an automobile radiator

The heat transfer of nanofluids through the radiator is analyzed using CNT/water nanofluid. The efforts are taken, to evaluate the comparative heat transfer performance of water, CNT/water and Al_2O_3/water with varied range of particle volume fraction (0.15%, 0.45%, 0.60%, and 1%). Tests were performed at ambient temperature 35±1^{0}C with a relative humidity of 65±5%. The inlet temperature of the coolant is maintained at 90^0C for all the test runs and the flow rate is varied between 2-5 lit/min. The observation obtained from the present investigation is summarized below.

1. The cooling performance in automobile radiator for both CNT/water and Al_2O_3/water nanocoolant increases with the increase in nanoparticles concentration. This may be due to facts that increase in nanoparticles concentration of nanofluids increases effective thermal conductivity of nanofluids.
2. The maximum heat transfer performance for 1.0 vol.% nanoparticle concentration was found to be 90.76% and 52.03% higher compared to pure water results for CNT/water and Al_2O_3/water, respectively.
3. With the increase in the coolant flow rate, the heat transfer performance increases for various coolants, namely, water, CNT/water and Al_2O_3/water.
4. The CNT/water nanofluid exhibits enormous enhancement in heat transfer compared to the Al_2O_3/water nanofluid. This may be due to the fact that carbon nanotubes offer a high thermal conductivity, high aspect ratio, low specific gravity, and large specific surface area (SSA) and low thermal resistance as compared Al_2O_3/water nanofluid.

Thermal performance of nanofluid charged thermosyphon in solar flat plate collector

An experimental investigation has been carried out to study the thermal performance of thermosyphon heat pipe using CNT/water nanofluid and pure water as working fluid. Tests have been conducted for varied range of CNT concentration (φ = 0.15%, 0.45%, 0.60% and 1%), collector tilt angle, filling ratio and coolant flow rate.

1. Solar heat pipe collector that uses CNT nanofluid as working fluid is found to be more efficient compared to the heat pipe

that uses pure water. The efficiency of the solar heat pipe collector is found to increase with the increase in the CNT nanoparticles concentration in water, the performance is found to decrease when the CNT concentration exceeds 0.60%.

2. Maximum instantaneous efficiency was found to be 73% for 0.60% volume concentration of the nanofluid. The efficiency of the heat pipe collectors for both water and nanofluids increases with the tilt angle and decreases when the tilt angle exceeds 50^0.
3. The increase in working fluid (CNT/water) filling ratio from 50% to 60% improves the thermal performance of wickless heat pipe collector. However, with further increase in filling ratio from 60% to 70% deteriorates the thermal performance. The optimum filling ratio of circular wickless heat pipe collector is found to be 60%.
4. The value of the absorbed energy parameter ($FR(\tau\alpha)$) is found to be highest at 60% filling ratio. While, the lowest value of and heat removed parameter ($F_R U_L$) is obtained for this filling ratio.
5. For 60% filling ratio of working fluid, the heat losses are found to higher for both the cases such as: lower coolant flow rate and higher coolant flow rate compared to ASHRAE standard coolant flow rate $0.02A_{coll}$ kg/sec.

Thermal performance of nanofluid charged heat pipe with PCM for electronics cooling

The present study experimentally investigates the thermal performance of a nanofluid (MCNT/water) charged heat pipe with phase change material (PCM) as energy storage material (ESM) for electronic cooling. Tests are conducted to obtain the thermal performance of heat pipe cooling module. The thermal performance of the cooling module is determined by the measured temperature of the storage tank under different charging and discharging processes. Present study utilizes two different ESM (water and paraffin), different fan speeds and heating powers in the PCM cooling module. The contributions from the present study are elaborated below.

1. The nanofluid charged heat pipe cooling module enhances the thermal performance compared to water charged heat pipe cooling module.
2. The heat pipe cooling module that uses paraffin (PCM) as ESM is found to be more efficient compared to the heat pipe that uses pure water as ESM.
3. The thermal performance of the heat pipe cooling module is found to increase with the increase in the CNT nanoparticles concentration in water, the performance decreases when the CNT concentration exceeds 2% by weight.
4. The study demonstrates that the heat pipe module with paraffin as PCM can reduce fan power consumption up to 66% compared with heat pipe module that uses water as energy storage material.
5. The cooling module that uses nanofluid (2% by weight) charged heat pipe and paraffin (PCM) as ESM exhibits maximum thermal performance.
6. The heat pipe cooling module automatically adjusts the heat transfer rate that depends on the fan voltage, heater temperature and mass of the PCM. This can be useful for designing the cooling of electronics components.

It may be mentioned that the findings of the present investigations could be helpful in designing various thermal systems as applied to scientific and engineering applications.

6.4 Suggestions for Future Work

It may be noted that nanofluids can be used as alternative coolant in various thermal devices. This would reduce the size of the system, consequently the cost of the thermal device. A better understanding of the stability behavior and anomalous increase in heat transfer enhancement of nanofluids may lead to an accurate design of the thermal device with nanofluid as the coolant. The investigation carried out in this dissertation may provide some useful information for further study in this area. In view of this, certain directions of future work are elaborated below.

1. More experiments with flow visualization are required to examine the anomalous enhancements in the heat transfer of nanofluids.
2. Experiments need to be conducted to evaluate the optimum ranges of concentration for maximum thermal performance.
3. There are certain technical challenges observed while using nanofluids in the real system. This includes the costs of production, long-term stability of nanoparticles dispersion, the increased pressure drop and pumping power. More experiments need to conduct in thermal devices to evaluate these issues.
4. Theoretical models need to be developed to evaluate the thermal performance of heat pipes. Also, efforts should be made to find the optimum concentration, filling ratio and tilt angle (orientation) for heat pipe to get maximum thermal performance.
5. Efforts should be made to analyze the thermal performance of nanofluid with boiling phenomenon.
6. Lack of study on optical properties of nanofluid in the solar collector and the other properties except the thermal conductivity is obvious and it needs more attention. The use of PCM in heat storage applications can be enhanced by using

PCM-nanoparticle composites. This will improve thermal performance in electronics cooling and solar collectors.

7. The addition of CNT to non-metallic oxide nanofluid can improve its thermal conductivity. In view of this, effort should be made to study heat transfer properties of non-metallic oxide/CNT hybrid nanofluids.
8. Experiments need to be conducted with hybrid nanofluid with more than one nanoparticle.

References

[1] S. U. S. Choi, D. A. Singer and H. Wang, "Development and application of non-newtonian flows," in *International Mechanical Engineering Congress and Exposition*, NY, 1995.

[2] J. C. Maxwell, Treatise on electricity and magnetism, Clarendon Press, Oxford, 1873.

[3] E. Serrano, G. Rus and J. Martinez, "Nanotechnology for sustainable energy," *Renew. Sust. Energy Rev.,* vol. 13, no. 9, pp. 2373-84, 2009.

[4] R. Saidur, K. Y. Leong and H. A. Mohammad, "A review on applications and challanges of nanofluids," *Renew. Sust. Energy Rev.,* vol. 15, pp. 1646-1668, 2011.

[5] P. Keblinski, S. R. Phillpot, S. U. S. Choi and J. A. Eastman, "Mechanism of heat flow in suspensions of nano-sized partciles (nanofluids)," *Int. Jou. Heat Mass Trans.,* vol. 45, pp. 855-863, 2002.

[6] W. Evans, R. Prasher, J. Fish, P. Meakin, P. Phelan and P. Keblinski, "Effect of aggregation and interfacial thermal resistance on thermal conductivity of nanocomposites and colloidal nanofluids," *Int. J. Heat Mass Transf.,* vol. 51, no. 5-6, pp. 1431–1438, 2008.

[7] J. Sarkar, "A critical review on convective heat transfer correlations of nanofluids," *Renewable and Sustainable Energy Reviews,* vol. 15, pp. 3271-3277, 2011.

[8] R. M. Mostafizur, M. U. Bhuiyan, R. Saidur and A. R. Abdul Aziz, "Thermal conductivity variation for methanol based nanofluids," *International Journal of Heat and Mass Transfer,* vol. 76, pp. 350-356, 2014.

[9] M. Hojjat, S. G. Etemad, R. Bagheri and J. Thibault, "Thermal conductivity of non-Newtonian nanofluids: Experimental data," *International Journal of Heat and Mass Transfer,* vol. 54, pp. 1017-10123, 2011.

[10] J. A. Eastman, S. U. S. Choi, S. Li., W. Yu and L. J. Thompson, "Anomalously increased effective thermal conductivities of ethylene glycol-based nanofluids containing copper nanoparticles," *Appl. Phys. Lett. ,* vol. 78, no. 6, pp. 718-20, 2001.

[11] L. Syam Sundar, N. T. Ravi Kumar, M. T. Naik and K. V. Sharma, "Effect of full length twisted tape inserts on heat transfer and friction factor enhancement with Fe_3O_4 magnetic nanofluid inside a plain tube: An experimental study," *International Journal of Heat and Mass Transfer,* vol. 55, pp. 2761–2768, 2012.

[12] M.-S. Liu, M.-C. Lin, C. Y. Tsai and C. C. Wang, "Enhancement of thermal conductivity with Cu for nanofluids using chemical reduction method," *Int. J. Heat. Mass Transfer,* vol. 49, no. 17-18, pp. 3028-33, 2006.

[13] Y. J. Hwang, Y. C. Ahn, H. S. Shin, C. G. Lee, G. T. Kim and H. S. Park, "Investigation on characteristics of thermal conductivity enhancement of nanofluids," *Curr. Appl. Phys.,* vol. 6, no. 6, pp. 1068-71, 2006.

[14] J. H. Lee, K. S. Hwang, S. P. Jang, B. H. Lee, J. H. Kim and S. U. S. Choi, "Effective viscosities and thermal conductivities of aqueous nanofluids containing low olume concentrations of Al_2O_3 nanoparticles," *Int. J. Heat Mass Transfer,* vol. 51, no. 11-12, pp. 2651-56, 2008.

[15] H. A. Mintsa, G. Roy, C. T. Nguyen and D. Doucet, "New temperature dependent thermal conductivity data for water-based nanofluids," *Int. J. Therm. Sci.,* vol. 48, no. 2, pp. 363–71, 2009.

[16] W. Yu, D. M. France, S. U. S. Choi and J. L. Routbort, "Review and

assessment of nanofluid technology for transportation and other applications," Energy Systems Division, Argonne National Laboratory, Chicago, USA, 2007.

[17] R. S. Vajjha and D. K. Das, "Experimental determination of thermal conductivity of three nanofluids and development of new correlations," *Int. J. Heat Mass Transfer,* vol. 52, no. 21-22, pp. 4675–8, 2009.

[18] B. Shen, "Minimum quantity lubrication grinding using nanofluids," PhD thesis, University of Michigan, Michigan USA, 2006.

[19] D. Wen and Y. Ding, "Experimental investigation into convective heat transferof nanofluids at the entrance region under laminar flow conditions," *International Journal of Heat and Mass Transfer,* vol. 47, pp. 5181–5188, 2004.

[20] K. B. Anoop, T. Sundararajan and S. K. Das, "Effect of particle size on the convective heat transfer in nanofluid in the developing region," *International Journal of Heat and Mass Transfer,* vol. 52, pp. 2189–2195, 2009.

[21] K. S. Hwang, S. P. Jang and S. U. S. Choi, "Flow and convective heat transfer characteristics of water-based Al_2O_3 nanofluids in fully developed laminar flow regime," *International Journal of Heat and Mass Transfer,* vol. 52, pp. 193-199, 2009.

[22] E. Esmaeilzadeh, H. Almohammadi, S. N. Vatan and A. N. Omrani, "Experimental investigation of hydrodynamics and heat transfer characteristics of Al_2O_3/water under laminar flow inside a horizontal tube," *Int. Jou. Ther. Sci.,* vol. 63, pp. 31-37, 2013.

[23] M. M. Heyhat, F. Kowsary, A. M. Rashidi, M. H. Momenpour and A. Amrollahi, "Experimental investigation of laminar convective heat transfer and pressure drop of water-based Al_2O_3 nanofluids in fully developed flow regime," *Experimental Thermal and Fluid Science,* vol. 44, pp. 483–489, 2013.

[24] Y. Ding, H. Alias, D. Wen and R. A. Williams, “Heat transfer of aqueous suspensions of carbon nanotubes (CNT nanofluids),” *International Journal of Heat and Mass Transfer,* vol. 49, pp. 240-250, 2006.

[25] P. Garg, J. L. Alvarado, C. Marsh, T. A. Carlson and D. A. Kessler, “An experimental study on the effect of ultrasonication on viscosity and heat transfer performance of multi-wall carbon nanotube-based aqueous nanofluids,” *International Journal of Heat and Mass Transfer,* vol. 52, pp. 5090–5101, 2009.

[26] A. Amrollahi, A. M. Rashidi, R. Lotfi, M. E. Meibodi and K. Kashefi, “Convection heat transfer of functionalized MWNT in aqueousfluids in laminar and turbulentflow at the entrance region,” *nternational Communications in Heat and Mass Transfer,* vol. 37, pp. 717–723, 2010.

[27] Z. H. Liu and L. Liao, “Forced convectiveflow and heat transfer characteristics of aqueous drag reducingfluid with carbon nanotubes added,” *International Journal of Thermal Sciences,* vol. 49, pp. 2331-2338, 2010.

[28] A. Abreu, B. Lamas, A. Fonseca, N. Martins and M. S. Oliveira, “Experimental characterization of convective heat transfer with MWCNT based nanofluids under laminar flow conditions,” *Heat Mass Transfer,* vol. 50, pp. 65-74, 2014.

[29] X. Q. Wang and A. S. Mujumdar, “Heat transfer characteristics of nanofluids: a review,” *International Journal of Thermal Sciences,* vol. 46, pp. 1-19, 2007.

[30] A. A. Abbasian Arani and J. Amani, “Experimental study on the effect of TiO_2–water nanofluid on heat transfer and pressure drop,” *Experimental Thermal and Fluid Science,* vol. 42, pp. 107-115, 2012.

[31] M. H. Kayhani, H. Soltanzadeh, M. M. Heyhat, M. Nazari and F.

Kowsary, "Experimental study of convective heat transfer and pressure drop of TiO_2/water nanofluid," *International Communications in Heat and Mass Transfer,* vol. 39, pp. 456–462, 2012.

[32] A. R. Sajadi and M. H. Kazemi, "Investigation of turbulent convective heat transfer and pressure drop of TiO_2/water nanofluid in circular tube," *International Communications in Heat and Mass Transfer,* vol. 38, pp. 1474–1478, 2011.

[33] Y. He, Y. Jin, H. Chen, Y. Ding, D. Cang and H. Lu, "Heat transfer and flow behaviour of aqueous suspensions of TiO_2 nanoparticles (nanofluids) flowing upward through a vertical pipe," *International Journal of Heat and Mass Transfer,* vol. 50, pp. 2272–2281, 2007.

[34] S. M. Fotukian and M. Nasr Esfahany, "Experimental study of turbulent convective heat transfer and pressure drop of dilute CuO/water nanofluid inside a circular tube," *International Communications in Heat and Mass Transfer,* vol. 37, pp. 214–219, 2010.

[35] P. Selvakumar and S. Suresh, "Convective performance of CuO/water nanofluid in an electronic heat sink," *Experimental Thermal and Fluid Science,* vol. 40, pp. 57–63, 2012.

[36] S. Zeinali Heris, T. H. Nassan and S. H. Noie, "CuO/water nanofluid convective heat transfer through square duct under uniform heat flux," *nt. J. Nanosci. Nanotechnol.,* vol. 7, no. 3, pp. 111-120, 2011.

[37] Y. Xuan and Q. Li, "Heat transfer enhancement of nanofluid," *International Journal of Heat and Fluid Transfer,* vol. 21, pp. 58–64, 2000.

[38] W. H. Azmi, K. V. Sharma, P. K. Sharma, R. Mamat, S. Anuar and V. Dharma Rao, "Experimental determination of turbulent forced convection heat transfer and friction factor with SiO_2 nanofluid,"

Experimental Thermal and Fluid Science, vol. 51, pp. 103-111, 2013.

[39] S. Ferrouillat, A. Bontemps, J. P. Ribeiro, J. A. Gruss and O. Soriano, "Hydraulic and heat transfer study of SiO_2/water nanofluids in horizontal tubes with imposed wall temperature boundary conditions," *International Journal of Heat and Fluid Flow,* vol. 32, pp. 424-439, 2011.

[40] J. E. Julia, L. Hernández, R. Martínez-Cuenca, T. Hibiki, R. Mondragón, C. Segarra and J. C. Jarque, "Measurement and modelling of forced convective heat transfer coefficient and pressure drop of Al_2O_3-water and SiO_2-water nanofluids," *Journal of Physics: Conference Series,* vol. 395, p. 012038, 2012.

[41] A. Bontemps, J. P. Ribeiro, S. Ferrouillat, J. A. Gruss, O. Soriano and B. Wang, "Experimental study of convective heat transfer and pressure loss of SiO_2/water nanofluids art 1: nanofluid characterization - imposed wall temperature," in *Thermal Issues in Emerging Technologies, ThETA 2* , Cairo, Egypt , 2008.

[42] W. Yu, D. M. France, D. S. Smith, D. Singh, E. V. Timofeeva and J. L. Routbort, "Heat transfer to a silicon carbide/water nanofluid," *International Journal of Heat and Mass Transfer,* vol. 52, pp. 3606–3612, 2009.

[43] L. Syam Sundar, M. T. Naik, K. V. Sharma, M. K. Singh and T. C. Siva Reddy, "Experimental investigation of forced convection heat transfer and friction factor in a tube with Fe_3O_4magnetic nanofluid," *Experimental Thermal and Fluid Science,* vol. 37, pp. 65-71, 2012.

[44] A. Hasanpour, M. Farhadi and K. Sedighi, "A review study on twisted tape inserts on turbulentflow heat exchangers: The overall enhancement ratio criteria," *International Communications in Heat and Mass Transfer,* vol. 55, pp. 53–62, 2014.

[45] S. Liu and M. Sakr, "A comprehensive review on passive heat

transfer enhancements in pipe exchangers," *Renewable and Sustainable Energy Reviews,* vol. 19, pp. 64–81, 2013.

[46] K. V. Sharma, L. S. Sundar and P. K. Sharma, "Estimation of heat transfer coefficient and friction factor in the transition flow with low volume concentration of Al_2O_3 nanofluid flowing in a circular tube and with twisted tape insert," *Int. Commun. Heat Mass Transf.,* vol. 36, pp. 503–507, 2009.

[47] L. S. Sundar and K. V. Sharma, "Heat transfer enhancements of low volume concentration Al_2O_3 nanofluid and with longitudinal strip inserts in a circular tube," *Int. J. Heat Mass Transf.,* vol. 53, pp. 4280–4286, 2010.

[48] L. S. Sundar and K. V. Sharma, "Turbulent Heat Transfer and Friction Factor of Al_2O_3 NanoFluid in Circular Tube with Twisted Tape Inserts," *Int. Commun. Heat Mass Transf.,* vol. 53, p. 1409–1416, 2010.

[49] K. Wongcharee and S. Eiamsa-ard, "Enhancement of heat transfer using CuO/water nanofluid and twisted tape with alternate axis," *Int. Commun. Heat Mass Transf.,* vol. 38, pp. 742–748, 2011.

[50] M. Chandrasekar., S. Suresh and A. Chandra Bose, "Experimental studies on heat transfer and friction factor characteristics of Al_2O_3/water nano-fluid in a circular pipe under laminar flow with wire coil inserts," *Exp. Thermal Fluid Sci.,* vol. 34, pp. 122-130, 2010.

[51] M. Chandrasekar., S. Suresh and A. Chandra Bose, "Experimental Studies onheat transfer and friction factor characteristics of Al_2O_3/water nanofluid in a circular pipe under transition flow with wire coil inserts," *Heat Transf. Eng.,* vol. 32, pp. 495–496, 2011.

[52] S. Suresh, K. P. Venkitaraj, P. Selvakumar and M. Chandrasekar, "Comparative study on thermal performance of helical screw tape inserts in laminar flow using Al_2O_3/water and CuO/water

nanofluids," *Superlattices Microstruct.,* vol. 49, pp. 608–622, 2011.

[53] S. Suresh, K. P. Venkitaraj, P. Selvakumar and M. Chandrasekar, "A comparison of thermal characteristics of Al_2O_3/water and CuO/water nanofluids in transition flow through a straight circular duct fitted with helical screw tape inserts," *Exp. Thermal Fluid Sci., vol. 39,* vol. 39, pp. 37–44, 2012.

[54] M. T. Naik and S. S. Lingala, "Heat transfer and friction factor with water/propylene glycol based CuO nanofluid in circular tube with helical inserts under transition flow regime," *Heat Transf. Eng.,* vol. 35, pp. 53-62, 2014.

[55] M. Kahani, S. Zeinali Heris and S. M. Mousavi, "Comparative study between metal oxide nanopowders on thermal characteristics of nanofluidflow through helical coils," *Powder Technology ,* vol. 246, pp. 82-92, 2013.

[56] M. Saeedinia, M. A. Akhavan-Behabadi and M. Nasr, "Experimental study on heat transfer and pressure drop of nanofluid flow in a horizontal coiled wire inserted tube under constant heat flux," *Experimental Thermal and Fluid Science,* vol. 36, pp. 158–168, 2012.

[57] S. U. S. Choi, "Nanofluids for improved efficiency in cooling systems," Heavy Vehicle Systems Review, Argonne National Laboratory, Argonne, IL, USA, 2006.

[58] D. P. Kulkarni, R. S. Vajjha, D. K. Das and D. Oliva, "Application of aluminum oxide nanofluids in diesel electric generators jacket water coolant," *Appl. Therm. Eng.,* vol. 28, pp. 1774–1781, 2011.

[59] R. S. Vajjha, D. K. Das and P. K. Namburu, "Numerical study of fluid ynamic and heat transfer performance of Al_2O_3 and CuO nanofluids in the flat tubes of a radiator," *Int. J. Heat Fluid Flow,* vol. 31, no. 4, pp. 613–621, 2010.

[60] S. M. Peyghambarzadeh, S. H. Hashemabadi, M. S. Jamnani and S.

H. Hoseini, “Improving the cooling performance of automobile radiator with Al_2O_3/water nanofluid,” *Appl. Therm. Eng.,* vol. 31, no. 10, pp. 1833–1838, 2011.

[61] K. Y. Leong, R. Saidur, S. N. Kazi and A. H. Mamun, “Performance investigation of an automotive car radiator operated with nanofluid-based coolants (nanofluid as a coolant in a radiator),” *Appl. Therm. Eng.,* vol. 30, no. 17-18, pp. 2685–2692, 2010.

[62] S. M. Peyghambarzadeh, S. H. Hashemabadi, S. H. Hoseini and M. S. Jamnani, “Experimental study of heat transfer enhancement using water/ethylene glycol based nanofluids as a new coolant in the car radiator,” *Int. Commun. Heat Mass Transfer,* vol. 38, no. 9, pp. 1283–1290, 2011.

[63] M. Naraki, S. M. Peyghambarzadeh, S. H. Hashemabadi and Y. Vermahmoudi, “Parametric study of overall heat transfer coefficient of CuO/water nanofluids in a car radiator,” *Int. J. Therm. Sciences,* vol. 66, pp. 82–90, 2013.

[64] A. Faghri, “Review and advances in heat pipe science and technology,” *Journal of Heat Transfer,* vol. 134, pp. 123001-1, 2013.

[65] Z. H. Liu, X. F. Yang and G. L. Guo, “Effect of nanoparticles in nanofluid on thermal performance in a miniature thermosyphon,” *Journal of Applied Physics,* vol. 102, p. 013526, 2007.

[66] Z. H. Liu, X. F. Yang, G. S. Wang and G. L. Guo, “Influence of car bon nanotubes suspension on the thermal performance of a miniature thermosyphon,” *Int. J. Heat Mass Transfer,* vol. 53, no. 9-10, pp. 1914–1920, 2010.

[67] H. Gabriela, H. Angel, M. Ion and D. Florian, “Experimental study of the thermal performance of thermosyphon heat pipe using iron oxide nanoparticles,” *Int. J. Heat Mass Transfer,* vol. 54, no. 1-3, pp. 656–661, 2011.

[68] M. Shanbedi, S. Zeinali, M. Baniadam, A. Amir and M. Maghrebi, "Investigation of heat transfer characterization of EDA-MWCNT/DI-water nanofluid in a two-phase closed thermosyphon," *Ind. Eng. Chem. Res.,* vol. 51, no. 3, pp. 1423–1428, 2012.

[69] S. H. Noie, S. Z. Heris, M. Kahani and S. M. Nowee, "Heat transfer enhancement using Al_2O_3/water nanofluid in a two-phase closed thermosyphon," *Int. J. Heat Fluid Flow,* vol. 30, no. 4, pp. 700-705, 2009.

[70] T. Paramatthanuwat, S. Boothaisong, S. Rittidech and K. Booddachan, "Heat transfer characteristics of a two-phase closed thermosyphon using deionized water mixed with silver nanoparticles," *Heat Mass Transfer,* vol. 46, pp. 281–285, 2010.

[71] L. Lu, Z.-H. Liu and H.-S. Xiao, "Thermal performance of an open thermosyphon using nanofluids for high-temperature evacuated tubular solar collectors part 1: Indoor experiments," *Solar Energy,* vol. 85, pp. 379–387, 2011.

[72] L. L. Vasiliev and A. G. Kulakov, "Developmentof advanced miniature copper heat pipes for cooling system of a mobile PC platform," *Heat Pipe Science and Technology,* vol. 1, no. 1, pp. 59–70, 2010.

[73] K. S. Kim, M. H. Won, J. W. Kim and B. J. Back, "Heat pipe cooling technology for desktop PC CPU," *Applied Thermal Engineering,* vol. 23, pp. 1137–1144, 2003.

[74] Y. W. Chang, C. H. Cheng, J. C. Wang and S. L. Chen, "Heat pipe for cooling of electronic equipment," *Energy Conversion and Management,* vol. 49, no. 11, pp. 3398-3404, 2008.

[75] J. Wang, "L-type heat pipes application in electronic cooling system," *Int. J. Therm. Sci.,* vol. 50, pp. 97–105, 2011.

[76] J. Choi, M. Jeong, J. Yoo and M. Seo, "A new CPU cooler design based on an active cooling heat sink combined with heat pipes,"

Appl. Therm. Eng., vol. 44, pp. 50-66, 2012.

[77] N. Putra, Yanuar and F. N. Iskandar, "Application of nanofluids to a heat pipe liquid-block and the thermoelectric cooling of electronic equipment," *Experimental Thermal and Fluid Science,* vol. 35, pp. 1274–1281, 2011.

[78] T. Yousefi, S. A. Mousavi, B. Farahbakhsh and M. Z. Saghir, "Experimental investigation on the performance of CPU coolers: effect of heat pipe inclination angle and the use of nanofluids," *Microelectronics Reliability,* vol. 53, pp. 1954–1961, 2013.

[79] K. Jahani, M. Mohammadi, M. B. Shafii and Z. Shiee, "Promising technology for electronic cooling nanofluidic micropulsating heat pipes," *Journal of Electronic Packaging,* vol. 135, p. 0210051, 2013.

[80] S. J. Kim, I. C. Bang, J. Buongiorno and L. W. Hu, "Effects of nanoparticle deposition on surface wettability influencing boiling heat transfer in nanofluids," *Appl. Phys. Lett.,* vol. 89, no. 15, pp. 153107/1-3, 2006.

[81] J. P. Tu, N. Dinh and T. Theofanous, "An experimental study of nanofluid boiling heat transfer," in *6th International Symposium on Heat Transfer*, Beijing, China, 2004.

[82] D. Wen and Y. Ding, "Experimental investigation into the pool boiling heat transfer of aqueous basedc-alumina nanofluids," *J. Nanoparticle Res. ,* vol. 7, no. 2, pp. 265–274, 2005.

[83] B. H. Truong, "Determination of pool boiling critical heat flux enhancement in nanofluids," Undergraduate Thesis, MIT, CA, USA, 2007.

[84] H. S. Ahn, V. Sathyamurthi and D. Banerjee, "Pool boiling experiments on a nanostructured surface," *IEEE Compon. Packaging Tech.,* vol. 32, pp. 156–165, 2009.

[85] I. C. Bang and S. H. Chang, "Boiling heat transfer performance and phenomena of Al_2O_3–water nano-fluids from a plain surface in a pool," *Int. J. Heat Mass Transfer,* vol. 48, no. 12, pp. 2420–2428, 2005.

[86] S. K. Das, N. Putra and W. Roetzel, "Pool boiling characteristics of nano-fluids," *Int. J. Heat Mass Transf.,* vol. 46, pp. 851-862, 2003.

[87] S. M. Kwark, R. Kumar, G. Moreno, J. Yoo and S. M. You, "Pool boiling characteristics of low concentration nanofluids," *Int. J. Heat Mass Transf.,* vol. 53, pp. 972-981, 2010.

[88] R. A. Taylor and P. E. Phelan, "Pool boiling of nanofluids: comprehensive review of existing data and limited pool boiling of nanofluid," *International Journal of Heat and Mass Transfer,* vol. 52, pp. 5339–5347, 2009.

[89] R. L. Hamilton and O. K. Crosser, "Thermal conductivity of heterogeneous two component systems," *Ind. Eng. Chem. Fundam.* , vol. 1, no. 3, pp. 187–191, 1962.

[90] S. M. Murshed, K. C. Leong and C. Yang, "Enhanced thermal conductivity of TiO_2–water based nanofluids," *Int. J. Therm. Sci.,* vol. 44, pp. 367–373, 2005.

[91] W. Yu and S. U. Choi, "The role of interfacial layers in the enhanced thermal of nanofluids: a renovated Maxwell model," *Journal of Nanoparticle Research,* vol. 5, no. 1-2, pp. 167-171, 2003.

[92] J. Koo and C. Kleinstreuer, "A new thermal conductivity model for nanofluids," *Journal of Nanoparticle Research,* vol. 6, no. 6, pp. 577–588, 2004.

[93] J. Koo and C. Kleinstreuer, "Laminar nanofluid flow in micro-heat sinks," *International Journal of Heat and Mass Transfer,* vol. 48, no. 13, pp. 2652–2661, 2005.

[94] R. Prasher, P. Bhattacharya and P. E. Phelan, "Thermal conductivity of nanoscale colloidal solutions (nanofluids)," *Physical Review Letters,* vol. 94, no. 2, pp. 025901/1–4, 2005.

[95] A. Einstein, "Investigation on the theory of brownian motion," *Annalen der Physik,* vol. 324, no. 2, pp. 289–306 , 1906.

[96] X. Q. Wang and A. S. Mujumdar, "A review on nanofluids - part I: theoretical and numerical investigations," *Brazilian Journal of Chemical Engineering,* vol. 25, no. 4, pp. 613 - 630, 2008.

[97] H. C. Brinkman, "The viscosity of concentrated suspensions and solution," *J. Chem. Phys.,* vol. 20, pp. 571–581, 1952.

[98] G. K. Batchelor, "The effect of Brownian motion on the bulk stress in a suspension of spherical particles," *J. Fluid Mech. ,* vol. 83, no. 1, pp. 97–117, 1977.

[99] W. J. Tseng and C. N. Chen, "Effect of polymeric dispersant on rheological behavior of nickel–terpineol suspensions," *Mater. Sci. Eng. A.,* vol. 347, no. 1, pp. 145–153, 2003.

[100] S. E. Maiga, C. T. Nguyen, N. Galanis and G. Roy, "Heat transfer behaviours of nanofluids in a uniformly heated tube," *Superlattices and Microstructures,* vol. 35, pp. 543–557 , 2004.

[101] S. E. Maiga, C. T. Nguyen, N. Galanis and G. Roy, "Hydrodynamic and thermal behaviours of a nanofluid in a uniformly heated tube," in *Advanced Computational Methods in Heat Transfer VIII*, Southampton, United Kingdom, WIT Press, pp. 453–462, 2004.

[102] D. P. Kulkarni, D. K. Das and G. Chukwu, "Temperature dependent rheological property of copper oxide nanoparticles suspension (Nanofluid)," *Journal of Nanoscience and Nanotechnology,* vol. 6, pp. 1150–1154, 2006.

[103] Z. Haddad, C. Abid, H. F. Oztop and A. Mataoui, "A review on how the researchers prepare their nanofluids," *International Journal of*

Thermal Sciences, vol. 76, pp. 168-189, 2014.

[104] N. A. C. Sidik, H. A. Mohammed, O. A. Alawi and S. Samion, "A review on preparation methods and challenges of nanofluids," *International Communications in Heat and Mass Transfer,* vol. 54, pp. 115-125, 2014.

[105] A. Ghadimi, R. Saidur and H. S. Metselaar, "A review of nanofluid stability properties and characterization in stationary conditions," *Int. Jou. Heat Mass Trans.,* vol. 54, pp. 4051-4068, 2011.

[106] L. Syam Sundar and M. K. Singh, "Convective heat transfer and friction factor correlations of nanofluid in a tube and with inserts: A review," *Renewable and Sustainable Energy Reviews,* vol. 20, pp. 23-35, 2013.

[107] C. Pang, J. W. Lee and Y. T. Kang, "Review on combined heat and mass transfer characteristics in nanofluids," *International Journal of Thermal Sciences,* vol. 87, pp. 49-67, 2015.

[108] A. G. Osorio, I. C. L. Silveira, V. L. Bueno and C. P. Bergmann, "$H_2SO_4/HNO_3/HCl$-functionalization and its effect on dispersion of carbon nanotubes in aqueous media," *Applied Surface Science*, vol. 255, pp. 2485–2489, 2008.

[109] A. Nasiri, M. Shariaty-Niasar, A. Rashidi, A. Amrollahi and R. Khodafarin, "Effect of dispersion method on thermal conductivity and stability of nanofluid," *Experimental Thermal and Fluid Science,* vol. 35, pp. 717-723, 2011.

[110] S. K. Das, N. Putra, P. Thiesen and W. Roetzel, "Temperature dependence of thermal conductivity enhancement for nanofluids," *J. Heat Transfer,* vol. 125, pp. 567–574, 2003.

[111] Y. Li, J. Zhou, S. Tung, E. Schneider and S. Xi, "A review on development of nanofluid preparation and characterization," *Powder Technology ,* vol. 196, pp. 89-101, 2009.

[112] J. Lee, Y. J. Yoon, J. K. Eaton, K. E. Goodson and S. J. Bai, "Analysis of oxide (Al_2O_3, CuO, and ZnO) and CNT nanoparticles disaggregation effect on the thermal conductivity and the viscosity of nanofluids," *International Journal of Precision Engineering and Manufacturing,* vol. 15, pp. 703-710, 2014.

[113] W. Duangthongsuk and S. Wongwises, "A critical review of convective heat transfer of nanofluids," *Renew. Sustain. Energy Rev.,* vol. 11, pp. 797–817, 2007.

[114] H. Chang, C. Jwo, P. Fan and S. Pai, "Process optimization and material properties for nanofluid manufacturing," *Int. J. Adv. Manf. Technol.,* vol. 34, no. 3, pp. 300-306, 2007.

[115] D. Lee, J. W. Kim and B. G. Kim, "A new parameter to control heat transport in nanofluids: surface charge state of the particle in suspension," *J. Phys. Chem.,* vol. 110, no. 9, pp. 4323-4328, 2006.

[116] X. Zhong, A. Crivoi and F. Duan, "Sessile nanofluid droplet drying," *Advances in Colloid and Interface Science,* vol. 217, pp. 13-30, 2015.

[117] G. Paul, M. Chopkar, I. Manna and P.K. Das, "Techniques for measuring the thermal conductivity of nanofluids: A review," *Renewable and Sustainable Energy Reviews,* vol. 14, pp. 1913–1924, 2010

[118] S.M.S. Murshed, K.C. Leong and C. Yang, "Investigations of thermal conductivity and viscosity of nanofluids," *International Journal of Thermal Sciences*, vol. 47, pp. 560–568, 2008.

[119] C.H. Chon and K.D. Kihm, "Thermal conductivity enhancement of nanofluids by Brownian motion," *ASME J. Heat Transfer*, vol. 127 p. 810, 2005.

[120] M. J. Assael, C. F. Chen, I. N. Metaxa and W.A. Wakeham, "Thermal conductivity of suspensions of carbon nanotubes in water," *Int. J. Thermophysics*, vol. 25, 971–985, 2004.

[121] L. Chen and H. Xie, "Surfactant-free nanofluids containing double and single-walled carbon nanotubes functionalized by a wet-mechanochemical reaction," *Thermochimica Acta*, vol. 497, pp. 67–71, 2010.

[122] A.A. Rabienataj Darzi, M. Farhadi, M., K. Sedighi, "Experimental investigation of convective heat transfer and friction factor of Al_2O_3/water nanofluid in helically corrugated tube," E*xperimental Thermal and Fluid Science*, vol. 57, pp. 188–199, 2014.

[123] L. Chen, H. Xie, Y. Li, W. Yu, "Nanofluids containing carbon nanotubes treated by mechanochemical reaction," *Thermochimica Act.*, vol. 477, pp. 21–24, 2008.

[124] R. K. Shah, “Thermal Entry Length Solutions for the Circular Tube and Parallel Plates,” in *Third National Heat Mass Transfer Conference*, Indan Institute of Technology Bombay, 1975.

[125] V. Gnielinski, "New equations for heat and mass transfer in turbulent pipe and channel flow", *Int. Chem. Eng.*, vol. 16, pp. 359–368, 1976.

[126] H. W. Coleman and W. G.Steele, "*Experimental and Uncertainty Analysis for Engineers*", Wiley, New York, 1989.

[127] ANSI/ASME, “Measurement Uncertainty,” *The American Society of Mechanical Engineers*, Paper No. PTC 19, 1989.

[128] R. Karwa, C. Sharma and N. Karwa, “Performance Evaluation Criterion at Equal Pumping Power for Enhanced Performance Heat Transfer Surfaces,” *Journal of Solar Energy,* vol. 2013, pp.1-9, 2013.

[129] P. Rathnakumar, K. Mayilsamy, S. Suresh and P. Murugesan, “Laminar Heat Transfer and Friction Factor Characteristics of Carbon Nano-tube/Water Nanofluids,” *Journal of Nanoscence Nanotechnology.*, vol. 13, pp. 1-8, 2013.

[130] H. Blasius, "Grenzschichten in Flussigkeiten mit kleiner Reibung (German)," *Z. Math. Phys*. vol. 56, p. 1–37, 1908.

[131] F. W. Dittus and L. M. K. Boelter, "*Heat Transfer in Automobile Radiators of Tubular Type*," University of California, Berkeley, CA, pp. 13–18, 1930.

[132] T. Yousefi, E. Shojaeizadeh, F. Veysi, and S. Zinadini, 2012, "An Experimental Investigation on the effect of pH variation of MWCNT–H_2O nanofluid on the efficiency of a flat-plate solar collector," *Solar Energy*, vol. 86, pp. 771–779, 2012.

[133] M. J. Assael, I. N. Metaxa, J. Arvanitidis, D. Christofilos, and C. Lioutas, "Thermal conductivity enhancement in aqueous suspensions of carbon multi-walled and double-walled nanotubes in the presence of two different dispersants," *Int. J. Thermophys.*, vol. 26, pp. 647–664, 2005.

[134] ASHRAE Standard 93-86, *"Methods of testing to determine the thermal performance of solar collectors,"* Atlanta, GA, 1986.

[135] P. Naphon, P. Assadamongkol and T. Borirak, "Experimental investi-gation of titanium nanofluids on the heat pipe thermal efficiency," *Int. Commun. Heat Mass Transfer*, vol. 35, no. 10, pp. 1316–1319, 2008.

[136] A. T. Pise and S. S. Chougule, "Experimental investigation heat transfer augmentation of solar heat pipe collector by using nanofluid," *21st National & 10th ISHMT-ASME Heat and Mass Transfer Conference*, IIT Madras, India, December 27–30, 2011.

[137] S. S. Chougule, A. T. Pise and P. A. Madane, 2012, "Performances of nanofluid-charged solar water heater by solar tracking system," *International Conference on Advances in Engineering, Science and Management(ICAESM)*, Nagapattinam, Tamil Nadu, March 30–31, pp. 247–253, 2012.

[138] Y. Cao, M. Gao and J. E. Beam, "Experiments and analyses of flat

miniature heat pipes," *J. Thermophys. Heat Transfer*, vol. 11, pp. 58–164, 1997.

[139] R. Hopkins, A. Faghri and D. Khrustalev, "Flat miniature heat pipes with micro capillary grooves," *ASME J. Heat Transfer*, vol. 121, pp. 102–109, 1999.

[140] Y. C. Weng, H. P. Cho, C. Chang and S. L. Chen, "Heat pipe with PCM for electronic cooling," *Appl. Energy*, vol. 88, pp. 1825–1833, 2011.

Appendix - A

Specifications of the Measuring Instruments/Equipments

In this study, several instruments have been used to measure various thermophysical properties and inspect stability of the nanofluid. Some of important equipments are listed below.

1. **Scanning Electron Microscope (SEM)**

Make:	Carl Zeiss NTS GmbH, Germany
Model:	SUPRA 55
Resolution:	1.0 nm @ 15 kV
	1.7 nm @ 1 kV
	4.0 nm @ 0.1 kV
Accleration Voltage:	0.1 - 30 kV
Magnification:	12x - 900,000 x
Stages:	5-Axes Motorised Eucentric Specimen Stage X = 130 mm, Y = 130mm, Z = 50mm, T = -3 - +70°, R = 360° (continuous)
Standard Detectors:	High efficiency In-lens detector Everhart-Thornley Secondary Electron Detector
Image Recording:	Camera and Printer

2. **Particle Size and Zeta Potential Analyzer**

Make:	Particle Sizing Systems, Inc., Santa Barbara, Calif., and USA
Model:	Nicomp 380
Size range:	0.3 nanometers – 6 microns
Analysis type:	Gaussian or Nicomp High Resolution Multi-modal
Dimensions:	W 17" x D 24" x H 10", 62 lbs (Approx depending on options)
Laser options:	5 mW HeNe, 12 mW, 15 mW, 35 mW, 50 mW, 100 mW Laser Diodes (red), 20 mW, 50 mW, 100 mW Laser Diodes (blue/green
Detector options:	PMT (Photomultiplier), CPM (Channel Photo Multiplier 4X Gain) & APD (Avalanche Photo Diode 7X Gain)
Angular range	Multi-Angle Goniometer 10 – 175 degree
Modular range:	Zeta Potential (Frequency and Phase Analysis PALS), High Concentration back Scattering, Auto-dilution, Auto-sampler, Multi-Angle, High Power Lasers, High Gain Detectors, 21 CFR Part 11 Complient Software, Online
Power requirement:	100-120 VAC, 60 Hz or 220-240 VAC, 50 HZ

3. Thermal Property Analyzer

Make:	Decagon Devices, USA
Model:	KD2
Sensor Type:	0 KS – 1 (Thermal conductivity/ Resistivity Sensor for liquids)
Sensor Needle Length:	6 cm
Needle Diameter:	1.27 cm
Operating Environment temperature:	50 to 150 ^{0}C
Accuracy :	± 5 % (0.2 to 2 $Wm^{-1}k^{-1}$) ± 0.01W $Wm^{-1}k^{-1}$ (0.02-0.2 $Wm^{-1}k^{-1}$)
Range of Measurement:	0.02 to 2 $Wm^{-1}k^{-1}$
Measurement Time:	60

4. Brookfield Cone and Plate Viscometer

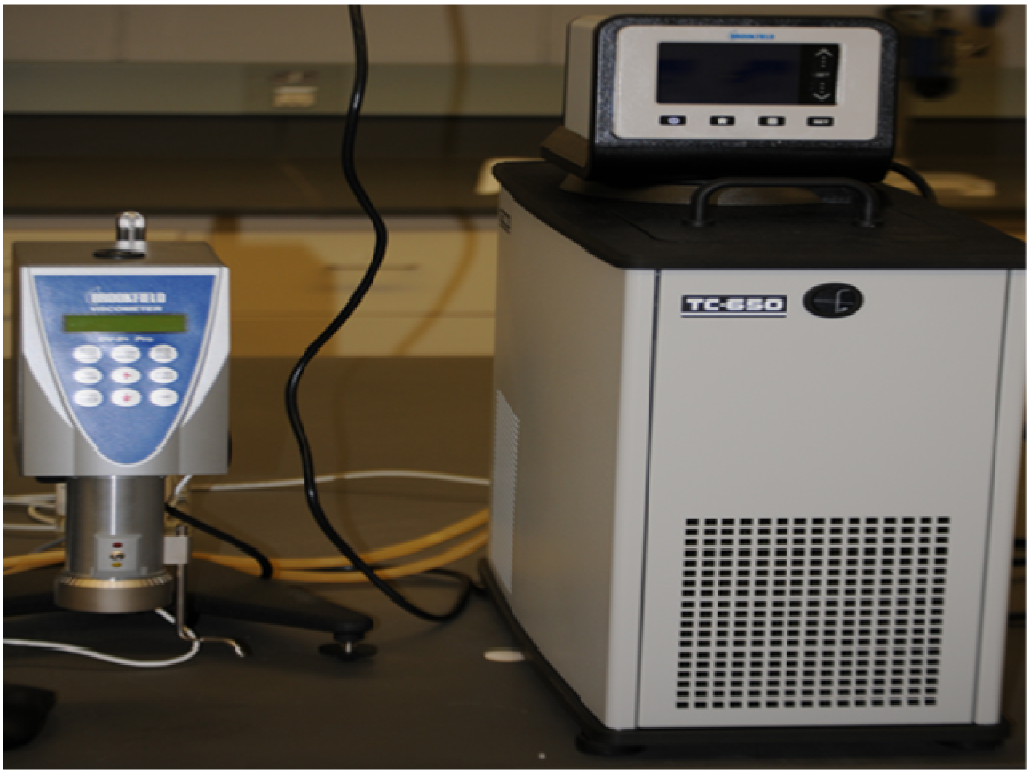

Make:	Brookfield Engineering Laboratories, Inc. , USA
Model:	Brookfield DV-II+ Pro (Cone and plate viscometer)
Temperature Sensing Range:	-100˚C to 300˚C
Viscosity Accuracy:	±1.0%
Viscosity Repeatability:	±0.2%
Operating Environment temperature:	0°C to 40°C
Temperature Accuracy:	±1°C I -100°C to +149°C ±2°C I +150°C to +300°C
Range of Measurement:	0.15 to 3065 cP
Spindle type:	CPE-40

5. Contact Angle Meter

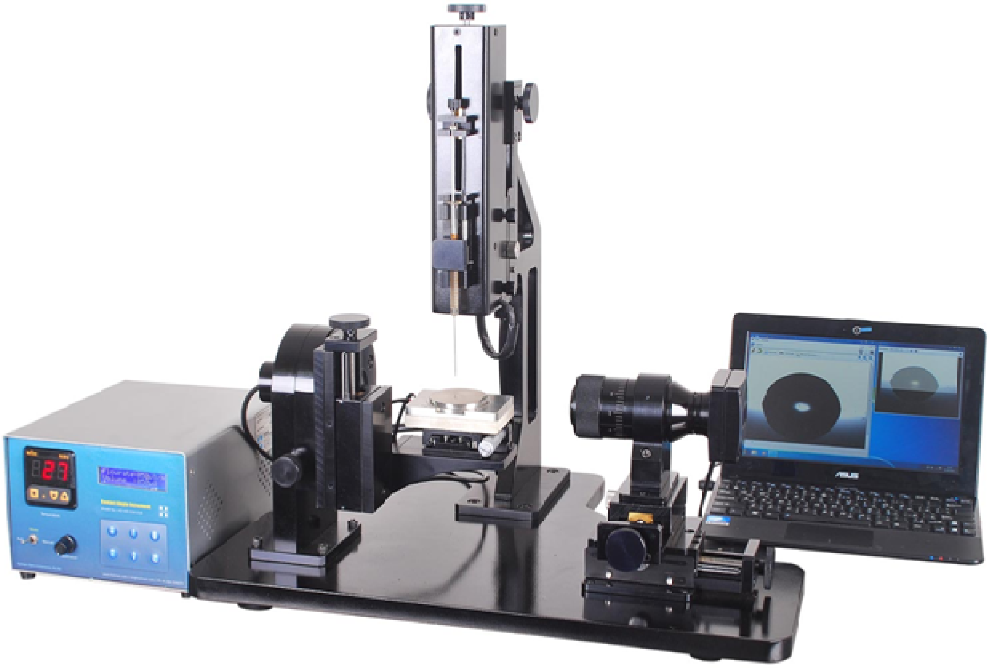

Make:	Holmarc Opto-mechatronics Pvt. Ltd
Model:	HO-IAD-CAM-01
Measuring method:	Sessile drop method
Analysis method:	Automatic curve fit analysis using drop snake method
Inaccuracy:	+/- 0.1 degree
Dispenser:	Mechanical dispenser with precise micrometer control. 50, 100 & 150 micro liter syringes are provided with the system
Dimension and Weight:	350 x 125 x 350mm, 30 kg (approx)
Power supply:	240VAC, 50 Hz
Optics:	High performance aberration corrected imaging lens with precise manual focus adjustment

Appendix - B

Uncertainty Analysis

In this study, synthesis and characterization of nanofluid is carried out to investigate the thermal performance of nanofluids in various practical applications including heat exchanging equipments, automobile radiator, flat plate solar collector and cooling of electronics components.

The present study involves measurement of various parameters such as: thermal conductivity, viscosity, temperature of test surface, coolant flow rate, solar insolation, voltage, current supplied, pressure drop, diameter and length of the test section. It is to be noticed that error in the test results initiates because of deviation of primary measured quantities, In view if this, attempts have been made to use pre-calibrated instruments to minimize the error in the measurement. Here, an error analysis is made to estimate the errors associated in the various parameters following the procedure suggested by Coleman and Steele [1] as:

If R is dependent variable and is function of n independent variables then,

$$R = f\,(v_1,\ v_2,\ v_3,\ldots\ldots\ldots..,v_n) \tag{B.1}$$

Let the uncertainties associated with independent variable be Δ_1, Δ_2, Δ_3, ……, Δ_n and resulting uncertainty of R be Δ and expressed as:

$$\Delta = \left[\left(\frac{\partial R}{\partial v_1}\Delta_1\right)^2 + \left(\frac{\partial R}{\partial v_2}\Delta_2\right)^2 + \left(\frac{\partial R}{\partial v_3}\Delta_3\right)^2 + \ldots\ldots + \left(\frac{\partial R}{\partial v_n}\Delta_n\right)^2\right]^{1/2} \tag{B.2}$$

In this study, several test facilities have been developed to evaluate the thermal performance of nanofluids in various thermal devices. Here, steel rule and vernier caliper is used to measure the dimensions of the test specimen. Various instruments such as: rotameter, graduated glass tube is used to measure the coolant flow rate. The temperatures of the coolant and test specimen are measured by using RTD during experiments. Here, differential pressure transmitter is used to measure the pressure drop between two different locations of the pipe. Solar insolation is measured by a calibrated pyranometer. Also, the voltage and current is measured by voltmeter and ammeter, respectively. The errors associated in the parameters are detailed below.

Heat transfer performance of nanofluids through uniformly heated circular tube with helical twisted tape inserts

In this study, various parameters such as: thermal conductivity, viscosity, temperature of test surface, coolant flow rate, voltage, current supplied, pressure drop, diameter and length of the test section are measured and the errors in these parameters are listed in table B.1. Considering errors in all basic measuring quantities, the maximum uncertainty in various parameters such as: Reynolds number, heat transfer coefficient, Nusselt number and friction factor are evaluated. This is detailed below

(a) Reynolds number, *Re*

$$\mathrm{Re} = \rho \bar{V} D / \mu$$

Following Eq. B.2, one can write

$$\frac{\Delta \mathrm{Re}}{\mathrm{Re}} = \frac{1}{\mathrm{Re}}\left[\left\{\frac{\partial \mathrm{Re}}{\partial \bar{V}}(\Delta \bar{V})\right\}^2 + \left\{\frac{\partial \mathrm{Re}}{\partial D}(\Delta D)\right\}^2 + \left\{\frac{\partial \mathrm{Re}}{\partial \mu}(\Delta \mu)\right\}^2\right]^{1/2}$$

Where, Δ presents error in parameters measured and above equation is reduced to,

$$\frac{\Delta \mathrm{Re}}{\mathrm{Re}} = \left[\left\{\frac{\Delta \bar{V}}{\bar{V}}\right\}^2 + \left\{\frac{\Delta D}{D}\right\}^2 + \left\{\frac{\Delta \mu}{\mu}\right\}^2\right]^{1/2} = \sqrt{(2)^2 + (0.19)^2 + (1)^2} = 2.24\ \%$$

Where,

$$\frac{\Delta \bar{V}}{\bar{V}} = \left[\left\{\frac{\Delta vol}{vol}\right\}^2 + \left\{\frac{\Delta t}{t}\right\}^2\right]^{1/2} = \left[(2)^2 + (0.027)^2\right]^{1/2} = 2.0\%$$

Table B1: Uncertainties in instruments for heat transfer performance of nanofluids through uniformly heated circular tube

Instrument	Range	Variable measured	Error	Min quantity	Max Uncertainty (%)
RTD	-50^0C to 200^0C	Bulk Temperature, (T_b)	$\Delta T=0.1^0C$ $\Delta T_b=[0.1^2+0.1^2]^{1/2}= 0.1414$	30.6	0.46
RTD	-50^0C to 200^0C	Surface Temperature, (T_w)	$\Delta T=0.1^0C$ $\Delta T_w=[6x(0.1)^2]^{1/2}= 0.2449$	31.3	0.78
Measuring Flask	0-200 ml	Volume, (vol)	1 ml	50	2
Stop watch	-	Time, (t)	0.01 sec	37	0.027
Voltammeter	0-240 V	Voltage, (V)	0.1 V	120	0.083
Ammeter	0-15 A	Current, (I)	0.01 A	6	0.166
Differential Pressure Transmitter	4-20 mA 0-250	Current, (mA) Pressure drop, (ΔP)	0.1 mA -	4.7 398	2.12 2.12
Measuring Tape	0-1.5 m	Length measurement, (L)	1 mm	1000	0.1
Vernier Caliper	0-150 mm	Diameter, (D)	0.02 mm	10.5	0.19
Thermal Property Analyzer	0.02 to 2.00 W/m.K	Thermal conductivity, (k)	-		1.68
Brookfield Viscometer	0.15-3065 cP	Viscosity, (μ)	-		1

(b) Heat flux, q

$$q = Q/A = VI/\pi DL$$

$$\frac{\Delta q}{q} = \frac{1}{q}\left[\left\{\frac{\partial q}{\partial V}(\Delta V)\right\}^2 + \left\{\frac{\partial q}{\partial I}(\Delta I)\right\}^2 + \left\{\frac{\partial q}{\partial D}(\Delta D)\right\}^2 + \left\{\frac{\partial q}{\partial L}(\Delta L)\right\}^2\right]^{1/2}$$

$$\frac{\Delta q}{q} = \left[\left\{\frac{\Delta V}{V}\right\}^2 + \left\{\frac{\Delta I}{I}\right\}^2 + \left\{\frac{\Delta D}{D}\right\}^2 + \left\{\frac{\Delta L}{L}\right\}^2\right]^{1/2}$$

$$= \sqrt{(0.083)^2 + (0.166)^2 + (0.19)^2 + (0.1)^2}$$

$$= 0.28\%$$

(c) Heat transfer coefficient, h

$$h = \frac{q}{(T_w - T_b)}$$

$$\frac{\Delta h}{h} = \frac{1}{h}\left[\left\{\frac{\partial h}{\partial q}(\Delta q)\right\}^2 + \left\{\frac{\partial h}{\partial (T_w - T_b)}\Delta(T_w - T_b)\right\}^2\right]^{1/2}$$

Where,

$$\frac{\Delta(T_w - T_b)}{(T_w - T_b)} = \left[\left\{\frac{\Delta T_w}{T_w}\right\}^2 + \left\{\frac{\Delta T_b}{T_b}\right\}^2\right]^{1/2} = \left[(0.78)^2 + (0.46)^2\right]^{1/2} = 0.90\%$$

$$\frac{\Delta h}{h} = \left[\left\{\frac{\Delta q}{q}\right\}^2 + \left\{\frac{\Delta(T_w - T_b)}{(T_w - T_b)}\right\}^2\right]^{1/2}$$

$$= \sqrt{(0.28)^2 + (0.90)^2}$$

$$= 0.94\%$$

(d) Nusselt number, Nu

$$Nu = hD/k$$

$$\frac{\Delta Nu}{Nu} = \frac{1}{Nu}\left[\left\{\frac{\partial Nu}{\partial h}(\Delta h)\right\}^2 + \left\{\frac{\partial Nu}{\partial D}(\Delta D)\right\}^2 + \left\{\frac{\partial Nu}{\partial k}(\Delta k)\right\}^2\right]^{1/2}$$

$$\frac{\Delta Nu}{Nu} = \left[\left\{\frac{\Delta h}{h}\right\}^2 + \left\{\frac{\Delta D}{D}\right\}^2 + \left\{\frac{\Delta k}{k}\right\}^2\right]^{1/2}$$

$$= \sqrt{(0.77)^2 + (0.19)^2 + (1.5)^2}$$

$$= 1.69\%$$

(e) Friction factor, f

$$f = \frac{1}{2}\left\{\frac{\Delta P}{L}\right\}\left\{\frac{\rho D^3}{\mathrm{Re}^2 \mu^2}\right\}$$

$$\frac{\Delta f}{f} = \frac{1}{f}\left[\begin{array}{l}\left\{\frac{\partial f}{\partial(\Delta P)}\Delta(\Delta P)\right\}^2 + \left\{\frac{\partial f}{\partial L}(\Delta L)\right\}^2 + \left\{\frac{\partial f}{\partial D}(\Delta D)\right\}^2 \\ + \left\{\frac{\partial f}{\partial \mathrm{Re}}(\Delta \mathrm{Re})\right\}^2 + \left\{\frac{\partial f}{\partial \mu}(\Delta \mu)\right\}^2\end{array}\right]^{1/2}$$

$$\frac{\Delta f}{f} = \left[\left\{\frac{\Delta(\Delta P)}{(\Delta P)}\right\}^2 + \left\{\frac{\Delta L}{L}\right\}^2 + \left\{\frac{3\Delta D}{D}\right\}^2 + \left\{\frac{2\Delta \mathrm{Re}}{\mathrm{Re}}\right\}^2 + \left\{\frac{2\Delta \mu}{\mu}\right\}^2\right]^{1/2}$$

$$= \sqrt{(2.5)^2 + (0.1)^2 + (3\times 0.19)^2 + (2\times 2.24)^2 + (2\times 1)^2}$$

$$= 5.53\%$$

Thermal performance of nanofluids through an automobile radiator

In this study various parameters such as: temperature, coolant flow rate, thermal conductivity and viscosity are measured. The rotameter is used for mass flow measurement. Table B.2 shows the uncertainty in measured basic quantities. The maximum uncertainty in various parameters such as: Reynolds number, heat transfer coefficient and Nusselt number are evaluated. This is detailed below

a) Reynolds number, *Re*

$$\mathrm{Re} = 4\dot{m}/\pi D\mu$$

$$\frac{\Delta \mathrm{Re}}{\mathrm{Re}} = \frac{1}{\mathrm{Re}}\left[\left\{\frac{\partial \mathrm{Re}}{\partial \dot{m}}(\Delta \dot{m})\right\}^2 + \left\{\frac{\partial \mathrm{Re}}{\partial D}(\Delta D)\right\}^2 + \left\{\frac{\partial \mathrm{Re}}{\partial \mu}(\Delta \mu)\right\}^2\right]^{1/2}$$

$$\frac{\Delta \mathrm{Re}}{\mathrm{Re}} = \left[\left\{\frac{\Delta \dot{m}}{\dot{m}}\right\}^2 + \left\{\frac{\Delta D}{D}\right\}^2 + \left\{\frac{\Delta \mu}{\mu}\right\}^2\right]^{1/2}$$

$$= \sqrt{(5)^2 + (0.66)^2 + (1)^2}$$

$$=5.1\ \%$$

(c) Heat transfer coefficient, *h*

$$h = \dot{m}C_P(T_{in} - T_{out})/A(T_b - T_w) = \dot{m}C_P(T_{in} - T_{out})/\pi DL(T_b - T_w)$$

$$\frac{\Delta h}{h} = \frac{1}{h}\left[\begin{array}{l}\left\{\frac{\partial h}{\partial \dot{m}}(\Delta \dot{m})\right\}^2 + \left\{\frac{\partial h}{\partial \Delta T}\Delta T\right\}^2 + \left\{\frac{\partial h}{\partial D}(\Delta D)\right\}^2 + \left\{\frac{\partial h}{\partial L}(\Delta L)\right\}^2 \\ + \left\{\frac{\partial h}{\partial (T_b - T_w)}\Delta(T_b - T_w)\right\}^2\end{array}\right]^{1/2}$$

Where,

$$\frac{\Delta(T_b - T_w)}{(T_b - T_w)} = \left[\left\{\frac{\Delta T_b}{T_b}\right\}^2 + \left\{\frac{\Delta T_w}{T_w}\right\}^2\right]^{1/2} = \left[(0.18)^2 + (0.40)^2\right]^{1/2} = 0.43\%$$

$$\frac{\Delta h}{h} = \left[\left\{\frac{\Delta \dot{m}}{\dot{m}}\right\}^2 + \left\{\frac{\Delta(\Delta T)}{\Delta T}\right\} + \left\{\frac{\Delta D}{D}\right\}^2 + \left\{\frac{\Delta L}{L}\right\}^2 + \left\{\frac{\Delta(T_b - T_w)}{(T_b - T_w)}\right\}^2\right]^{1/2}$$

Table B2: Uncertainties in instruments for thermal performance of automobile radiator

Instrument	Range	Variable measured	Error	Min quantity	Max Uncertainty (%)
RTD	-50^0C to 200^0C	Bulk Temperature, (T_b)	$\Delta T=0.1^0C$ $T_b=[0.1^2+0.1^2]^{1/2}=0.1414$	75.6	0.18
RTD	-50^0C to 200^0C	Surface Temperature, (T_w)	$T=0.1^0C$ $T_w=[8x(0.1)^2]^{1/2}=0.2828$	70.3	0.40
Rotameter	0-5 lpm	Mass flow rate, ($\dot{m}$)	0.1 lpm	2	5
Measuring Tape	0-1.5 m	Length, (L)	1 mm	310	0.33
Vernier Caliper	0-150 mm	Diameter, (D)	0.02 mm	3	0.66
KD2 Pro sensor	0.02 to 2.00 W/m.K	Thermal conductivity, (k)	-		1.68
Brookfield Viscometer	0.15-3065 cP	Viscosity,(μ)	-		1

Table B3: Uncertainties in instruments for thermal performance of solar heat pipe collector

Instrument	Range	Variable measured	Error	Min quantity	Max Uncertainty (%)
RTD	-50^0C to 200^0C	Temperature, (T)	0.1^0C	35	0.28
Pyranometer	$0 – 1500$ W/m^2	Solar radiation measurement, (I_t)	10 W/m^2	660	1.5
Measuring Tape	0-1.5 m	Length, (L)	1 mm	630	0.15
	0-150 mm	Width, (W)	1 mm	360	0.27
Measuring Flask	0-200 ml	Volume, (vol)	1 ml	56	1.78
Stop watch	-	Time, (t)	0.01 sec	30	0.03

$$= \sqrt{(5)^2 + (0.18)^2 + (0.66)^2 + (0.33)^2 + (0.43)^2}$$

$=5.06\%$

(c) Nusselt number, *Nu*

$$Nu = hD/k$$

$$\frac{\Delta Nu}{Nu} = \frac{1}{Nu}\left[\left\{\frac{\partial Nu}{\partial h}(\Delta h)\right\}^2 + \left\{\frac{\partial Nu}{\partial D}(\Delta D)\right\}^2 + \left\{\frac{\partial Nu}{\partial k}(\Delta k)\right\}^2\right]^{1/2}$$

$$\frac{\Delta Nu}{Nu} = \left[\left\{\frac{\Delta h}{h}\right\}^2 + \left\{\frac{\Delta D}{D}\right\}^2 + \left\{\frac{\Delta k}{k}\right\}^2\right]^{1/2}$$

$$= \sqrt{(5.06)^2 + (0.66)^2 + (1.5)^2}$$

$=5.32\%$

Thermal Performance of Two-Phase Thermosyphon Flat Plate Collector by using Nanofluids

Here, the coolant temperature at inlet and outlet of the collector is measured by RTD during experiments. The coolant flow rate is adjusted by using flow control valve and measured by using a stop watch of 0.01 s accuracy and a graduated glass bottle of tolerance 1cm^3. The solar radiations are measured by using a pyranometer. The uncertainties in measured quantities are tabulated in Table B.3. The maximum uncertainty in various parameters such as: heat gain (Q_g) and efficiency of collector (η) are evaluated and is detailed below:

(a) Heat gain, Q_g

$$Q_g = \dot{m}C_p(T_o - T_i) = \dot{m}C_p\Delta T$$

$$\frac{\Delta Q_g}{Q_g} = \frac{1}{Q_g}\left[\left\{\frac{\partial Q_g}{\partial \dot{m}}(\Delta \dot{m})\right\}^2 + \left\{\frac{\partial Q_g}{\partial(\Delta T)}\Delta(\Delta T)\right\}^2\right]^{1/2}$$

$$\frac{\Delta Q_g}{Q_g} = \left[\left\{ \frac{\Delta \dot{m}}{\dot{m}} \right\}^2 + \left\{ \frac{\Delta(\Delta T)}{(\Delta T)} \right\}^2 \right] = \sqrt{(1.78)^2 + (0.28)^2} = 1.80\%$$

Where,

$$\frac{\Delta \dot{m}}{\dot{m}} = \left[\left\{ \frac{\Delta V}{V} \right\}^2 + \left\{ \frac{\Delta t}{t} \right\}^2 \right]^{1/2} = \left[(1.78)^2 + (0.03)^2 \right]^{1/2} = 1.78\%$$

(b) Efficiency of collector, η

$$\eta = \frac{Q_g}{Q_{in}} = \frac{Q_g}{I_t A_{coll}} = \frac{Q_g}{I_t (L \times W)}$$

$$\frac{\Delta \eta}{\eta} = \frac{1}{\eta} \left[\left\{ \frac{\partial \eta}{\partial Q_g} (\Delta Q_g) \right\}^2 + \left\{ \frac{\partial \eta}{\partial I_t} (\Delta I_t) \right\}^2 + \left\{ \frac{\partial \eta}{\partial L} (\Delta L) \right\}^2 + \left\{ \frac{\partial \eta}{\partial W} (\Delta W) \right\}^2 \right]^{1/2}$$

$$\frac{\Delta \eta}{\eta} = \left[\left\{ \frac{\Delta Q_g}{Q_g} \right\}^2 + \left\{ \frac{\Delta I_t}{I_t} \right\}^2 + \left\{ \frac{\Delta L}{L} \right\}^2 + \left\{ \frac{\Delta W}{W} \right\}^2 \right]^{1/2}$$

$$= \sqrt{(1.80)^2 + (1.5)^2 + (0.15)^2 + (0.27)^2} = 2.36\%$$

Reference

[1] H. W. Coleman and W. G.Steele, "*Experimental and Uncertainty Analysis for Engineers*", Wiley, New York, 1989

List of Publications

International Journal

1. **Chougule, S.S.** and Sahu, S.K., 2015, "Heat Transfer and Friction Characteristics of Al_2O_3/water and CNT/water Nanofluids in Transition flow using Helical Screw Tape Inserts - A Comparative Study," **Chemical Engineering and Processing**, 88, pp. 77-88.
2. **Chougule, S.S.** and Sahu, S.K., 2014, "Thermal Performance of Nanofluid Charged Heat Pipe With Phase Change Material for Electronics Cooling," **ASME- Journal of Electronics Packaging**, 137 (2), p. 021004.
3. [a]Modak, M., Srinivasan, S., Garg, K., **Chougule, S.S.**, Agarwal, M.K., Sahu, S.K., 2015 "Experimental investigation of heat transfer characteristics of the hot surface using Al_2O_3/water nanofluids," **Chemical Engineering and Processing**, 91, pp. 104-113.
4. **Chougule, S.S.**, and Sahu, S.K., 2015, "Performance of Wickless Heat Pipe Flat Plate Solar Collectors Having Different Filling Ratios," **ASME - Journal of Solar Energy**, 137 (2), p. 024501.
5. **Chougule, S.S.** and Sahu, S.K., 2013, "Comparative Study on Heat Transfer Enhancement of Low Volume Concentration of Al_2O_3/water and Carbon Nanotube/Water Nanofluids in Laminar Regime using Helical Screw Tape Inserts," **ASME- Journal of Nanotechnology in Engineering and Medicine**, 4 (4), p. 040904.
6. **Chougule, S.S.** and Sahu, S.K., 2014, "Comparative Study on Heat Transfer Enhancement of Low Volume Concentration of Al_2O_3/water and Carbon Nano-tube/Water Nanofluids in Transition Regime using Helical Screw Tape Inserts," **Experimental Heat Transfer** (accepted).
7. **Chougule, S.S.**, and Sahu, S.K., 2014, "Thermal Performance of Automobile Radiator Using Carbon Nanotube-Water Nanofluid—

Experimental Study," **ASME - Journal of Thermal Science and Engineering applications**, 6 (4), p. 041009.

8. **Chougule, S. S.**, Sahu S.K. and Pise A.T., 2014, "Thermal Performance of Two Phase Thermosyphon Flat-Plate Solar Collectors by Using Nanofluid," **ASME - Journal of Solar Energy**, 136 (1), p. 014503.
9. **Chougule, S.S.** and Sahu S.K., 2014, "Comparative Study of Cooling Performance of Automobile Radiator using Al_2O_3/water and Carbon Nanotube/Water Nanofluid," **ASME - Journal of Nanotechnology in Engineering and Medicine**, vol. 5, pp. 010901.
10. [b]**Chougule, S.S.** and Sahu, S.K., and Pise A.T. 2013, "Performance Enhancement Of Two Phase Thermosyphon Solar Water Heater By using Surfactant," **Frontiers in Heat Pipe**, 4(1), pp. 1-5.
11. [c]**Chougule, S.S**., and Sahu, S.K., 2015, "Experimental Study on Laminar Forced Convection of Al_2O_3/waterr and CNT/Water Nanofluid of Varied Particle Concentration with Helical Twisted Tape Inserts in Pipe Flow," **Chemical Engineering and Technology** (Under Review).

International Conference

12. **Chougule, S. S.,** and Sahu, S.K., 2014, "An Integrated Effect of PCM and Nanofluid Charged Heat Pipe for Electronics Cooling," ***ASME-12th International Conference on Nanochannels, Microchannels, and Minichannels,*** **Illinois Chicago, USA**, August 13-17.
13. **Chougule, S.S.,** and Sahu, S.K., 2013, "Experimental Investigation of Heat Transfer Augmentation in Automobile Radiator with CNT/Water Nanofluid," ***4th ASME-International Conference on***

Micro/Nanoscale Heat & Mass Transfer (MNHMT), **Hong Kong, China**, December 11-14.

14. **Chougule, S.S.,** and Sahu, S.K., 2013, "Performance of Wickless Heat Pipe Flat Plate Solar Collectors Having Different Filling Ratios," ***11th ISHMT-ASME and 21st National Heat and Mass Transfer International Conference,*** **IIT Kharagpur, India**, December 28-31.
15. **Chougule, S.S.,** and Sahu, S.K., 2013, "Comparison of Augmented Thermal Performance of CNT/Water and Al_2O_3/Water Nanofluids In Transition Flow Through A Straight Circular Duct Fitted With Helical Screw Tape Inserts," ***11th ISHMT-ASME and 21st National Heat and Mass Transfer International Conference*****,** **IIT Kharagpur, India**, December 28-31.
16. **Chougule, S.S.,** and Sahu, S.K., 2013, "Comparative Study of Cooling Performance of Automobile Radiator Using Al_2O_3/Water and CNT/Water Nanofluid," ***11th ISHMT-ASME and 21st National Heat and Mass Transfer International Conference*****, IIT Kharagpur, India**, December 28-31.
17. [d]**Chougule, S.S.,** and Sahu, S.K., 2013, "Augmentation of Convective Heat Transfer by Addition of High-Alcohol Surfactant (HAS)," ***11th ISHMT-ASME and 21st National Heat and Mass Transfer International Conference*****, IIT Kharagpur, India**, December 28-31.
18. [e]**Chougule, S.S.,** Sahu S.K., and Pise, A.T., 2013, "Performance Enhancement of Two Phase Thermosyphon Solar Water Heater by using Surfactant," ***17th International Heat Pipe Conference (IHPC),*** **IIT Kanpur, India**, October 13-17.
19. [f]**Chougule, S.S.**, and Sahu, S.K, 2013, "Model of Heat Conduction in hybrid nanofluid," ***International conference on emerging trends in computing, communication and nanotechnology (ICE-CCN),*** **India**, March 25-26.

20. [g]Shewale, S.P., **Chougule, S.S.,** Sahu, S.K., and Pise, A.T., 2014, "A Review of Heat Pipe with Nanofluid for Electronic Cooling," *IEEE - **4th International Conference on Advances in Engineering and Technology (ICAET 2014),*** **Nagapattiam, India**, May 2-3 .
21. [h]Shewale, S.P., **Chougule, S.S.,** Sahu, S.K., and Pise, A.T., 2014, "A Review on Applications of PCM for Electronic Cooling," ***IEEE - 4th International Conference on Advances in Engineering and Technology (ICAET 2014),*** **Nagapattiam, India**, May 2-3.

[a, b, c, d, e, f, g, h] articles are not included in the present dissertation

SANDESH S. CHOUGULE | RESUME

Doctoral Research Scholar
Indian Institute of Technology, Indore
Madhya Pradesh, India, 453446
TEL: +91-8109747596
E-mail: sandesh_chougule@yahoo.com
Google Scholar Profile:
https://scholar.google.co.in/citations?user=sygGWRsAAAAJ&hl=en

RESEARH AND TEACHING INTERESTS

Nanofluid, Enhanced Heat Transfer, Heat pipes, Solar Energy, Electronics Cooling and Biodiesel….

EDUCATION

- **Indian Institute of Technology Indore** — **Indore, MP, India**
  Ph.D. - Mechanical Engineering — 2012-Present
- **Government College of Engineering** — **Karad, Maharashtra, India**
  M.E. (Master of Engineering)-Mechanical Engineering — 2010-2012
- **Shivaji University** — **Kolhapur, Maharashtra, India**
  B.E. (Bachelor of Engineering)-Mechanical Engineering — 2004-2008

RELATED WORK EXPERIENCE

- **Indian Institute of Technology Indore** — **Indore, MP, India**
  Teaching Assistant-Discipline of Mechanical Engineering — July 2012 – present
- **Government College of Engineering** — **Karad, Maharashtra, India**
  Lecturer – Department of Mechanical Engineering — August 2010 – October 2011
- **D. Y. Patil College of Engineering** — **Kolhapur, Maharashtra, India**
  Lecturer – Department of Mechanical Engineering — July 2008 – May 2010

HONORS AND AWARDS

- Travel Support from **Science and Engineering Research Board,** Government of India to present research paper at **ASME (ICNMM-14)** conference, **Chicago, USA**.
- Travel Support from **Council of Scientific and Industrial Research**, Government of India to present research paper at **ASME (MNHMT-13)** conference, **Hong Kong**.
- **MHRD scholarship** for Ph.D. program at Indian Institute Technology, Indore, India.
- **Ranked 1st** in Master Engineering Program at GCE, Karad.
- **Referee:** *Journal of Nanoparticle research* (Springer), *Applied Thermal Engineering* (Elsevier), *Thermal Sciences* (Elsevier), *Heat Transfer-Asian Research* (Wiley), *Frontiers in Heat Pipes* (Thermal Fluid Central), *Magnetism and Magnetic Materials* (Springer), *Advances in Materials Science and Engineering*, *Physical Sciences*

Publications

International Journals (11), **Refereed Conferences** (17)

Participation in Short Term Courses

• **Introduction to Research Methodology**, IIT Bombay	June 25 - July 4, 2012
• **Computational Fluid Dynamics**, IIT Bombay	June 12 - 22, 2012
• **Phase-change Thermal System**, IIT Kanpur	March 19-20, 2012
• **Solar Photovoltaic**, IIT Bombay	Dec. 12 – 22, 2011
• **Heat Transfer**, IIT Bombay	Nov.29 – Dec.10, 2011
• **Advanced Nanomaterials**, NIT Calicut	July 6-12, 2011
• **Advances in Hybrid Energy**, NIT Calicut	June 26 - July 2, 2011
• **Thermodynamics in Mechanical Engineering**, IIT Bombay	June 14 - 24, 2011
• **Condition Monitoring of Plant and Machinery**, NIT Hamirpur	June 21-25, 2010
• **Alternative Energy Option for I.C. Engine**, NIT Calicut	June 28 - July 3, 2010
• **Recent Trends in Numerical Method**, NIT Calicut	May 24 - June 5, 2010
• **Recent Trends in Heat Exchangers**, GCE Karad	Dec. 21 – Jan. 2, 2010
• **High Impact Skills**, Wipro	December 7-11, 2009

Personal Details

Date of Birth	May 26, 1987 (Kognoli, Karnataka, India)
Nationality	Indian
Languages known	English, Hindi, Marathi, Kannada
Contact	+91- 8109747596
E-mail	sandesh_chougule@yahoo.com phd12110304@iiti.ac.in
Permanent Address	A/P: Lakhanapur Tal: Chikodi, Dist: Belgaum, Karnataka, India, 591211
Present Address	Indian Institute of Technology Indore PACL Campus, Harniya Khedi, Opposite to Veterinary College, Rasalpura P.O., MHOW, Madhya Pradesh, India, 453446
Countries Visited	USA, Hong Kong, Macau